OPTIMUM POSITION ESTIMATION FOR OMEGA

Cecil Jerome Waylan

NAVAL POSTGRADUATE SCHOOL
Monterey, California

THESIS

OPTIMUM POSITION ESTIMATION
FOR OMEGA

by

Cecil Jerome Waylan

June 1974

Thesis Advisor: J. E. Ohlson

Approved for public release; distribution unlimited.

SECURITY CLASSIFICATION OF THIS PAGE (When Data Entered)

REPORT DOCUMENTATION PAGE

READ INSTRUCTIONS BEFORE COMPLETING FORM

1. REPORT NUMBER	2. GOVT ACCESSION NO. / 3. RECIPIENT'S CATALOG NUMBER
4. TITLE (and Subtitle): Optimum Position Estimation for Omega	5. TYPE OF REPORT & PERIOD COVERED: Doctor of Philosophy, June 1974
	6. PERFORMING ORG. REPORT NUMBER
7. AUTHOR(s): Cecil Jerome Waylan	8. CONTRACT OR GRANT NUMBER(s)
9. PERFORMING ORGANIZATION NAME AND ADDRESS: Naval Postgraduate School, Monterey, California 93940	10. PROGRAM ELEMENT, PROJECT, TASK AREA & WORK UNIT NUMBERS
11. CONTROLLING OFFICE NAME AND ADDRESS: Naval Postgraduate School, Monterey, California 93940	12. REPORT DATE: June 1974 / 13. NUMBER OF PAGES: 195
14. MONITORING AGENCY NAME & ADDRESS (if different from Controlling Office): Naval Postgraduate School, Monterey, California 93940	15. SECURITY CLASS. (of this report): Unclassified / 15a. DECLASSIFICATION/DOWNGRADING SCHEDULE

16. DISTRIBUTION STATEMENT (of this Report)

Approved for public release; distribution unlimited.

17. DISTRIBUTION STATEMENT (of the abstract entered in Block 20, if different from Report)

18. SUPPLEMENTARY NOTES

19. KEY WORDS (Continue on reverse side if necessary and identify by block number)

20. ABSTRACT (Continue on reverse side if necessary and identify by block number)

Omega is a worldwide VLF navigation system which utilizes phase differencing techniques. The VLF signals of Omega are perturbed by phase uncertainties caused by factors such as diurnal effects which are quite predictable and other factors which are not so predictable. This dissertation models the effective phase velocity uncertainties which result from the less predictable phase uncertainties as jointly Gaussian perturbations to the phase velocities. This approach of modeling VLF propagation for Omega has not previously been taken.

DD FORM 1 JAN 73 1473 EDITION OF 1 NOV 65 IS OBSOLETE
S/N 0102-014-6601 |
(Page 1)

SECURITY CLASSIFICATION OF THIS PAGE (When Data Entered)

The more predictable factors are incorporated into determination of the mean values of the phase velocities. This model allows any interfrequency and interstation correlation to the phase disturbances of Omega to be readily taken advantage of to improve the estimation performance. From this model, the maximum likelihood position estimation equations are derived for Omega with an arbitrary number of frequencies. Monte Carlo simulation results are reported for four-frequency Omega as SNR and phase velocity uncertainty are varied. These results allow quantitative error prediction for Omega utilizing different fourth frequencies to be made for the first time. Several fourth frequencies which can be easily implemented by the Omega stations, to place less stringent requirements on ambiguity resolution techniques, are examined. The requirement for resolving the inherent lane ambiguity of Omega arises when application of Omega to search and rescue systems such as the planned worldwide Global Rescue Alarm Net (GRAN) is considered. Four-frequency experimental data was processed with the maximum likelihood estimator and the results, which demonstrate the potential of the estimator, are presented.

Optimum Position Estimation for Omega

by

Cecil Jerome Waylan
Lieutenant Commander, United States Navy
B.S., Kansas University, 1965
M.S., Naval Postgraduate School, 1973

Submitted in partial fulfillment of the
requirements for the degree of

DOCTOR OF PHILOSOPHY

from the
NAVAL POSTGRADUATE SCHOOL
June 1974

ABSTRACT

Omega is a worldwide VLF navigation system which utilizes phase differencing techniques. The VLF signals of Omega are perturbed by phase uncertainties caused by factors such as diurnal effects which are quite predictable and other factors which are not so predictable. This dissertation models the effective phase velocity uncertainties which result from the less predictable phase uncertainties as jointly Gaussian perturbations to the phase velocities. This approach of modeling VLF propagation for Omega has not previously been taken. The more predictable factors are incorporated into determination of the mean values of the phase velocities. This model allows any interfrequency and interstation correlation to the phase disturbances of Omega to be readily taken advantage of to improve the estimation performance. From this model, the maximum likelihood position estimation equations are derived for Omega with an arbitrary number of frequencies. Monte Carlo simulation results are reported for four-frequency Omega as SNR and phase velocity uncertainty are varied. These results allow quantitative error prediction for Omega utilizing different fourth frequencies to be made for the first time. Several fourth frequencies which can be easily implemented by the Omega stations, to place less stringent requirements on ambiguity resolution techniques, are examined. The requirement for resolving the inherent lane ambiguity of Omega arises when application of Omega to search and rescue systems such as the planned worldwide Global Rescue Alarm Net (GRAN) is considered. Four-frequency experimental data was processed with the maximum likelihood estimator and the results, which demonstrate the potential of the estimator, are presented.

TABLE OF CONTENTS

LIST OF TABLES

LIST OF FIGURES

ACKNOWLEDGMENTS

The author wishes to express his appreciation to Dr. J. E. Ohlson for his guidance throughout this research. His efforts to always provide time in a busy schedule for guidance and assistance are recognized and appreciated. Thanks are given to Professor J. A. Pierce of Harvard University for his time in discussing considerations involved in VLF propagation. Thanks are also given to CDR. W. R. Crawford and Mr. W. E. Rupp of Naval Air Test Center, Patuxent River, Maryland for providing the requirement for this research and the funding to support it. Mr. W. Hoover of Texas Instruments Corporation, Dallas, Texas is thanked as well for his aid in providing experimental data.

For my wife and son, their patience and understanding during this period when little of my time has been available to them has been most appreciated.

This work was supported by Naval Air Test Center, Patuxent River, Maryland.

I. INTRODUCTION

The Omega navigation system is being developed with the intent of achieving a worldwide navigational aid. It is anticipated [1], that the eight station Omega system will be fully operational by 1976. There are, at this writing, two fully operational stations radiating the prescribed 10 kw of power at the three present Omega frequencies; 10.2 kHz, 11 1/3 kHz, and 13.6 kHz. These stations are located in North Dakota and Norway. The exact locations are contained in Table I. The Trinidad station, which will eventually be replaced by the station in Liberia, is operational at reduced power; and the Hawaii station is expected to be fully operational at full power by 1975.

The choice and number of frequencies for the Omega system has been predicated on the use of Omega as a navigation aid by ships and aircraft which would have dead reckoning (DR) and alternate fix capabilities. In the recent past, however, the United States Navy [2] and the United States Air Force [3], along with several other organizations, have been investigating the use of Omega for applications such as search and rescue (SAR). The requirements of a SAR System, using Omega as a position location information source, are much more demanding than those of navigation systems. In general, no a priori position information is available at a SAR incident location. On the basis of what information

TABLE I

OMEGA STATION LOCATIONS*

Station	Latitude	Longitude
Aldra, Norway	66°25'15" N	13°09'10" E
Trinidad**	10°42'06.2" N	61°38'20.3" W
Liberia** (proposed)		
Haiku, Hawaii	21°24'16.9" N	157°49'52.7" W
La Moure, North Dakota	46°21'57.2" N	98°20'08.8" W
Reunion	20°58'26.5" S	55°17'24.2" E
Trelew, Argentina	43°03'12.5" S	65°11'27.7" W
Australia (proposed)		
Tsushima, Japan	34°36'53.3" N	129°27'12.5" E
Forestport, New York***	43°26'40.9" N	75°05'09.8" W

* Information for this table was obtained from the Defense Mapping Agency, Washington, D. C.

** The Trinidad station is expected to be replaced by a station in Liberia.

*** The Forestport station remains only as an experimental station and is not part of the Omega system.

can be received at the SAR incident and relayed to rescue forces, the SAR position must be determined.

A. INTRODUCTORY BACKGROUND

The first proposal to use satellite relayed Omega information for SAR purposes was by Samek and Pike [4]. The principle was taken from the Omega position locating experiment (OPLE) proposed by NASA's Goddard Space Flight Center. The OPLE was carried out in 1967[5] utilizing the ATS-1 and 3 satellites and demonstrated that Omega navigation signals could be received at a remote site and retransmitted via satellite to a ground center which uses these signals to determine the location of the retransmitter. The success of this experiment engendered the advanced OPLE concept. Advanced OPLE was to use a UHF satellite link frequency (402 MHz) instead of the VHF link frequency (149 MHz) of OPLE, smaller transceivers (platforms), random access techniques for the satellite link, and an ambiguity resolution technique for the Omega information. Omega ambiguities are described later in this chapter. These changes to OPLE allowed for much more diversified anticipated usage of the concept. The random access technique (many users using a single satellite at arbitrary times) obviated the requirement to interrogate the platforms and thus they could be much smaller and lighter. This allowed for planned application of the concept to tasks such as tracking of animals for zoological purposes. Resolution capability for the ambiguity problem would mean no

a priori position information would be required to locate the transceiver. The advanced OPLE concept was not carried out because of fund limitations and the interest of Naval Air Test Center (NAVAIRTESTCEN), Patuxent River, Maryland in using the equipment for their GRAN program.

1. GRAN

In 1969, NAVAIRTESTCEN, Patuxent River, Maryland, proposed the Global Rescue Alarm Net (GRAN) as a worldwide SAR system based on the advanced OPLE concept. GRAN will utilize hand-held transceivers called SAR communicators (SARCOM's) to receive Omega signals and relay them, shifted in frequency and occupying reduced spectrum, via SAR satellites (SARSAT's) to ground SAR centers (SARCEN's), Figure 1. At the SARCOM, unit identification information is added to the spectrum. In 1970, NAVAIRTESTCEN carried out experiments utilizing low transmitted powers and demonstrated the feasibility of low power SARCOM's for GRAN [6]. The 100 kHz band of frequencies from 406.0 MHz to 406.1 MHz was assigned for use in a SAR satellite link such as GRAN at the World Administrative Radio Conference for Space Telecommunications (WARC-ST) in Geneva in 1971 [2].

It is anticipated by the originators that GRAN will serve all countries. GRAN will be available to any military and civilian users who purchase a SARCOM. In keeping with this concept, the cost of the SARCOM units must be kept to the minimum possible level. This constraint prohibits preprocessing of the received Omega information in the SARCOM.

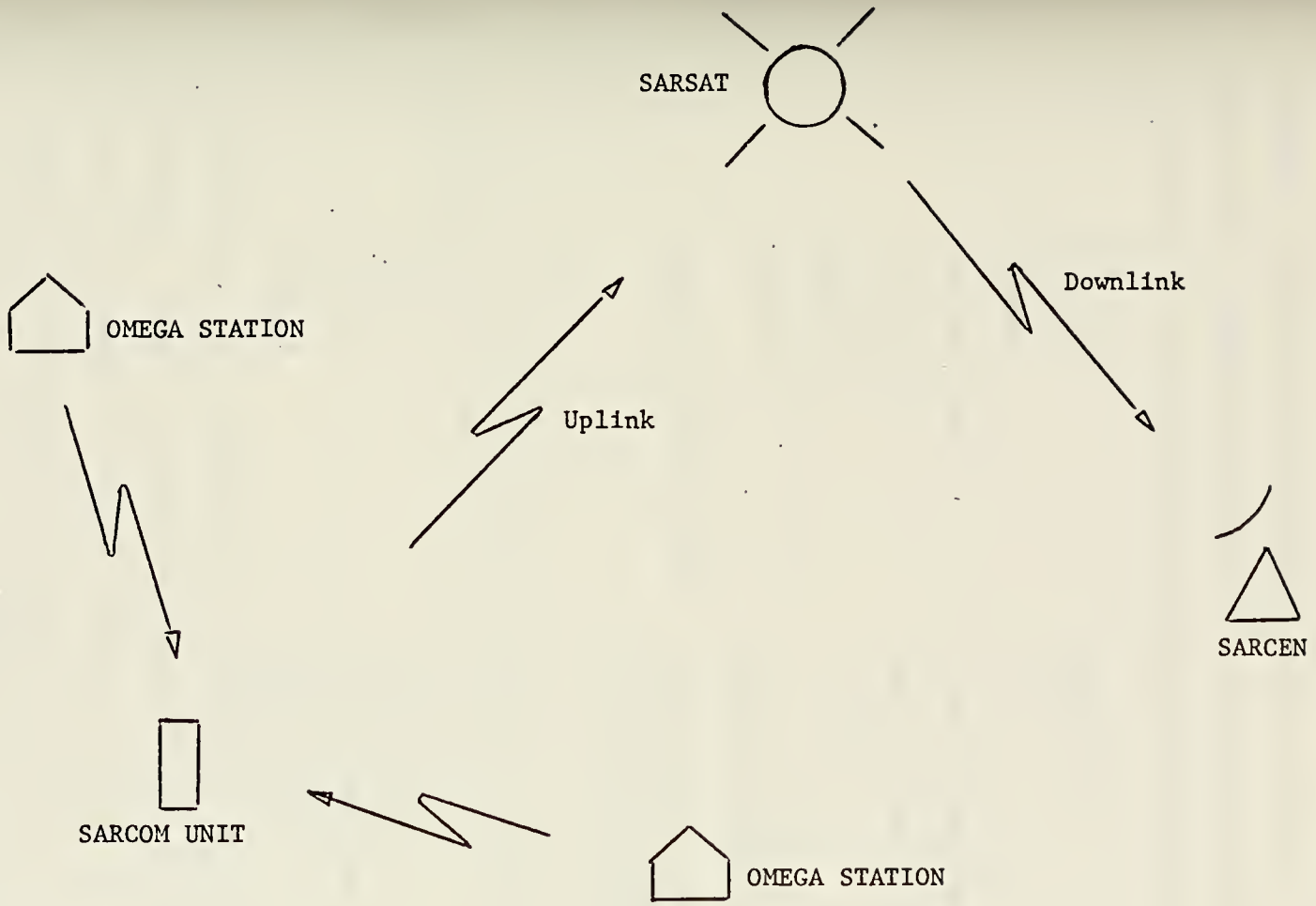

Figure 1. The GRAN System.

In order to meet the portability requirements necessary so pleasure craft and perhaps even hikers can carry the units, weight and size of the SARCOM units must also be kept to a minimum. Studies by NASA [7] have demonstrated the feasibility of the following characteristics for the SARCOM's:

Volume	1000 in^3
Weight	1 kg
Output Power	5 watts maximum
Frequency	406.0 - 406.1 MHz
Bandwidth	2.5 kHz
Transmission Period	3 min. broadcast, repeated as battery power allows
Identification Data	36 (bits) - sufficient for nine digit number such as a social security number

The SARCOM units will operate sequentially in three modes when activated. The modes are:

Mode 1.	Acquisition
Mode 2.	Identification Data
Mode 3.	Omega Data

In mode one, the SARCOM will transmit only an internally generated Acquisition/Recognition (A/R) tone in the allotted band of frequencies for a period of about 12 seconds. The maximum power capability of the unit will be concentrated in this tone to allow the SARCEN phase-locked-loop receivers to acquire the retransmitted tone and switch to a narrow tracking bandwidth for signal-to-noise ratio improvement.

The second mode is then commenced automatically and SARCOM unit identification information is transmitted digitally by phase-shift-keying the A/R tone with a code preassigned to the SARCOM unit. The second mode will consist of about six seconds of transmissions. In the final mode, the received Omega information is retransmitted along with the A/R tone. The total transmitted power of the SARCOM will be divided between the A/R tone (approximately .5 w) and the retransmitted Omega signals (remaining power equally divided). This third mode is expected to last for approximately 180 seconds, which would allow for 18 of the ten second Omega format periods (see the following section) to be relayed. A possible spectrum of signals to be retransmitted if four-frequency Omega is adopted and the fourth signal is at 10.88 kHz is shown in Figure 2. The signals in the spectrum correspond to frequency shifted versions of the Omega signals; signal number one corresponds to the 10.2 kHz signal, signal two to the 10.88 kHz signal, signal three to the 11 1/3 kHz signal and signal four to the 13.6 kHz signal. The actual number of different frequency Omega signals and the options available in choosing these frequencies is discussed in detail later in this thesis. The center frequency of the spectrum in Figure 2 is referred to only as f_o. This is done since to utilize the entire 100 kHz bandwidth of the SARSAT as well as to avoid concurrent identical spectra to be transmitted from several SARCOM's, the 2.5 kHz SARCOM spectra will have to be spread throughout the 406.0 MHz - 406.1 MHz

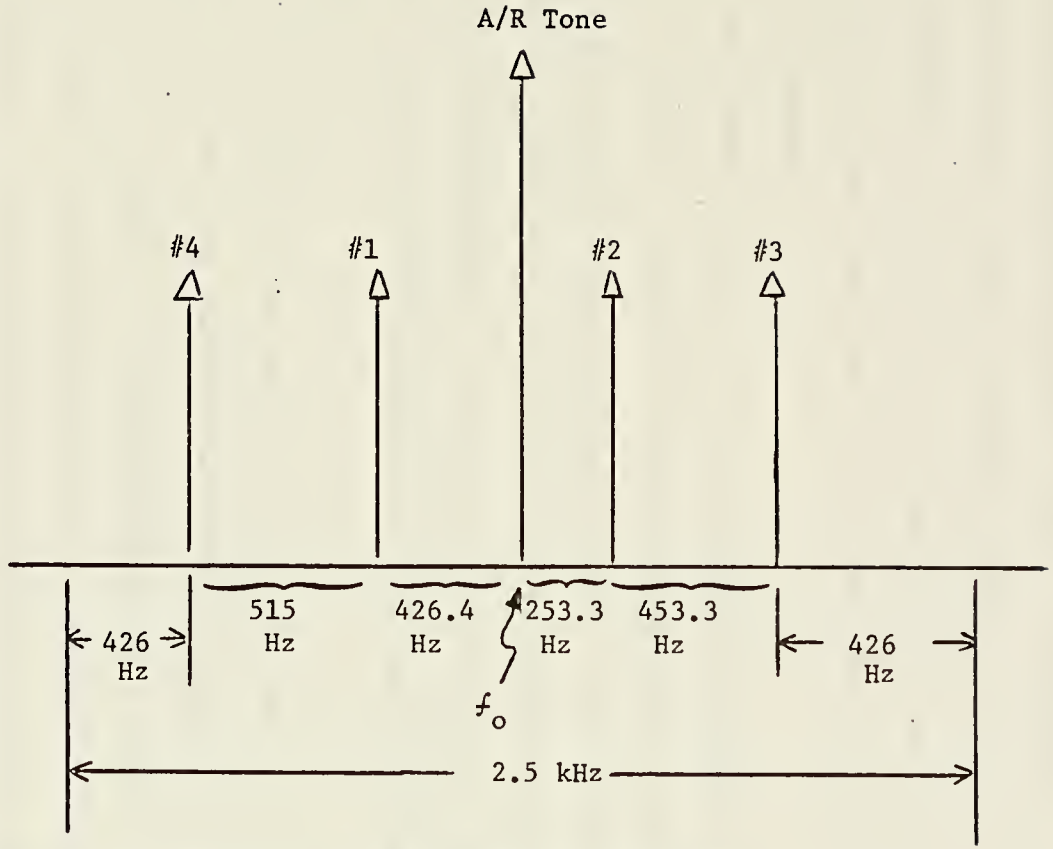

Figure 2. A Possible GRAN Retransmitted Spectrum.

band of the SARSAT. This may be accomplished by assigning different frequency A/R tones to different users. Reference [8] contains additional discussion in this area. The spacing of the retransmitted Omega signals relative to the A/R tone will be accurately controlled by the SARCOM. Thus, when the phase-locked-loop receiver in the SARCEN locks on and tracks the A/R tone, the Omega signals may be recovered with essentially all of the frequency drift and doppler shifts which affect the spectrum, after its creation in the SARCOM, eliminated.

The SARSAT system to be utilized for GRAN will consist of a system of three to four geosynchronous satellites and additional polar orbiting satellites. The exact number and types of orbits of the satellites is still being considered by NAVAIRTESTCEN. A discussion of the requirements for the satellite system as well as link calculations is contained in [8].

The SARCEN system will consist of several SARCEN's in order to allow some SARCEN to continuously be in the coverage of each SARSAT. Each SARCEN will search the preassigned band of frequencies with a set of phase-locked-loop (PLL) receivers. The bandwidth of the PLL in the search mode will be larger than when tracking a SARCOM relayed message in order for the acquisition time to be small. When an A/R tone has been acquired, the bandwidth of the PLL will be decreased to improve the SNR from the PLL and allow

lock to be maintained after the power of the A/R tone is decreased for the third mode of SARCOM transmission.

After the SARCEN has acquired a retransmitted SAR message, identified the sending SARCOM from the identification data, and recorded the retransmitted Omega signals, the position of the SAR incident must be determined. The optimum method for locating the retransmitting SARCOM position is determined by this thesis.

2. Omega

a. History of Omega

Following World War II, the MIT Radiation Laboratory which had been actively developing military navigation aids, was closed [9]. Loran A and Loran C, as presently used, were results of their work. A small group from Division 11 of the Laboratory moved to Cruft Laboratory, Harvard University. In 1947, Professor J. A. Pierce of this group proposed Radux [4] as a navigation system. The technique of Radux was very similar to Loran except that the transmitted signals were phase modulated with a 200 Hz signal. Because of the extremely stable phase characteristics of signals in the proposed frequency range of 40 kHz to 50 kHz, it was expected that the modulation could be used in phase comparison with quite accurate results.

The results of experiments with Radux by the Navy Electronics Laboratory indicated that the accuracy of Radux could resolve ambiguities which would result from a 10 kHz signal. This, along with the fact that VLF

frequencies were relatively unusable for communications purposes, resulted in a composite system Radux-Omega which radiated the 40 kHz signals of Radux interrupted by 10 kHz bursts of a coherent signal. The 10 kHz signal yielded nominally eight nmi (nautical miles) ambiguities which could be resolved by the 200 Hz modulation of the 40 kHz signal.

It was soon found that this system was not as good as could be obtained. The 10 kHz signal had a much longer usable range than the 40 kHz signal and could thus have much longer baselines (the great circle connecting two Omega stations) thus improving the accuracy of the system markedly.

b. Present Omega

Several different frequencies in the 10-14 kHz range were used in experiments with Omega. The frequencies decided upon for final implementation were 10.2 kHz, 11 1/3 kHz, and 13.6 kHz common to all Omega stations and other frequencies unique to the stations to be transmitted for other than phase difference navigation. A total of eight stations were decided upon to achieve worldwide coverage with a station redundancy sufficient to assure an adequate fix anywhere in the world. The three common frequencies are radiated as on-off-keyed, time-division-multiplexed signals in a ten second format as shown in Figure 3. The nominally one-second pulses are all separated by 0.2 seconds. Each station transmits the common frequencies in the same sequence, but starting at a different time.

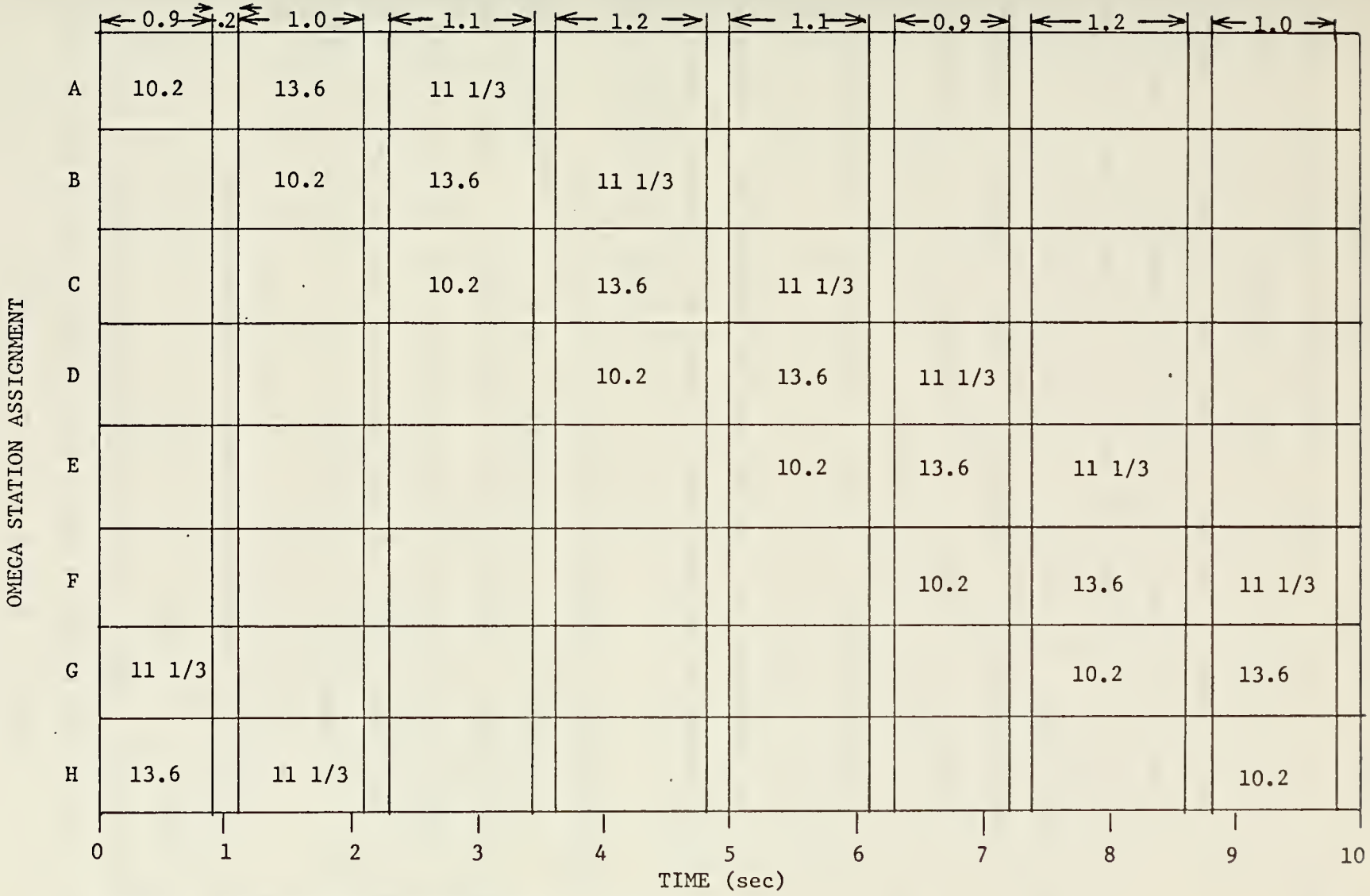

Figure 3. Omega Station Transmission Format.

Omega, being a phase differencing navigation system is necessarily a hyperbolic system. That is, the isophase contours of two stations (lines on the earth for which the phase difference of two common frequency signals from two stations is constant) form a set of hyperbolas shown in Figure 4, which has as foci the two stations radiating the signals. As shown in Figure 4, two adjacent hyperbolic lines, henceforth called "lines of position" or LOP, separated by a distance d_1 on the baseline can be shown to be spaced by $d_2 = d_1 \csc(\theta/2)$ off the baseline [10]. The angle θ is that angle formed by the two great circles passing through the stations and a point midway between the adjacent LOP off the baseline. The spacing of two LOP off the baseline of two stations then will be equal to the spacing of these LOP on the baseline multiplied by $\csc(\theta/2)$.

Because it is a phase difference system, Omega has naturally occurring ambiguities. On the baseline of two stations, the same phase difference of a common frequency f radiated from the stations will be seen every $\frac{1}{2}\lambda$ where λ is the wavelength of the frequency f. This results in lanes between unambiguous LOP of width $\frac{1}{2}\lambda$ on the baseline. Off the baseline this spacing will be $\frac{1}{2}\lambda \csc(\theta/2)$.

This concept is easily extended to multiple frequency transmissions by considering a signal of frequency f_r which is a common clock frequency to all Omega stations and is utilized to create the K transmitted signals f_i ($i = 1, 2, \ldots, K$). In the present Omega system K is three. In order

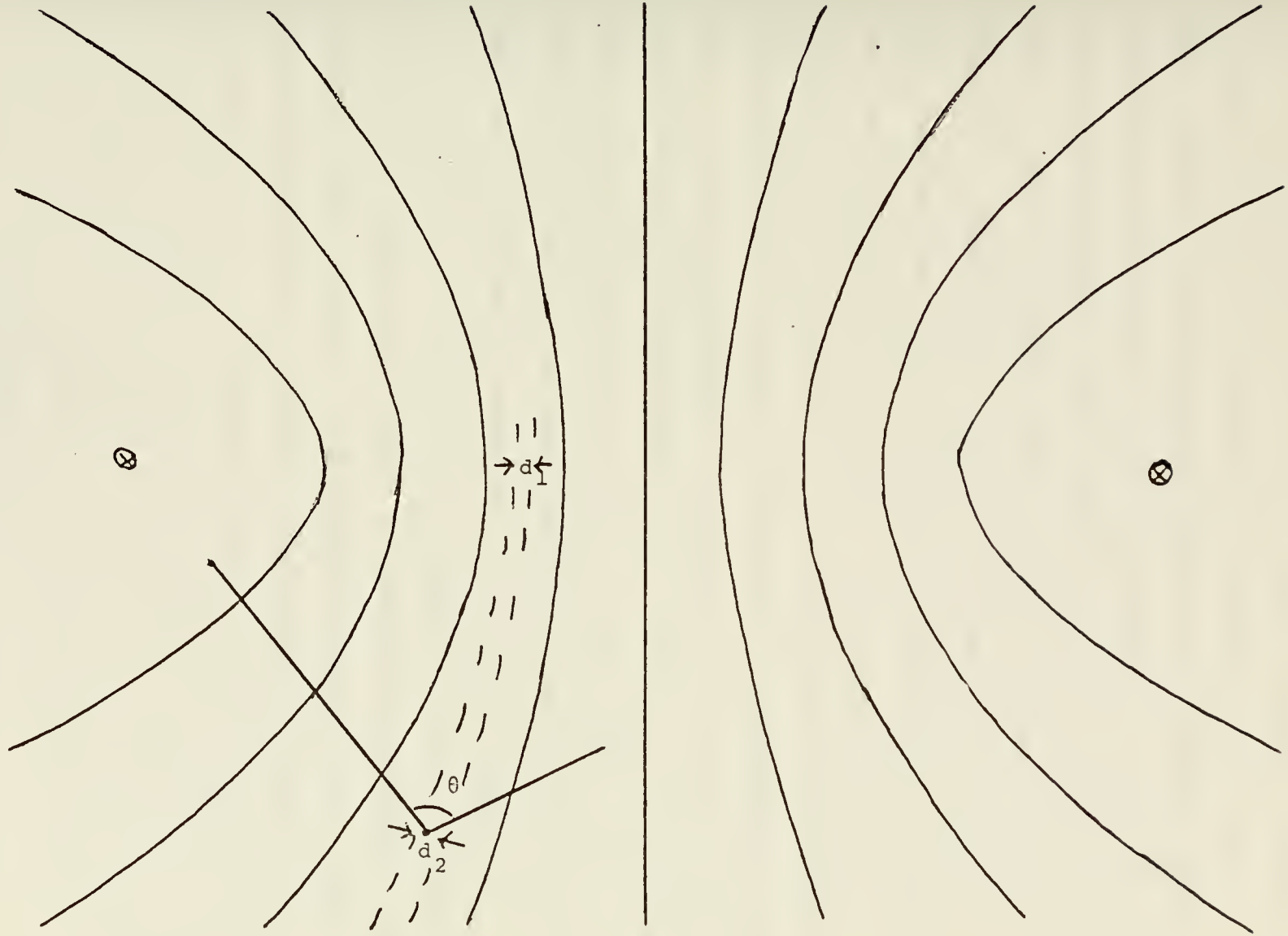

Figure 4. Hyperbolic LOP between Two Omega Stations.

for phase comparison of the common frequencies from the stations to be useful in locating a remote receiver site, the frequency f_r at all stations are maintained very nearly phase coherent. The ith Omega signal to be transmitted is created from division of f_r by an integer n_i. The baseline lane width associated with frequency f_i will be $\frac{1}{2}\lambda_s = v_s/2f_s$, where f_s is the largest common multiple frequency of the transmitted frequencies. This is the smallest frequency which can be obtained by frequency differencing techniques from the K transmitted frequency. The value of v_s, the effective phase velocity of f_s, is determined by the phase velocities of the K signals. However, v_s is nominally equal to c, the velocity of light in vacuum, so we can get a nominal value for $\frac{1}{2}\lambda_s$ by assuming $v_s \approx c$. The term "unambiguous lane" will be used in this thesis to refer to $\frac{1}{2}\lambda_s$. The nominal baseline size of the unambiguous lane may be determined by the following procedure. The integer divisors, n_i (i = 1, 2, ..., K) are first separated into the products of powers of their prime number components (see example which follows). The product of the largest powers of all prime numbers which occur, then gives the divisor n_s which yields f_s from $f_s = f_f/n_s$. Baseline unambiguous lane width is then $\approx c/2f_s = c \cdot n_s/2f_r$. The present value of f_r(816 kHz) used by the Omega stations allows a simple rule of thumb to find a nominal baseline unambiguous lane width easily from n_s.

$$\frac{1}{2}\lambda_s(\text{nmi}) \approx \frac{161{,}875.2(\text{nmi/sec}) \cdot n_s}{2 \cdot 816{,}000 \text{ Hz}} = .0992\ n_s \approx n_s/10 \quad (1)$$

The present three frequencies transmitted by the Omega system; 10.2 kHz, 11 1/3 kHz, and 13.6 kHz yield $n_s = 2^4 \cdot 3^2 \cdot 5 = 720$ since $n_1 = 2^4 \cdot 5 = 80$, $n_2 = 2^3 \cdot 3^2 = 72$, and $n_3 = 2^2 \cdot 3 \cdot 5 = 60$. Thus from (1) the baseline width of the unambiguous lanes is nominally 72 nmi.

3. VLF Propagation

Since the Omega system depends upon phase comparison, unexpected phase shifts in the propagation path cause position estimation errors. The causes of the anomalous phase shifts must therefore be considered. For the Omega system, frequencies in the 10-14 kHz region have been chosen because of the extremely long ranges which VLF signals propagate and because of the remarkable phase stability of these signals. The propagation problem at VLF has been studied both experimentally and theoretically by many researchers for many years. References [11, 12, 13, and 14] contain very detailed and thorough discussions of VLF propagation.

In general, for distances less than several Megameters (Mm) from the transmitter, the easiest theoretical analysis of VLF propagation can be obtained by a combination of ground and sky wave contributions. The ground wave provides the field which would be seen in the absence of the ionosphere and its attenuation with distance from the transmitter is generally attributable to earth curvature [11]. The sky wave is the transmitted wave which is reflected in the earth ionosphere cavity. The contribution to the total field from skywaves can be determined by summing all of the skywaves

present at any distance from the transmitter using ray theory [11]. At distances beyond a few Mm, the number of skywave contributions becomes unwieldy and waveguide theory of propagation becomes much easier to use.

Waveguide theory for VLF is generally used for making theoretical predictions for Omega. Propagation predictions (to be discussed later) do attempt to predict phases of signals at ranges where ground wave effects are significant; however, Omega is considered most predictable and thus most reliable at distances in excess of 2-3 Mm from the transmitters. At these distances, single mode waveguide theory seems to describe the propagation quite well.

Waveguide theory of propagation describes the earth and ionosphere as forming a spherical waveguide. The height of the ionosphere above the earth, nominally 90 km at night and 70 km during the day, is on the order of several wavelengths for the 10-14 kHz signals of Omega and thus waveguide theory would seem to apply if the boundaries of the waveguide could be adequately described. It is generally accepted [15], that the propagation effects causing phase variation, which is what is of concern for a phase comparison system such as Omega, can be divided into two categories, temporal and spatial. Among the temporal variations, the diurnal variations have the most dramatic affect and are probably one of the most predictable factors. This variation is in general accounted for by using different effective phase velocities for each frequency for dark and for lighted

transmission paths. Professor J. A. Pierce of Harvard University has conjectured that adequate position estimation using Omega may be attainable using the single waveguide mode phase velocities given in Table II. These values were obtained from [16] and from personal communication with Professor Pierce. Other temporal variations are long term dependence on solar cycle, lunar, and annual variations.

The spatial variations of importance appear to vary with propagation bearing, earth conductivity over the transmission path, geomagnetic latitude, and the ionosphere conditions. The magnetic field has an apparent marked effect on the ionosphere and thus creates phase variations dependent upon the transmission path. These spatial variation causes are not independent quantities and thus must be treated together [15].

The Defense Mapping Agency attempts to account for all of the above phase variation sources as well as other lesser known sources in the Omega Propagation Correction Tables which are published regularly for the 10.2 kHz and 13.6 kHz Omega signals. The computer programs which accomplish this are described in [15]. Additionally, force fitting of the corrections to actual data is continually carried out. The use of these tables is simple; knowing the date and the approximate receiver location, phase correction factors to be added to the observed phase of a known frequency signal from a known station are looked up in prepublished tables. After these corrections are made, the

TABLE II

PREDICTED FIRST MODE PHASE VELOCITY RATIOS

f(kHz)	v/c Day	v/c Night
10.2	1.00270	.99960
11 1/3	1.00139	.99869
13.6	.99965	.99751
10.88	1.00187	.99902

phase difference for a particular station pair and frequency choice is computed and the corresponding LOP is determined from specially prepared Omega charts. Figure 5 shows a sample section of an Omega chart. These charts are prepared based upon a phase velocity 1.00261 times the speed of light in vacuum and thus the phase corrections attempt to correct the phase to this effective phase velocity in determining the receiver location.

B. PROBLEM STATEMENT AND APPROACH

This dissertation determines the optimum procedure to establish an Omega receiver's location. In order to accomplish this task, a model for the Omega problem was first formulated in which the effective phase velocities of the transmitted Omega signals were assumed known. Since true phase velocities of the signals are continuously varying along the transmission path as ionospheric densities and many other factors change, effective phase velocity is used. This velocity is that which satisfies the equation

$$v = \frac{\omega d}{\phi} \tag{2}$$

where d is the distance measured on the globe which the signal travels, ω is the angular frequency of the signal, and ϕ is the observed phase in radians of the signal at a distance d trom the transmitter.

Utilizing this assumption and the assumptions about the noise which will be given in Chapter II, the maximum likelihood LOP estimation equation for two-station, multiple

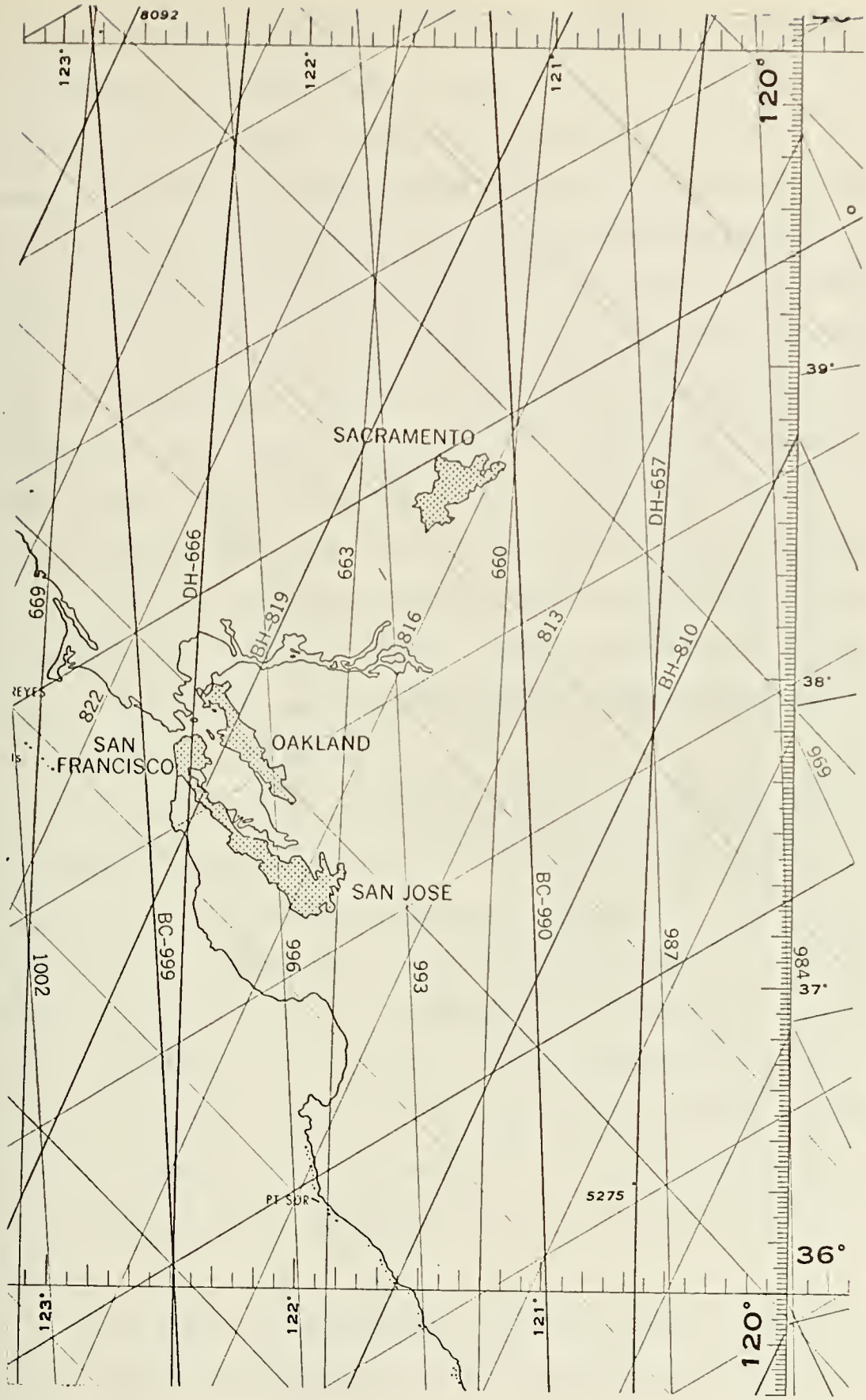

Figure 5. A Sample Portion of an OMEGA Chart.

frequency Omega was derived. This derivation is presented in Appendix C. Using this result and the effective phase velocities for single mode propagation given in Table II, some four-frequency experimental Omega data was processed. The data was collected preliminary to the four frequency Omega experiment described in detail in Chapter VI. The results of this effort were no lane errors (defined in Chapter IV) for transmission paths in daylight, but a significant number of lane errors for dark or partially dark transmission paths. The conclusion which was reached then was that the Table II effective phase velocities were not sufficient predictions of phase velocities actually being experienced. Accounting for diurnal effects only, in predicting effective phase velocities, and assuming single mode propagation was not apparently justified.

A further search into the literature revealed that at reasonably long ranges from VLF transmitters, predicted phase velocities using propagation prediction methods disagreed with experimental results by a few parts in 10^{-4} [17]. This indicated that the best available methods of predicting the disturbances to the phase of VLF signals for typical distances could yield errors in phase differences of signals from two stations on the order of one radian or more. This realization led to the model which was used in this dissertation.

Since phase is related to effective phase velocity by (2), phase disturbances can equivalently be considered as

due to effective phase velocity uncertainties. The many effects which cause phase uncertainties and thus effective phase velocity uncertainties imply, as a result of the central limit theorem, a model of the phase velocities of jointly Gaussian random variables. This new approach not previously considered in the literature allows any correlation between the phase disturbances of signals from the same station or different stations to be taken into account in the estimation process. The effective phase velocity can be predicted as accurately as necessary or possible for the different frequency signals and these values used for the mean values of the jointly Gaussian phase velocities. The entries in the covariance matrix of the phase velocities reflect the uncertainties of these predictions and the correlation of the uncertainties. This is the first model for position estimation which allows advantage to be taken of the correlation between different frequency signals from an Omega station.

References [18, 19, and 20] reveal a significant correlation between phase perturbations of Omega signals transmitted from a single station. The interstation correlation is in general considered to be negligible [19]. If some appropriate standard deviations of the phase velocities on the order of a few parts in 10^{-4} are assumed and the correlation between all signals are assumed known, the probability density functions of the assumed jointly Gaussian phase velocities are completely known. These parameters must be

experimentally determined. Professor J. A. Pierce of Harvard University is presently investigating the correlation of phase disturbances of Omega signals.

Utilizing this new approach and the assumption of additive white noise, which is justified in Chapter II, the maximum likelihood estimation equations for Omega were derived (Chapter IV) for high SNR. The performance of the resultant estimator for various fourth frequencies which could be easily added to the present three-frequency Omega format was investigated by Monte Carlo simulation. The results of these simulations (see Chapter V) allow for the first time, a quantitative measure, in terms of expected errors, of the performance of Omega with different fourth frequencies which could be added to Omega to yield larger unambiguous lanes. The maximum likelihood estimator was used to process experimental four-frequency data (Chapter VI) and the performance was found to conform in general to the simulation results. Preliminary comparison of the estimator performance indicates it is superior in terms of lane errors (defined in Chapter IV), the most important consideration for SAR systems particularly, to any other known estimation procedure.

The equation for the maximum likelihood estimator requires prior estimates of the doppler shifts, signal amplitudes and noise spectral density heights for the Omega signals received by the SARCOM. The maximum likelihood estimation equations for these quantities are contained in Appendices A and B. The results of application of the signal

amplitude and noise density estimation equations to experimental data are presented in Appendix B also. These equations allow optimum estimates of signal-to-noise ratios to be found for Omega signals. The optimum method for determining SNR of Omega signals has not been presented before.

A four frequency experiment utilizing a satellite link is planned by Naval Air Test Center, Patuxent River, Maryland for late 1974. A prototype portable transceiver is being constructed and will be transported to various sites in Europe and the eastern United States for relay of four frequency Omega signals. The LES-6 satellite will be used. The processor for the ground station which has been selected for use is the maximum likelihood estimation program presented in Appendix E of this dissertation.

C. ORGANIZATION OF THESIS

Chapter II of this thesis presents the mathematical model of the estimation problem. The assumptions necessary to describe the problem so that a solution can be obtained and their justification are presented.

Chapter III addresses the resolution of the ambiguity problem which arises in a differencing system. The size of the unambiguous lanes, determined by the number of signals and the choice of their frequencies, determines the requirements from an ambiguity resolution technique. Several potential techniques and their anticipated capabilities, which will thus determine frequency choice for a SAR system, are presented.

Chapter IV contains the derivation of the maximum likelihood estimate of the LOP resulting from two stations each transmitting an arbitrary number, K, of common frequencies. Since there are only eight locations in the Omega format for the nominally one second pulses of different frequencies, K will necessarily be less than or equal to eight unless more than one frequency is allowed to occupy a pulse by time sharing. The resultant estimation equation when K is set equal to four, the number of frequencies presently being considered by the managers of GRAN, is presented. The estimation equation which resulted when deterministic, known phase velocities were assumed is addressed in Appendix C.

Chapter V presents the results of Monte Carlo simulation which was carried out for several easily implemented fourth frequency choices, an expected range of variances of the phase velocities, and a range of SNR. The simulations were carried out to aid in selection of a fourth frequency for Omega which will allow an ambiguity resolution technique to resolve the unambiguous lane problem. The trade off in performance in terms of estimation error which is experienced as unambiguous lane size is increased as a function of the necessary parameters is presented. Although the addition of one frequency to the Omega format is expected to be acceptable to the program managers as well as the Omega station host countries, additional frequencies and/or modulation of a frequency has been stated to be unacceptable by the Omega program office and is, therefore, not considered.

Chapter VI presents the results of processing four-frequency Omega data from two stations with the maximum likelihood estimator. The data for the experiment was collected by Texas Instruments Corporation of Dallas, Texas for NAVAIRTESTCEN in the fall of 1973. The fourth frequency which was transmitted by the two experimental Omega stations (Trinidad and Forestport, New York) in addition to the standard three Omega signal frequencies was 10.88 kHz. A discussion of the results and an explanation of the errors which were experienced is presented. The estimation was done first by assuming the effective phase velocities given in Table II for single mode propagation and second by using propagation correction factors provided by the Defense Mapping Agency. A comparison of the results is presented.

Chapter VII presents the derivation of the multiple station estimation equation and the prospects of being able to implement its computer solution. An alternative approach to the multiple station problem which requires less computation time but is nonoptimum is presented.

Chapter VIII presents the conclusions drawn from the previous chapters. Several appendices contain important methods and results which are not required in the general flow of the chapters.

II. MATHEMATICAL MODEL

Consider two Omega stations each transmitting K frequencies occupying K of the eight nominally one second positions in the predetermined format shown in Figure 3. Let Y(t) be a 2K dimensional column vector, where the first K components represent the signals received from station one and the last K components represent the signals received from station two. We shall represent Y(t) as

$$Y(t) = S(t) + N(t) \tag{3}$$

where S(t) represents the signal portion of the received vector and N(t) represents an additive noise process. We can express the ith component of S(t) in (3) as

$$s_i(t) = A_i \cos [(\omega_i + \Delta_i)t - \phi_i + \theta_i] \tag{4}$$

where A_i is the amplitude of the ith signal, ω_i is the angular frequency of the ith signal, Δ_i is the doppler frequency shift of the ith signal, ϕ_i is the propagation phase delay of the ith signal and θ_i is the contribution of other than propagation delay to the phase of the ith signal. The components of the 2K dimensional signal vector will be ordered so that the angular frequency ω_i equals the angular frequency ω_{K+i}. Since quite accurate common frequency signals from the two Omega stations are necessary for navigation, $\omega_{K+i} = \omega_i$ will be assumed.

For GRAN, an acquisition and reference signal (A/R tone) will be generated in the SARCOM and transmitted with the Omega data. The transmitted information will occupy 2.5 kHz, Figure 2, a smaller bandwidth than the 3.4 kHz received signal bandwidth, for spectrum conservation and will be centered at a frequency in the allocated band of frequencies from 406.0 - 406.1 MHz. The A/R tone will serve two functions. For a short period at the beginning of the transmission period it will be radiated alone by the SARCOM so the SARCEN phase-locked-loop receiver can achieve lock and track the subsequent transmission. The other function of the A/R tone is to allow phase shifts and frequency drifts in the transmission channel through the SARSAT to the SARCEN to be eliminated. The particular contributors to these effects will be satellite link delays and frequency drift in the satellite frequency translator. Proper processing at the SARCEN will then result in Δ_i values in (4) being caused only by relative motion of the SARCOM with respect to the Omega stations. The frequency drifts in the SARCEN or Omega stations during the transmission period will be negligible because of the accurate frequency standards which will be used.

The same transmission channel will be used to receive, relay, and process the (K+i)th frequency as the ith since they must be at the same frequency. Therefore, with the exception of timing errors at the stations, the phase shift

$\theta_{K+i} = \theta_i$, (i = 1, 2, ..., K). The phase shifts in the K different channels will result from different phase shifts at different frequencies in the transmission channel from the SARCOM to the SARCEN and from the frequency division in the SARCOM. The compacting of the spectrum in the SARCOM must be accomplished by multiplication in each receiving channel with an appropriate frequency signal created by frequency division of a local oscillator signal. The frequency division will be done by digital counting circuits whose initial counting level will be a random quantity. The phase shifts in the K channels which result will thus be mutually independent random variables, uniformly distributed on the interval $(-\pi, \pi]$. It can be shown that this assumption is not affected by the addition of constant phase shifts to the signals due to Omega station timing errors since a uniformly distributed random variable plus a constant remains uniformly distributed.

The propagation phase shifts of the signals from station one and station two will be written as

$$\phi_i = \omega_i \int_o^{x_1} \frac{d\gamma}{v_i(\gamma)} - 2\pi m_i \qquad 1 \leq i \leq K \quad (5a)$$

and

$$\phi_{K+i} = \omega_i \int_o^{x_2} \frac{d\eta}{v_{K+i}(\eta)} - 2\pi m_{K+i} \qquad 1 \leq i \leq K \quad (5b)$$

In (5), $v_i(\ )$ is the effective phase velocity of the ith signal from the Omega station to the SARCOM receiver. These

phase velocities are written as a function of the distance from the transmitter to allow for incorporation of changes in the predicted value of the phase velocities, e.g., from daylight path to dark path conditions. The integers m_i are the number of whole cycles of phase delay the ith signal has experienced from the Omega transmitters to the SARCOM receiver. The values x_1 and x_2 are the great circle distances from the respective Omega stations to the SARCOM.

It is convenient since only an LOP estimate can result from two stations, to estimate only one variable rather than two (x_1 and x_2) in (5). The graphical description of this method is contained in Chapter IV. It consists of defining the sum $x_1 + x_2 = L$ and replacing x_1 by x. Then, by holding the value of L constant the only variable to estimate is x. Substitutions of these definitions into (5) yield

$$\phi_i = \omega_i \int_o^x \frac{d\gamma}{v_i(\gamma)} - 2\pi m_i \qquad 1 \leq i \leq K \quad (6a)$$

and

$$\phi_{K+i} = \omega_i \int_x^L \frac{d\gamma}{v_{K+i}(L-\gamma)} - 2\pi m_{K+i} \qquad 1 \leq i \leq K. \quad (6b)$$

Equations (5) and (6) are written as two equations in order to emphasize that $\omega_i = \omega_{K+i}$ and to allow the limits of the integrals to be written. The value of x is the great circle distance from the first station to the receiver at the

beginning of the data collection period (t=0) and L is the sum of the great circle distances to the two stations for t = 0. Any SARCOM motion must be accounted for by using the doppler estimation information from Appendix A and the position estimate.

The large range over which VLF signal strengths can be expected to vary and the impulsive nature of the atmospheric noise at VLF frequencies [11] dictate the use of a limiter in the receiver. This thesis will assume that the receiver will use a hard limiter which will yield the necessary dynamic range as well as minimize the effect of the impulsive noise.

The components of the noise column vector N(t) in (3) will be assumed to be sample functions from white Gaussian random processes, the ith component of N(t) having two-sided noise spectral density height of $N_i/2$. The ith and (K+i)th noise components will be received in the same channel of the receiver since they are associated with signals of equal frequency. But, as shown by Figure 3, they are received at different times and will, therefore be uncorrelated. The noise will actually be the sum of thermal and atmospheric noise and the rationale for the Gaussian assumption is as follows. The atmospheric noise, expected to dominate at the VLF frequencies, will be the sum of many atmospherics from around the globe. The distant noise impulses will have insufficient amplitude to dominate the hard limiter in the receiver, but nearby impulses will dominate the hard limiter.

Since VLF signals propagate very well over long distances, the small amplitude impulses of noise will occur quite frequently and by the central limit theorem their sum will approach a Gaussian random process. The strong impulses which dominate the hard limiter, yielding approximately zero SNR to the receiver during their existence, will occur much less frequently and with a wise choice of bandwidth for the K channels of the receiver, each impulse will capture the hard limiter for only a small time. It can be shown that this time will be on the order of the inverse of the bandwidth of the filter, so that a 100 Hz filter will allow the hard limiter to be captured for a time of about 0.01 sec. by an impulse.

The 2K dimensional phase velocity vector V will be used to represent the effective phase velocities which are modeled as jointly Gaussian random variables. The covariance matrix of the components of V will be written as K_v. Since inadequate evidence is presently available to justify different uncertainties for the effective phase velocities when modeled in this fashion, it is convenient for the simulations reported on in Chapter V to assume

$$K_v = E[V V^T] = \sigma^2 \begin{bmatrix} \underset{\sim}{\rho} & \underset{\sim}{0} \\ \underset{\sim}{0} & \underset{\sim}{\rho} \end{bmatrix} . \quad (7)$$

In (7), σ^2 is the scalar variance, assumed equal for all signals. The symbol $\underset{\sim}{\rho}$ represents the K-by-K correlation

matrix for the signals from a single station. The symbol $\underset{\sim}{0}$ represents a K-by-K zero matrix, indicating interstation correlation is negligible. The rationale and justification for these assumptions is contained in Chapter I.

III. AMBIGUITY RESOLUTION

Phase differencing systems such as Omega necessarily are ambiguous. The size of the unambiguous lanes (the lanes formed by indistinguishable LOP from a station pair) is determined by the choice of frequencies. A discussion of how the frequencies determine the lane size is contained in Chapter I.

The Radux navigation system [9] which immediately preceded the Omega system had a 200 Hz modulation of its carrier frequency, 40 kHz. This allowed for nominally 400 nmi unambiguous lanes which were considered to be adequate for navigation. It was the short baselines, due to the short propagation ranges, which caused Radux to be abandoned and not its ambiguities. The short baselines caused the divergence of the LOP off the baseline to occur very rapidly as distances from the baseline increased, thus reducing the accuracy of the system. When Omega was in the design stage, dead reckoning (DR) systems and the reliability of receivers were improving markedly. This influenced the final design of Omega to concentrate on one or two frequencies which would be used for navigation. Many Omega navigators presently use only the 10.2 kHz Omega signal. Also, the Defense Mapping Agency only publishes propagation prediction correction factors for the 10.2 kHz and 13.6 kHz Omega signals. As shown in Chapter I, the three navigation signals presently radiated by the Omega stations yield nominally 72 nmi unambiguous lanes at the baseline.

This has been adequate for all systems using Omega to date. The SAR applications such as GRAN, which prompted this study, however, require an ambiguity resolution technique in order to be successful. Since the retransmitter at the SAR incident will in general have no prior knowledge of position which can be relayed to the SAR forces, the assumption must be made that complete position estimation must be accomplished from the retransmitted Omega data. There are presently five methods which are seriously being investigated as potential ways to solve the ambiguity problem. They are: 1) addition of frequencies to the Omega format, 2) pulse time-of-arrival measurement, 3) ratio of signal-to-noise ratios, i.e., signal-to-signal ratios, 4) multiple LOP examination, and 5) modulation of one of the Omega signals with a large period tone. The fifth technique has been stated by the Omega Project Office in Naval Electronic Systems Command as being unacceptable to the host countries for the Omega stations and will not be considered here in detail. The United States Air Force, however, is funding an experiment which Cincinnati Electronics Corporation and NELC of San Diego are to carry out by 1975 which will modulate one of the signals from the experimental Omega station in Forestport, New York with a 226 2/3 Hz tone. Since the Omega Project Office has stated that a final implementation using modulation on an Omega signal is not feasible, the experiment appears to be academic.

As discussed in Chapter I, the choice of frequencies determines the size of the unambiguous lanes. It is reasonable then to expect that different or additional frequency signals for Omega could yield larger unambiguous lanes. It is very likely, however, that the three present frequencies must remain and that, for political reasons, at most only one more frequency common to all stations can be added to the Omega format. This statement is made because of the many existing receivers designed for the three existing Omega frequencies and the great demand for the remaining Omega format slots for other applications. Chapter V of this dissertation is dedicated to the study of the performance of four-frequency Omega for several easily implemented fourth frequencies. One additional frequency is not expected to be able to completely solve the ambiguity problem; however, it can place much less demand on other ambiguity resolution techniques by expanding the unambiguous lane size.

Reference [21] discusses the use of the relative times-of-arrival of the Omega pulses from station pairs at a receiver to determine a lane of LOP which contains the receiver. One of the conclusions of [21] is that the existing three-frequency Omega, 72 nmi, baseline ambiguity cannot be resolved in high noise areas with .95 confidence with less than on the order of one hour of data. The pulse time-of-arrival technique is, however, expected to be able to resolve nominal 360 nmi baseline lanes with three minutes of Omega data.

These lanes result from four-frequency Omega utilizing 10.88 kHz in addition to the existing Omega tones. This resolution is expected even for worst case noise.

Reference [22] reports on an experiment which examined the potential Omega lane size which could be resolved using the relative powers of the signals received from a station pair. The OPLE ground station in Dallas, Texas was utilized in measuring satellite relayed Omega data retransmitted by a bread-boarded SARCOM from various locations on the globe. It was assumed that the noise averaged to a constant over the essentially concurrent measurement interval for signals from two stations. The ground station was used to estimate the SNR from the two stations and with the above assumption about the noise, the ratio of the SNR's from the stations for a given frequency is a signal power ratio. The conclusion of [22] was that signal-to-signal power ratios are feasible for use in ambiguity resolution, but the limited experiment performed did not allow for a conclusion about the lane size which could be resolved. The SNR for the experiment was measured at the ground station by a non-optimal technique and it is possible that the maximum likelihood estimate of SNR derived in Appendix B of this dissertation could be used to advantage if this technique is applied in a final system.

Reference [23] reports on simulations which were carried out for three-frequency multiple station Omega utilizing multiple LOP intersections to resolve ambiguity. All the

polygons formed by LOP from stations treated pairwise are examined for an area of radius 250 nmi on the globe and the one which maximizes a likelihood function is selected as being the most likely position estimate. The likelihood function is formed by assuming additive Gaussian phase uncertainties affecting the phase differences which correspond to the LOP estimates of the receiver location when the Omega stations are treated pairwise. The conclusion drawn from the simulations is that the multiple LOP method of ambiguity resolution does have promise in terms of resolving the Omega ambiguities if multiple position estimates along with their associated relative probabilities are taken as a solution set.

Additional information concerning the simulations reported upon in [23] is contained in [24, 25]. It can be found from these references that the standard deviations used for the additive Gaussian phase uncertainties for the simulations was 0.003291 rad for three stations and 0.010408 rad for the remainder. This corresponds to LOP estimate standard deviations on the order of 0.0047 to 0.0142. These values are said to be derived from a 10 db-Hz SNR expected from three stations and 0 db-Hz SNR from the remaining stations. It was found by experiment and is discussed in a later chapter of this thesis that standard deviations of the LOP estimate on the order of 0.1 to 0.2 baseline nmi are experienced with daylight paths and SNR in excess of 10 db-Hz for a station

pair using the optimum estimator. The equation

$$\sigma_{\phi} = \sigma_{x}(2\pi/360) \tag{8}$$

allows these standard deviations to be converted to standard deviation of phase difference since 2π radians of phase difference corresponds to one unambiguous lane on the baseline (nominally 360 nmi for the four frequencies which were used in the experiment). Therefore, standard deviations of phase difference uncertainties which were experienced in the experiment were, for best conditions, on the order of 0.00^2 to 0.004 radians. When unambiguous lane size is increased by the addition of a fourth frequency as was the case for the experiment, the same number of polygons as were considered in [23] occur in a larger area on the globe. If this area is expanded sufficiently both by addition of frequencies and consideration of more polygons, the multiple LOP method of ambiguity resolution may be a viable technique for SAR systems.

The pulse time-of-arrival technique and the multiple LOP technique appear to have the most promise as ambiguity resolution techniques which can be implemented. The multiple LOP is an alternative, although nonoptimal, technique for treating the multiple station problem to be discussed in Chapter VII. The conservation of computer time which it allows would be a reason for adopting it as a method over the optimum estimator. An estimation procedure using the multiple LOP technique would be to obtain the two-station

LOP estimates optimally and determine the set of most likely position estimates from a multiple LOP approach as described in [23]. Use of pulse time-of-arrival information with this approach will be very helpful in reducing the area on the globe over which LOP intersections must be examined.

IV. TWO-STATION LOP ESTIMATION

A. TWO-STATION ESTIMATION FOR K FREQUENCIES

In order to establish an estimation problem which will yield an unambiguous estimate of LOP for two stations and K frequencies, we assume that an ambiguity resolution technique has resolved the lane ambiguity. Thus, the estimation is performed within one unambiguous lane. Within the presupposed unambiguous lane we can only estimate a LOP for any station pair. Therefore, referring to the mathematical model of Chapter II, an essentially equivalent problem is to fix L in (6a) and vary x in (6a) and (6_b) over a range of values necessary to traverse all candidate LOP in the unambiguous lane given for the two stations being considered. Figure 6 illustrates the geometry of the problem. This method is convenient for the following reasons. First, only one parameter, x, need be varied in the estimation procedure; and second, for a fixed step size in an iterative solution, the total range over which x is varied (one unambiguous baseline lane width) is the same for any receiver position. A reasonable value to assign to L is the sum of the great circle distances from the two stations to the center of the presupposed area. If x_t is defined as the great circle distance from the reference station, henceforth referred to as station one, to the center of the presupposed area, the range of values over which x must be varied is $x_t \pm$ one-half the unambiguous

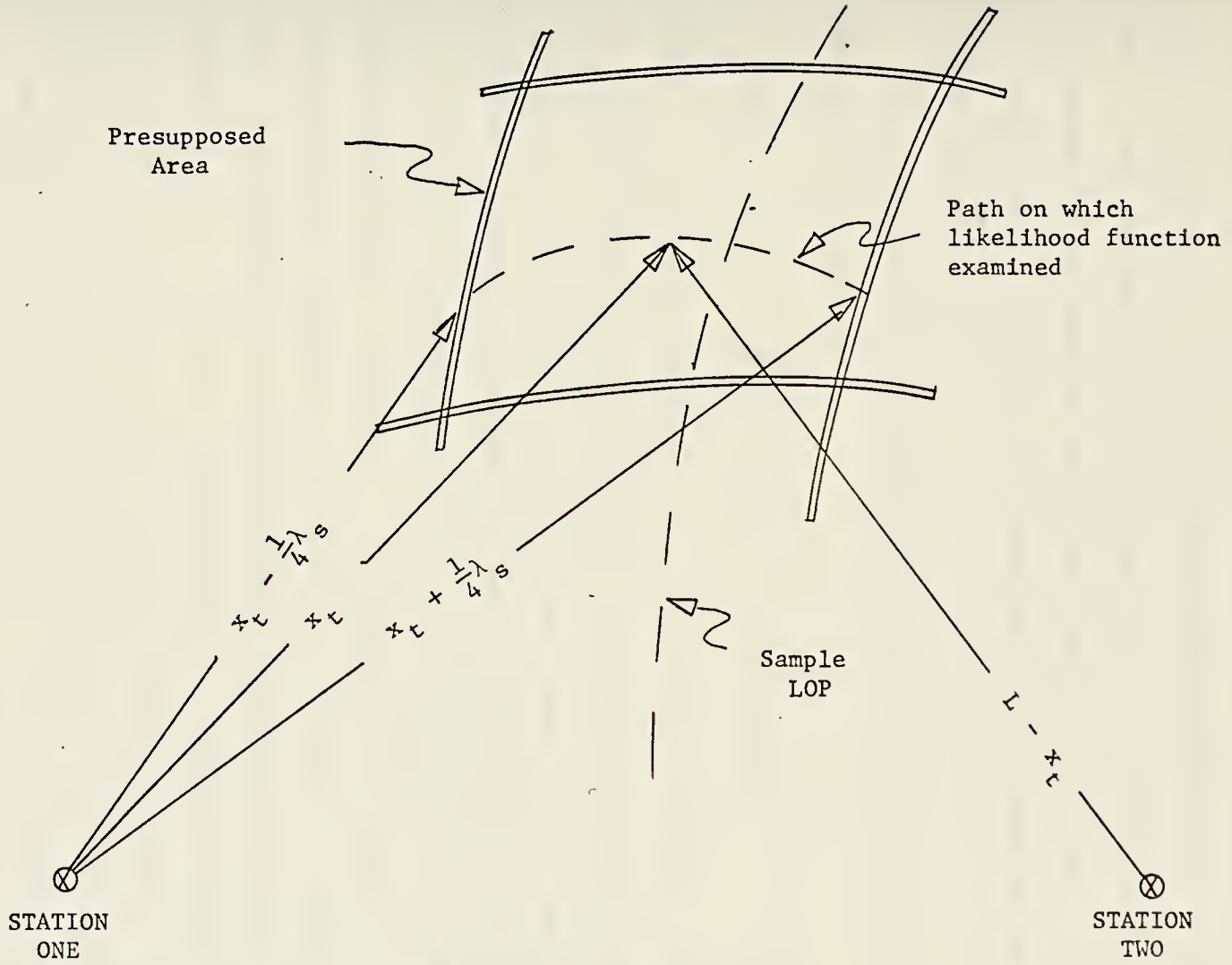

Figure 6. Geometry for the Estimation Problem.

lane size. The fact that this range of values for x actually traverses an unambiguous lane is easily seen if one assumes two artificial stations separated by a baseline distance L. Estimation of x on the artificial baseline formed is equivalent to estimating x off the baseline in the real problem if the manner of estimation explained above is followed. Thus, the range of x which must be examined is one baseline unambiguous lane width.

To estimate x in the problem posed, we form the likelihood function [26] as

$$\Lambda(x) = f(Y/x) = \int\int f(Y/V,\theta,x)f(V)f(\theta)dVd\theta \qquad (9)$$

where V is the 2K-dimensional phase velocity column vector, θ is the K dimensional random phase vector and $f(V)$ and $f(\theta)$ are the joint probability density functions of the components of V and θ which are assumed mutually independent. $f(Y/x)$ is the joint probability density of the components of the vector Y conditioned upon knowing x. Since our only interest in the likelihood function is to find the values of x which yield its maxima, we can equivalently maximize any monotonic function of it. Factors multiplying the likelihood function but not containing x, v_i or θ_i will be dropped without redefining the likelihood function throughout the dissertation.

Ambiguity resolution information can be conveniently incorporated in the maximum likelihood estimator in the following way. Consider the ambiguity resolution information as a priori information about x in the form of a probability

density f(x). Equation (9) when multiplied by f(x) is proportional to the a posteriori density of x. The maximum a posteriori (MAP) estimate of x is then that x which maximizes this equation and is the optimum estimate of x for the problem [26]. When f(x) is a uniform density function, as would be the case if exactly one unambiguous lane were given by an ambiguity resolution technique with no information about where in the lane the correct LOP might be, the MAP estimator is equivalent to the maximum likelihood estimator.

It can be shown [26] that for the density function of N(t) assumed for the mathematical model in Chapter II,

$$f(Y/V,\theta,x) \propto \prod_{i=1}^{2K} \exp\left[(2/N_i)\int_0^T y_i(t)s_i(t,x)dt\right] \qquad (10)$$

where T is the total data collection period. Substituting (4) in (10) and using the trigonometric identity for the cosine of the sum of angles, (10) can be written as

$$f(Y/V,\theta,x) \propto \prod_{i=1}^{2K} \exp\left\{(2A_i/N_i)[C_i \cos(\phi_i-\theta_i) + S_i \sin(\phi_i-\theta_i)]\right\} \qquad (11)$$

In (11) C_i and S_i are defined as

$$C_i = \sum_{j=1}^{M} \int_{10(j-1)}^{10(j-1)+T_i} y_i(t) \cos[(\omega_i+\Delta_i)t]dt \qquad (12a)$$

and

$$S_i = \sum_{j=1}^{M} \int_{10(j-1)}^{10(j-1)+T_1} y_i(t) \sin[(\omega_i+\Delta_i)t]dt \qquad (12b)$$

where M is the number of T_i sec. duration pulses contained in the data collection period.

The quantities A_i, N_i and Δ_i $(1\leq i\leq 2K)$ must be estimated from the collected data. The estimation equations for these quantities are derived in Appendix A and Appendix B. From this point in the two-station estimation derivation it will be assumed that the values of A_i and N_i have been estimated from the data and the estimates are available. The values of Δ_i will be assumed to have been estimated and the data corrected for doppler shift utilizing this information. Following these assumptions, we define

$$R_i^2 = (C_i^2 + S_i^2)(2A_i/N_i)^2 \qquad 1\leq i\leq 2K \qquad (13a)$$

and

$$\mu_i = \tan^{-1}(S_i/C_i) \qquad 1\leq i\leq 2K. \qquad (13b)$$

The likelihood function (9) may then be written by substitution of (13) into (11) into (9) as

$$\Lambda(x) = E_V \int f(\theta)\exp\left\{ \sum_{i=1}^{K} [R_i\cos(\phi_i-\mu_i)+R_{i+K}\cos(\phi_{i+K}-\mu_{i+K})]\cos\theta_i + \sum_{i=1}^{K} [R_i\sin(\phi_i-\mu_i)+R_{i+K}\sin(\phi_{i+K}-\mu_{i+K})]\sin\theta_i \right\} d\theta \qquad (14)$$

where $E_V(\cdot)$ denotes expectation with respect to V.

Since the θ_i were argued to be independent, uniformly distributed random variables on the interval $(-\pi, \pi]$ in Chapter II, we may use the relationship

$$(2\pi)^{-1} \int_{-\pi}^{\pi} \exp[A \cos \theta + B \sin \theta] d\theta = I_o[(A^2+B^2)^{1/2}], \quad (15)$$

some algebra and some trigonometric identities to write the likelihood function as

$$\Lambda(x) = E_V \prod_{i=1}^{K} I_o\{[R_i^2 + R_{K+i}^2 + 2R_i R_{K+i} \cos \psi_i]^{1/2}\} \quad (16)$$

where

$$\psi_i = \text{principal value}^1 \text{ of } [\mu_{K+i} - \mu_i - \phi_{K+i} + \phi_i]. \quad (17)$$

In (15) and (16) $I_o(\cdot)$ is the zero order modified Bessel function of the first kind. At this point, no approximations have been made and the assumed random nature of the effective phase velocities has not been utilized. Therefore, if the phase velocity column vector V is assumed to have deterministic components as was first thought to adequately model the problem, the maximum likelihood estimation equation for known phase velocities can be obtained. This estimation equation is derived in Appendix C. As was discussed in Chapter I, the phase velocities are not well enough known

---

[1] The value of θ which lies in the interval $-\pi < \theta \leq \pi$ is called the principal value of θ.

to use this model, so we continue with the derivation of the estimator assuming Gaussian phase velocities.

A few minutes of data collection is expected to be adequate to insure high SNR in one Hz even for worst case noise [2]. The arguments of the I_o function associated with the ith frequency are on the order of the sum of the SNR in one Hz of the signals received from the two stations at the ith frequency. This allows the replacement of the I_o functions in (16) by their large argument approximation [27],

$$I_o(z) \simeq (2\pi z)^{-1/2} \exp(z). \qquad (18)$$

Using (18), the likelihood function (16) may then be written as

$$\Lambda(x) = E_V \frac{\exp\{\sum_{i=1}^{K} [R_i^2 + R_{K+i}^2 + 2R_i R_{K+i} \cos \psi_i]^{1/2}\}}{\prod_{i=1}^{K} [R_i^2 + R_{K+i}^2 + 2R_i R_{K+i} \cos \psi_i]^{1/4}} \cdot (19)$$

The numerator of (19) is a rapidly varying function of x, sharply peaked at all the local maxima of the function. The denominator is a more slowly varying function and for regions near a local maximum can be considered to be nearly constant. The denominator will have different values from peak to peak of the likelihood function, but the magnitude of the change from peak to peak will be quite small compared to the change in the magnitude of the numerator for the same peaks. For

the peaks in the vicinity of the global maximum which we are seeking to find, the denominator in (19) can be considered to have relatively little effect on the likelihood function and will be ignored, yielding

$$\Lambda(x) = E_V \exp\{ \sum_{i=1}^{K} [R_i^2 + R_{K+i}^2 + 2R_i R_{K+i} \cos \psi_i]^{1/2} \}. \quad (20)$$

It is convenient to write

$$v_i(x) = \bar{v}_i(x) + p_i \quad (21)$$

where $\bar{v}_i(x)$ is the expected value and p_i some random perturbation of the ith phase velocity. The expected value of the phase velocities are all very near c [10], so we can approximate (6a) and (6b) by

$$\phi_i \simeq \omega_i \int_o^x \frac{d\gamma}{\bar{v}_i(\gamma)[1+\varepsilon_i]} - 2\pi m_i \qquad 1 \leq i \leq K \quad (22a)$$

$$\phi_{K+i} \simeq \omega_i \int_x^L \frac{d\gamma}{\bar{v}_{K+i}(L-\gamma)[1+\varepsilon_{K+i}]} - 2\pi m_{K+i} \qquad 1 \leq i \leq K \quad (22b)$$

where

$$\varepsilon_i = p_i/c \simeq p_i/\bar{v}_i(x). \quad (23)$$

The random variables ε_i, $1 \leq i \leq 2K$ will be taken as jointly Gaussian with zero means and as components of the 2K dimensional vector ε. This follows directly from the assumption of the components of V being jointly Gaussian and the

definition of ε. The covariance matrix of ε will be

$$K_\varepsilon \simeq \frac{1}{c^2} K_v \tag{24}$$

where K_v is the covariance matrix of the 2K dimensional vector V. Utilizing this result and the approximation $\frac{1}{1+\eta} \approx 1 - \eta$ for $|\eta| << 1$, we can now write

$$\phi_i \simeq \bar{\phi}_i - \frac{\omega_i x}{c} \varepsilon_i - 2\pi m_i \qquad 1 \leq i \leq K \tag{25a}$$

and

$$\phi_{K+i} \simeq \bar{\phi}_{K+i} - \frac{\omega_i (L-x)}{c} \varepsilon_{K+i} - 2\pi m_{K+i} \qquad 1 \leq i \leq K \tag{25b}$$

where

$$\bar{\phi}_i = \omega_i \int_o^x \frac{d\gamma}{\bar{v}_i(\gamma)} \qquad 1 \leq i \leq K \tag{26a}$$

and

$$\bar{\phi}_{K+i} = \omega_i \int_x^L \frac{d\gamma}{\bar{v}_{K+i}(L-\gamma)} \qquad 1 \leq i \leq K. \tag{26b}$$

Recalling the definition of ψ_i from (17), for high SNR ψ_i will be small near the local maxima of the likelihood function and we write

$$\cos \psi_i \simeq 1 - \frac{\psi_i^2}{2} . \tag{27}$$

This allows the likelihood function to be written as

$$\Lambda(x) = E_{\varepsilon} \exp \{ \sum_{i=1}^{K} (R_i + R_{K+i})[1 - \frac{R_i R_{K+i} \psi_i^2}{(R_i+R_{K+i})^2}]^{1/2} \}. \quad (28)$$

Again, using the fact that ψ_i and thus ψ_i^2 is small in the vicinity of the local maxima of the likelihood function and the approximation

$$(1 - \eta)^{1/2} \simeq 1 - \eta/2, \quad (29)$$

an equivalent likelihood function can be written as

$$\Lambda(x) = E_{\varepsilon} \exp [\sum_{i=1}^{K} Q_i \psi_i^2] \quad (30)$$

where

$$Q_i = - \frac{R_i R_{K+i}}{2(R_i+R_{K+i})} . \quad (31)$$

Using vector notation, the likelihood function can be written as

$$\Lambda(x) = E_{\varepsilon} \exp [\varepsilon^T A \varepsilon + B^T \varepsilon + D]. \quad (32)$$

The 2K-by-2K matrix A is defined by jth row and nth column entries

$$a_{jn} = \frac{\omega_j^2 x^2 Q_j}{c^2} \qquad 1 \leq j = n \leq K \quad (33a)$$

$$a_{jn} = \frac{\omega_{j-K}^2 x^2 Q_{j-K}}{c^2} \qquad K+1 \leq j = n \leq 2K \quad (33b)$$

$$a_{jn} = \frac{-\omega_j^2 x(L-x)Q_j}{c^2} \qquad 1 \leq j = |(n \pm K)| \leq 2K \qquad (33c)$$

$$a_{jn} = 0 \qquad \text{elsewhere.} \qquad (33d)$$

The 2K-dimensional column vector B is defined by ith entry

$$b_i = -\frac{2}{c} Q_i W_i \omega_i x \qquad 1 \leq i \leq K \qquad (34a)$$

$$b_i = \frac{2}{c} Q_{i-K} W_{i-K} \omega_{i-K} (L-x) \qquad K+1 \leq i \leq 2K \qquad (34b)$$

where

$$W_i = \text{principal value of } [\mu_{i+K} - \mu_i - \bar{\phi}_{i+K} + \bar{\phi}_i]. \qquad (35)$$

The scalar D is defined as

$$D = \sum_{i=1}^{K} Q_i W_i^2. \qquad (36)$$

The expected value in (32) under the conditions given is shown in Appendix D to yield

$$\Lambda(x) = \frac{\exp[D + (1/2) B^T K_\varepsilon (I - 2AK_\varepsilon)^{-1} B]}{|I - 2AK_\varepsilon|^{1/2}} \qquad (37)$$

where I is the 2K by 2K identity matrix and $|\cdot|$ denotes the determinant of a matrix. The value of x which maximizes the likelihood equation can be determined by allowing x in

(37) to range over the necessary values as shown in Figure 6. Other less likely LOP can be determined and a measure of the probability of their being correct can be found by dividing the value of Λ for the less likely LOP by the value of Λ for the most likely LOP. If the LOP being estimated is considered to be a random variable, uniformly distributed across one unambiguous lane, this ratio is a ratio of the a posteriori probability densities of the two LOP.

Figure 7 is a drawing of the envelope of a typical likelihood function as it varies with x. Within the "envelope" the function will be a more rapidly varying function of x. The number of local maxima in an unambiguous lane, determined by the values and number of Omega frequencies, will in general be many more than shown. The value of x_t, the distance from the first station to the center of some presupposed area, serves only as a means to establish the fixed value of L to use in the estimation. In Figure 7, x_{ml}, the value of x which yields the maximum value of Λ cannot be used as a valid measure of the distance of the receiver from the reference station, but serves only to identify the resulting LOP estimate.

B. TWO-STATION ESTIMATION FOR FOUR FREQUENCIES

The general estimation equation for K frequencies received from two stations is given by (37). This equation can be applied to the four-frequency case with the size of the matrices A and K_ε being 8-by-8 and the column vector B

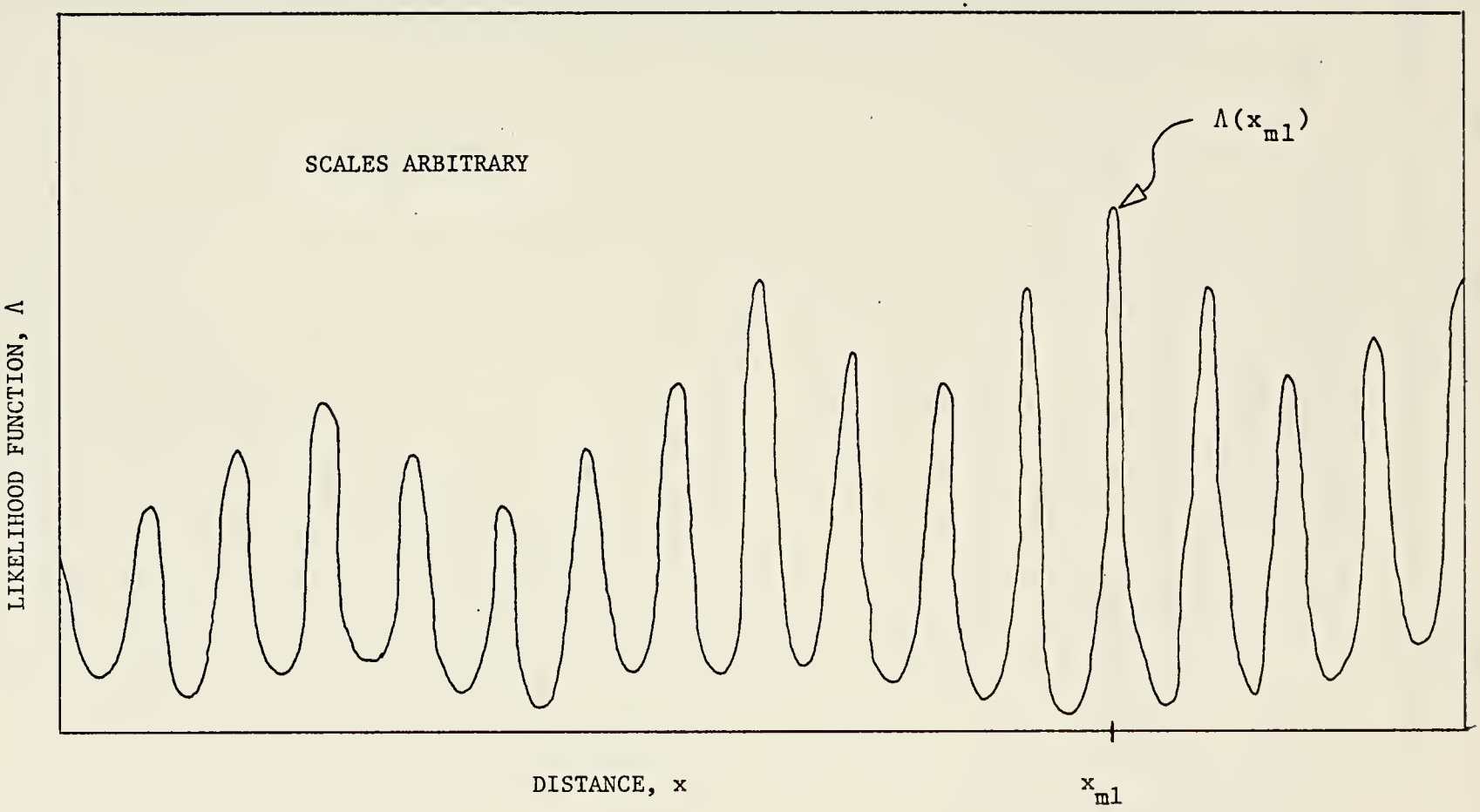

Figure 7. A Typical Likelihood Function.

being 8 dimensional. For the four-frequency, two-station problem then, the likelihood function is given by

$$\Lambda(x) = \frac{\exp[D+(1/2)B^T K_\varepsilon (I-2AK_\varepsilon)^{-1} B]}{|I - 2AK_\varepsilon|^{1/2}} \qquad (38)$$

where K_ε is the 8-by-8 covariance matrix of the normalized effective phase velocity vector ε. The 8-by-8 matrix A is given by

$$A = \frac{1}{c^2}\begin{bmatrix}
\omega_1^2 Q_1 x^2 & 0 & 0 & 0 & -\omega_1^2 Q_1 x(L-x) & 0 & 0 & 0 \\
0 & \omega_2^2 Q_2 x^2 & 0 & 0 & 0 & -\omega_2^2 Q_2 x(L-x) & 0 & 0 \\
0 & 0 & \omega_3^2 Q_3 x^2 & 0 & 0 & 0 & -\omega_2^2 Q_2 x(L-x) & 0 \\
0 & 0 & 0 & \omega_4^2 Q_4 x^2 & 0 & 0 & 0 & -\omega_4^2 Q_4 x(L-x) \\
-\omega_1^2 Q_1 x(L-x) & 0 & 0 & 0 & \omega_1^2 Q_1 (L-x)^2 & 0 & 0 & 0 \\
0 & -\omega_2^2 Q^2 x(L-x) & 0 & 0 & 0 & \omega_2^2 Q_2 (L-x)^2 & 0 & 0 \\
0 & 0 & -\omega_3^2 Q_3 x(L-x) & 0 & 0 & 0 & \omega_3^2 Q_3 (L-x)^2 & 0 \\
0 & 0 & 0 & -\omega_4^2 Q_4 x(L-x) & 0 & 0 & 0 & \omega_4^2 Q_4 (L-x)^2
\end{bmatrix} \tag{39}$$

where Q_i, $1 \leq i \leq 4$, is given by (31). The column vector B in (38) is given by

$$B = \frac{2}{c} \begin{bmatrix} -Q_1 W_1 \omega_1 x \\ -Q_2 W_2 \omega_2 x \\ -Q_3 W_3 \omega_3 x \\ -Q_4 W_4 \omega_4 x \\ Q_1 W_1 \omega_1 (L-x) \\ Q_2 W_2 \omega_2 (L-x) \\ Q_3 W_3 \omega_3 (L-x) \\ Q_4 W_4 \omega_4 (L-x) \end{bmatrix} \tag{40}$$

where W_i, $1 \leq i \leq 4$, is given by (35). The scalar D is given by

$$D = \sum_{i=1}^{4} Q_i W_i^2 \ . \tag{41}$$

C. ESTIMATION ERROR TYPES

The cyclic nature of the likelihood function yields LOP estimates which fall into three categories:

1. Estimates which fall within nominally 1 or 2 nmi or less of the correct LOP,
2. Estimates which are nominally one half wavelength of the fundamental four frequencies from the correct LOP, referred to as "minor lane" errors and
3. Estimates which are farther from the correct LOP than the previous two types, which we refer to as "major lane" errors.

The latter two types of estimates are considered as erroneous estimates for the purposes of this thesis. An important consideration to note is that the probability of making a position error when using data from several stations will very likely be less than the probability of making a lane error in the two station case for the following reasons. The transmissions of at least three Omega stations will be available (this number being required for a position fix) and it is very likely that one or more additional stations will be usable given the great distances of VLF propagation and the planned worldwide location of eight transmitters in the Omega system. This redundancy will reduce the probability of large position estimation errors. The multiple station problem is considered in Chapter VII.

V. FOUR-FREQUENCY SIMULATION

In the interest of achieving unambiguous lane widths which can be identified by an ambiguity resolution technique, additional frequencies may be added to the Omega format. Assuming that the present three Omega frequencies are retained, adequate widening for ambiguity resolution by time-of-arrival techniques [21] is expected to be achieved by addition of a fourth frequency. A fifth frequency and/or frequency modulation of one of the signals by a signal with wavelength on the order of several thousand miles would yield better estimator performance and perhaps inherent ambiguity resolution as well. This chapter considers the performance of the four-frequency Omega maximum likelihood estimator for several candidate fourth frequencies which can be added to the Omega format with minimum modification.

A. FREQUENCY CHOICE

The criteria used in selection of the fourth frequencies were:

1. Retention of the present three Omega frequencies (10.2 kHz, 11 1/3 kHz, and 13.6 kHz),
2. Separation of the fourth frequency from any of the existing three Omega frequencies or other known existing or planned VLF transmissions by at least 250 kHz to avoid interference in present receivers,

3. A resultant unambiguous lane size greater than the present three frequency baseline size of nominally 72 nmi and
4. Selection of a fourth frequency which can be generated using the present Omega signal format generator frequency of 816 kHz.

In addition to these criteria, preliminary four-frequency simulations were carried out for SNR which are to be expected for reasonably long transmission paths and assuming that exact phase velocity predictions were available. These simulations, discussed in Appendix C, indicate that four-frequency unambiguous lane widths must be restricted to about 1000 nmi or less for estimation performance "acceptable" for SAR application. The frequencies which met the four criteria above, the integer divisor of the fundamental station frequency (816 kHz) and the resultant nominal baseline unambiguous lane width are presented in Table III. Figure 8 shows the Omega frequency spectrum with the present three frequencies and the potential fourth frequencies.

B. SIMULATION DATA AND PROCESSOR

Monte Carlo simulation of the four-frequency Omega problem was carried out utilizing the maximum likelihood estimator given by (37) in Chapter IV with $K = 4$. The parameters which were varied were the choice of fourth frequency, the SNR in one Hz and the uncertainties of the phase velocities. It is shown in Appendix A that C_i and S_i, when conditioned

TABLE III

CANDIDATE FOURTH FREQUENCIES

Frequency (f_4)	Divisor (n_4)	Nominal Unambig. Lane ($1/2\ \lambda_s$)
10.4615 kHz	78	928 nmi
10.8800 kHz	75	357 nmi
11.6571 kHz	70	500 nmi

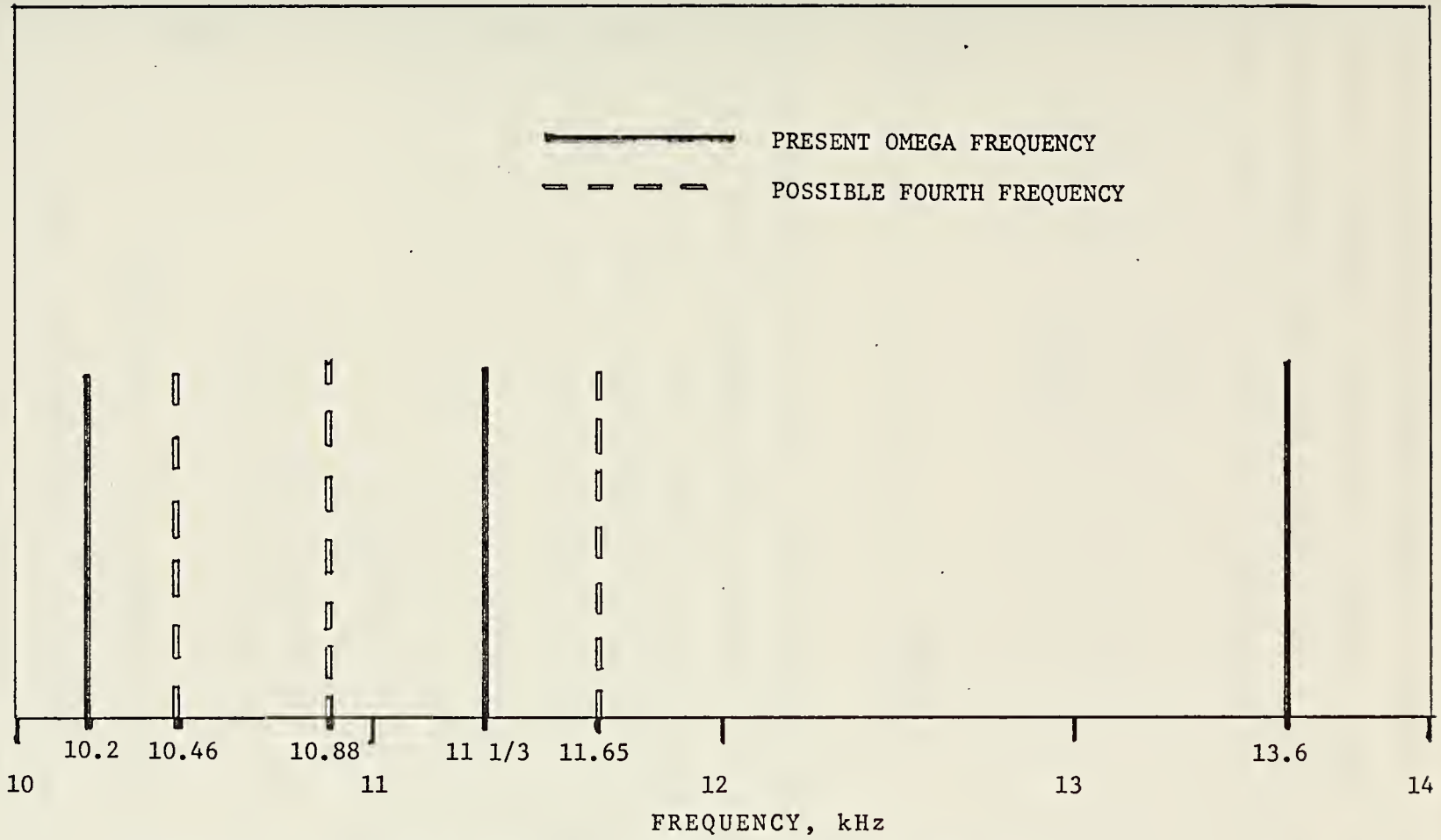

Figure 8. Frequency Spectrum of Four Frequency Omega

upon knowing ϕ_i and θ_i and also under the assumption that N(t) is a vector whose components are sample functions of a white, Gaussian process, are Gaussian random variables. The conditional means and variances of C_i and S_i when doppler shift is assumed to be negligible are given by

$$E[C_i|\phi_i,\theta_i] = \frac{A_i MT_i}{2} \cos(-\phi_i + \theta_i) , \tag{42a}$$

$$E[S_i|\phi_i,\theta_i] = \frac{A_i MT_i}{2} \sin(-\phi_i + \theta_i) , \tag{42b}$$

and

$$VAR[C_i|\phi_i,\theta_i] = VAR[S_i|\phi_i, \theta_i] = \frac{N_i MT_i}{4} . \tag{42c}$$

For the simulation, Δ_i and θ_i were assumed equal to zero and A_i and N_i were determined from the SNR in one Hz, assumed the same for all i. The product MT_i was assumed equal to 18 for all i, this choice being influenced by the GRAN anticipated 180 second data retransmission time, equivalent to 18 nominally one second pulses of Omega data for each frequency from each station. With these assumptions, the means and variances of C_i and S_i conditioned upon ϕ_i and θ_i become

$$E[C_i|\phi_i, \theta_i] = 9A_i \cos\phi_i , \tag{43a}$$

$$E[S_i|\phi_i, \theta_i] = 9A_1 \sin\phi_i , \tag{43b}$$

and

$$VAR[C_i|\phi_i, \theta_i] = VAR[S_i|\phi_i, \theta_i] = \frac{9N_i}{2} . \tag{43c}$$

The eight phase velocities used to generate the data were generated by a correlated Gaussian random number generating

computer program using the mean vector with all components equal to c and the covariance matrix

$$K_v = c^2\sigma^2 \begin{bmatrix} \rho & \underset{\sim}{o} \\ \underset{\sim}{o} & \rho \end{bmatrix} . \qquad (44)$$

In (44) ρ is a symmetric 4 by 4 correlation matrix referring to the interfrequency correlation of transmissions from each station and $\underset{\sim}{o}$ represents a 4 by 4 zero matrix indicating uncorrelated interstation phase velocities. In (44) σ^2 is the variance of all ε_i (equal to the variance of v_i/c) which is varied as a parameter in the simulation. The correlation matrix was chosen to reflect uncorrelated interstation transmissions because in the general case very low correlation is expected [19]. The inter-frequency correlation matrix ρ was formed by assuming the correlation of 10.2 kHz and 13.6 kHz frequencies from one station to be .7, which seems to be a reasonably good choice [16, 18, and 19] and linear interpolation using the equation

$$\rho_{ij} = 1 - \frac{.3}{3400} \left| (f_i - f_j) \right| \qquad (45)$$

where ρ_{ij} is the ith row, jth column entry in the matrix ρ and f_i is the ith frequency. These assumptions resulted in the symmetric matrix

$$\rho = \begin{bmatrix} 1.00 & .90 & .70 & \rho_{14} \\ .90 & 1.00 & .80 & \rho_{24} \\ .70 & .80 & 1.00 & \rho_{34} \\ \rho_{41} & \rho_{42} & \rho_{43} & 1.00 \end{bmatrix} \quad (46)$$

where the first three rows/columns of the matrix correspond to the frequencies 10.2 kHz, 11 1/3 kHz, and 13.6 kHz respectively. The values used for $\rho_{i4} = \rho_{4i}$, $i = 1, 2, 3$ were chosen from Table IV depending upon the fourth frequency being used.

The values for L and x used in the creation of the simulation data were 8000 nmi and 3000 nmi respectively. In the final Omega system implementation, these values should be typical of values to be expected. With all the above assumptions, the simulation data was generated by computer using random number generating programs for the random variable sample values.

The processing of the data with the four-frequency maximum likelihood estimator, was accomplished using c as the mean value for all phase velocities and the covariance matrix

$$K_\varepsilon = \frac{1}{c^2} K_V \quad (47)$$

where K_V is given by (44) and the value of the parameter σ^2. Using c for the mean value of phase velocity for processing is equivalent to having a reasonably good predicted mean value of phase velocity since the data were created using this mean value.

TABLE IV

FOURTH FREQUENCY CORRELATION COEFFICIENTS

Frequency (f_4)	i	ρ_{i4}
10.4615 kHz	1	.98
	2	.92
	3	.72
10.8800 kHz	1	.94
	2	.96
	3	.76
11.6571 kHz	1	.87
	2	.97
	3	.83

Figures 9, 10, and 11 illustrate the results of the simulation for each of the three choices of fourth frequency. Each point plotted consists of a number of "runs" which correspond to a three minute data collection period. The fraction of the total number of runs for each point which yielded lane errors (either major or minor, as defined in Chapter IV) are plotted as a function of SNR in one Hz and σ, the standard deviation of the phase velocities. Table V gives the number of runs which were utilized in the generation of each point and a breakdown of the number of the lane errors which were major and minor.

The number of runs which were used in generating the points in Figures 9, 10, and 11 are quite small for simulation, particularly considering the small number of resultant lane errors. The reason for this is the computer time which is required, 15 to 40 seconds on the IBM 360 per run depending on the lane size. However, the reasonably consistent increase in lane errors with increasing lane width and phase velocity standard deviation influences the decision that the general results are valid.

The results of this simulation prompt the conclusion that with adequate knowledge of the phase velocity variance and correlation and with reasonable signal-to-noise ratios, the unambiguous lane size can be increased beyond the present nominal 72 nmi obtained with three frequency Omega. The controlling factors in the selection of a fourth frequency for Omega to be used for SAR purposes are (1) the capability

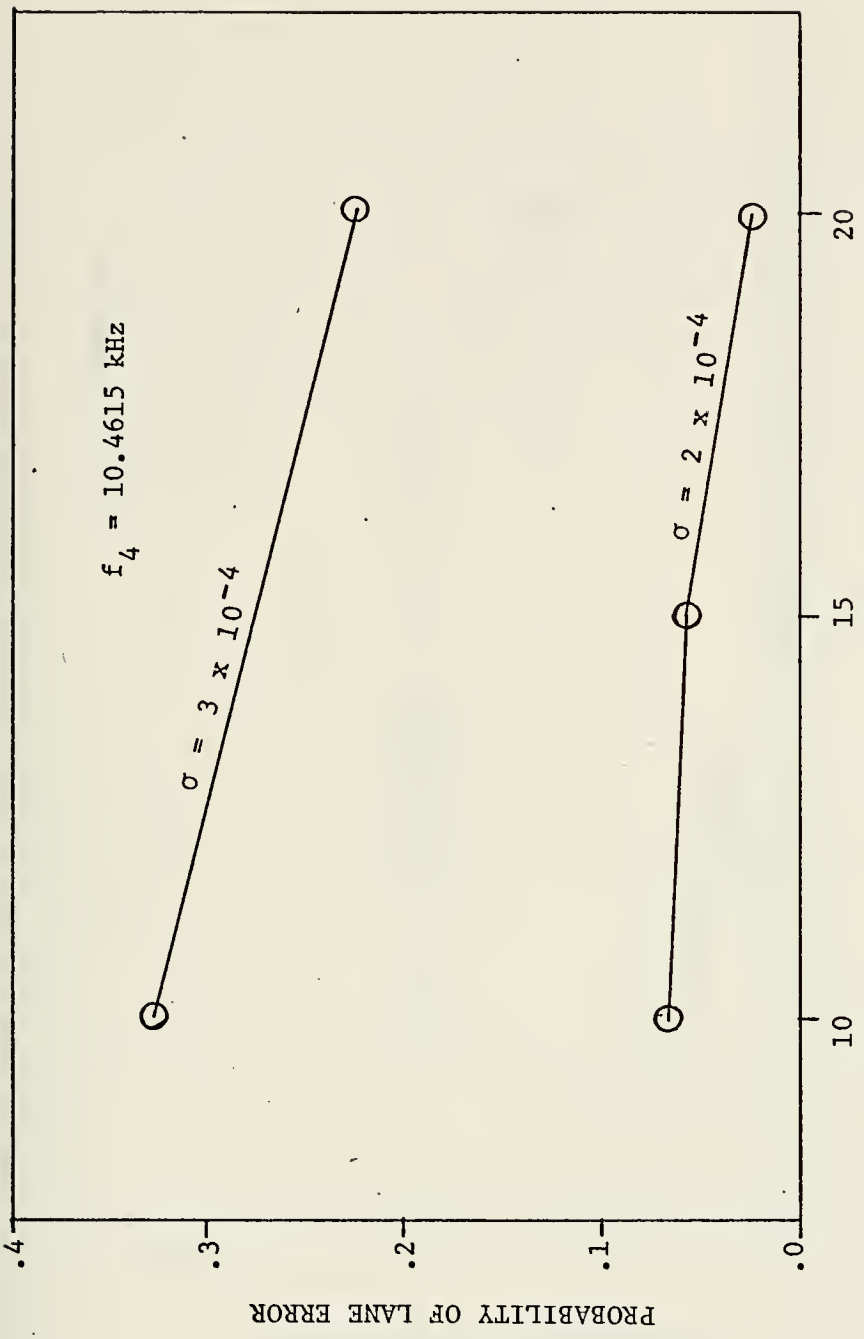

Figure 9. Probability of Lane Error for f_4 = 10.4615 kHz.

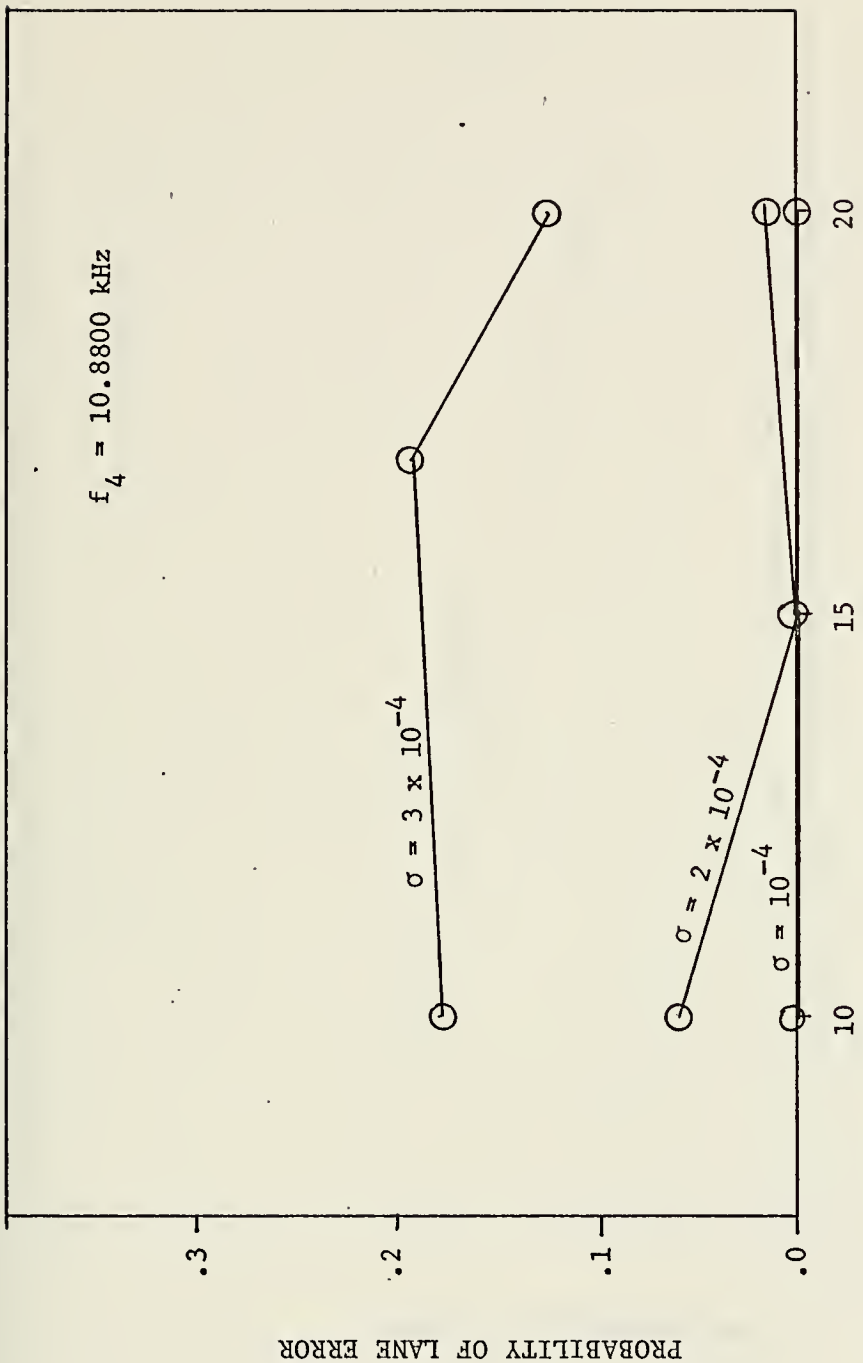

Figure 10. Probability of Lane Error for f_4 = 10.8800 kHz.

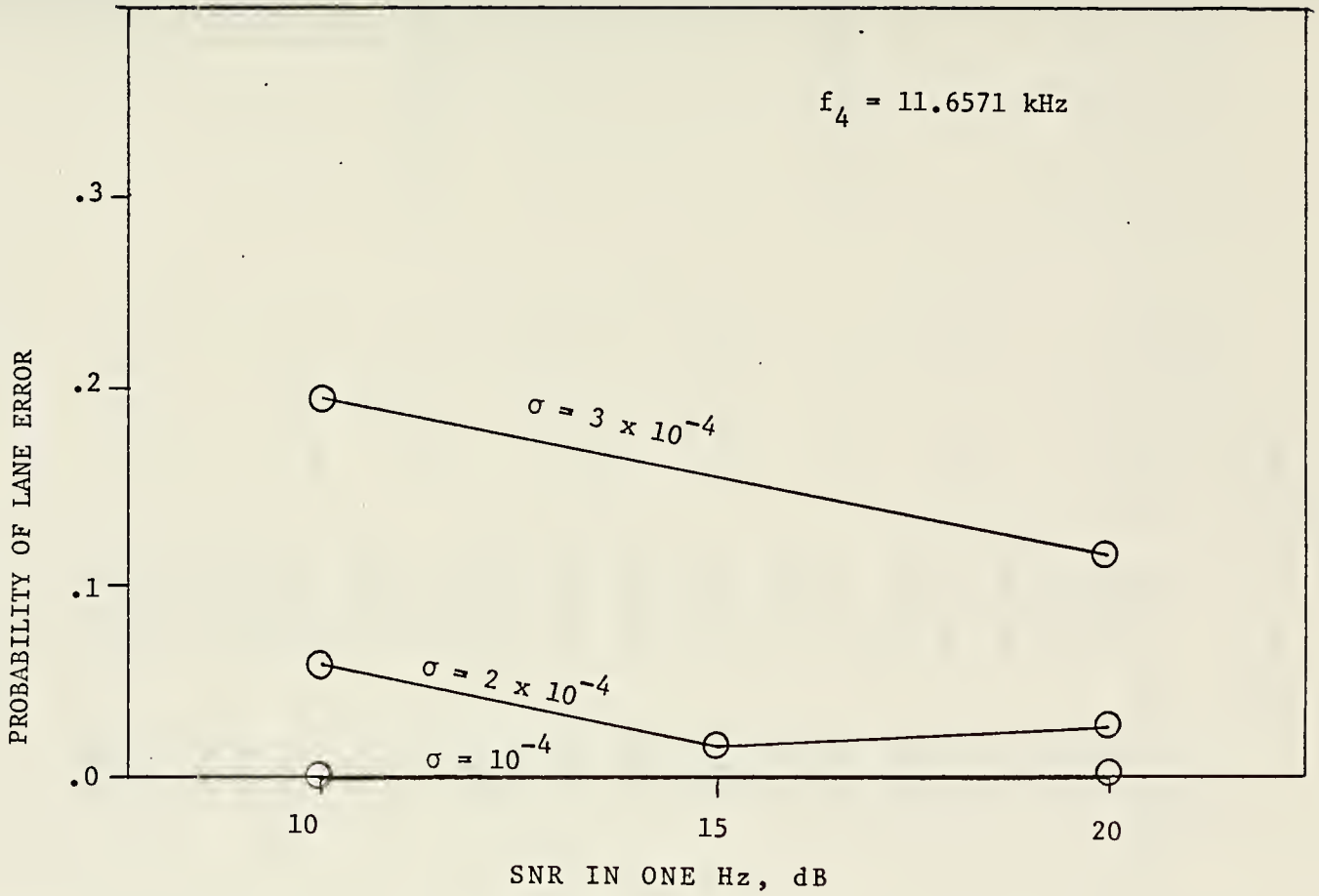

Figure 11. Probability of Lane Error for f_4 = 11.6571 kHz.

TABLE V

SIMULATION RESULTS

Frequency (f_4)	Std. Dev.(σ)	SNR	No. Runs	Lane Errors (major)	Lane Errors (minor)
10.4615 kHz	2×10^{-4}	10 dB	100	7	0
	"	15 dB	100	4	2
	"	20 dB	190	3	2
	3×10^{-4}	10 dB	100	17	16
	"	20 dB	100	6	17
10.8800 kHz	1×10^{-4}	10 dB	100	0	0
	"	20 dB	100	0	0
	2×10^{-4}	10 dB	100	0	6
	"	15 dB	100	0	0
	"	20 dB	200	0	3
	3×10^{-4}	10 dB	100	0	18
	"	17 dB	100	0	20
	"	20 dB	200	0	26
11.6571 kHz	1×10^{-4}	10 dB	100	0	0
	"	20 dB	100	0	0
	2×10^{-4}	10 dB	100	1	5
	"	15 dB	100	1	1
	"	20 dB	200	0	6
	3×10^{-4}	10 dB	100	3	17
	"	20 dB	100	2	10

of ambiguity resolution techniques to resolve the lane ambiguity with restricted amounts of Omega data and (2) the accuracy with which the phase velocities of the Omega frequencies can be predicted.

One of the results of the Monte Carlo simulation as shown by Figures 9, 10, and 11 is that as unambiguous lane size is increased, the probability of lane error increases. However, the estimator provides several estimates along with their relative probabilities of being correct. Thus, even when a lane error occurs, the second or third most likely estimate is nearly always correct. This fact, in conjunction with the reduced probability of position error expected when redundant information from additional stations is available, makes a .1 or .2 probability of lane error more acceptable as a trade-off for the larger unambiguous lane size.

VI. A FOUR-FREQUENCY OMEGA EXPERIMENT

All of the ambiguity resolution techniques discussed in Chapter III, which appear practical to implement, require an unambiguous lane width in excess of the nominal 72 nmi which the present three Omega frequencies yield. The performance which can be expected from a maximum likelihood estimator if used with four-frequency Omega for several easily implemented fourth frequencies was presented in Chapter V. Naval Air Test Center, Patuxent River, Maryland conducted a four-frequency experiment utilizing one of these frequencies (10.88 kHz) in the fall of 1973. The maximum likelihood estimator derived in Chapter IV was utilized to process this data, the results of which are reported in this chapter.

A. DATA COLLECTION

The four-frequency Omega data was collected by Texas Instruments Corporation at Dallas, Texas [29]. The receiver location was 1197.53 nmi from the Forestport, New York experimental Omega station and 2349.62 nmi from the Trinidad Omega station. The data was collected over the two five-day periods 17-21 October 1973 and 14-18 November 1973. Data was taken for three-minute intervals four times per hour beginning on the hour and half hour and seven minutes past the hour and half hour for the entire periods. Each of these three-minute collection periods, herein referred to as "runs," consisted

of 18 nominally one-second pulses of signal for each frequency from each station. On the last day of the first data collection period, the Forestport station reduced transmitted power to very low levels. This portion of the data is not included in the estimation results as it is considered not to be representative of actual conditions to be expected.

The receiver used for the data collection was the Omega Position Locating Equipment (OPLE) ground station modified to receive four frequencies [29]. A block diagram of the receiving equipment is shown in Figure 12.

B. MAXIMUM LIKELIHOOD ESTIMATION

The maximum likelihood estimator for high SNR Omega was derived in Chapter IV. Quite high SNR were experienced as shown in Appendix B. As described in Chapter II, the effective phase velocities are modeled as being jointly Gaussian. The eight element column vector V is defined as the effective phase velocity vector

$$V^T = [v_1, v_2, \ldots v_8] . \qquad (48)$$

The first four elements of V correspond to the four signals at frequencies 10.2 kHz, 11 1/3 kHz, 13.6 kHz, and 10.88 kHz, in that order, from Forestport. The last four elements of V correspond to the same frequency signals from Trinidad. The mean values of the Gaussian vector V which were used in the estimation were those provided by Professor J. A. Pierce of Harvard in [16] and in private correspondence. These values

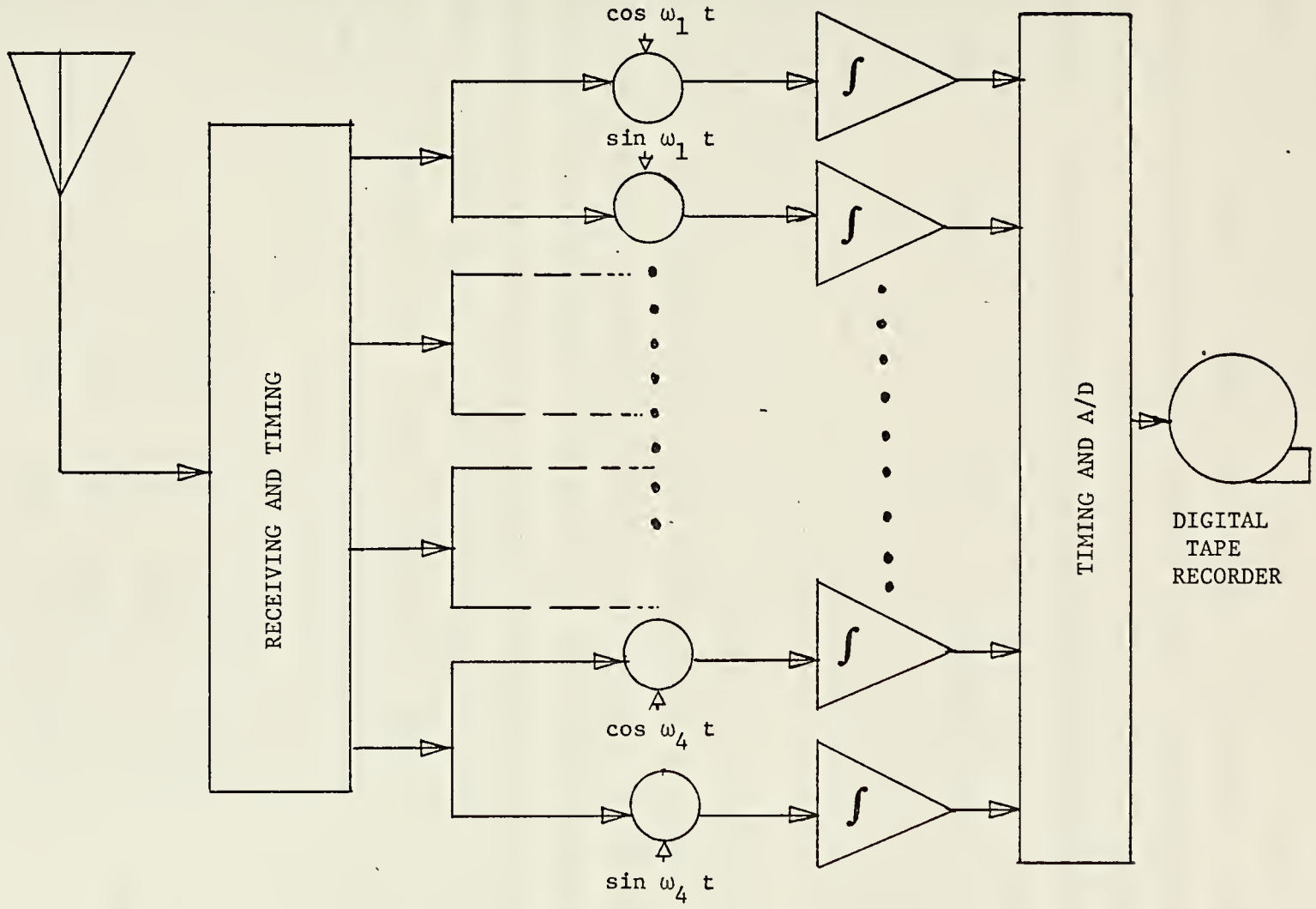

Figure 12. Data Collection Receiver.

are given as ratios of the phase velocity and the velocity of light in vacuum (v/c) in Table II. Because of the significant diurnal effects of phase velocity, different values for v/c are required for day (all lighted transmission path) and night (all dark transmission path). For transition periods, when a path was not all lighted or all dark, weighted averages of the day and night path phase velocity values from Table II based upon the fraction of the path which was light was used. In general, this would not be justified, but since the values of phase velocity for day and night are so close and because of the phase velocity uncertainties, it is considered acceptable to use this technique.

Since the phase velocities are considered to be jointly Gaussian, a covariance matrix must be specified in order to do the estimation. The inter-station correlation of phase velocities was considered to be zero and the inter-frequency correlation was determined by assuming the phase velocities of the 13.6 kHz signal and the 10.2 kHz signal to have a 0.7 correlation coefficient. These assumptions, taken from [16, 18, and 19], allow the matrix ρ to be determined as in Chapter V, Equation (46)

$$\rho = \begin{bmatrix} 1.00 & .90 & .70 & .94 \\ .90 & 1.00 & .80 & .96 \\ .70 & .80 & 1.00 & .76 \\ .94 & .96 & .76 & 1.00 \end{bmatrix} . \quad (49)$$

The matrix ρ is used, as in Chapter V, to form

$$K_v = c^2 \sigma^2 \begin{bmatrix} \rho & \underset{\sim}{o} \\ \underset{\sim}{o} & \rho \end{bmatrix} \qquad (50)$$

where c is the speed of light in vacuum, σ is the standard deviation of v/c which was assumed to be the same for all frequencies, and $\underset{\sim}{o}$ is the 4-by-4 zero matrix. The final parameter which must be specified for the estimation procedure is σ. As discussed throughout this thesis, the value of v/c is expected to be predictable to a few parts in 10^{-4}. Values of σ from 10^{-4} to 5×10^{-4} were used in the estimation presented here. It is expected that future analysis of Omega data for these frequencies with the idea of considering predicted phase velocities will yield better values for ρ and σ. It is not unlikely that different standard deviations of predicted phase velocities will result for different frequencies. If this does occur, K_v in (50) can easily be modified.

With the assumptions delineated above, the estimation can be performed. As discussed in Chapter IV, the estimation procedure consists of assuming a priori knowledge of an unambiguous, nominally 360 nmi, lane which contains the correct receiver LOP. This information must be provided by an ambiguity resolution technique in a final system implementation. Then, the sum of the great circle distances from the two stations to some point in the region of the receiver

is fixed equal to L. Since two stations can yield only an LOP, this sum of distances can be quite approximate, as will be the case, since this sum must actually be obtained from a coarse ambiguity resolution technique. Finally, x is defined as the distance from a reference station (Forestport was chosen for this processing) to a potential receiver site. Evaluation of the likelihood function as x is varied over the known unambiguous lane provides a function which has its maximum value for that x which is the maximum likelihood estimate. This estimate of x (x_{ml}) is equivalent to estimation of an LOP as can be seen from Figure 6. The path over which the evaluation is done is shown by the dashed line, a convenient path for the following reasons. First, only one parameter, x, need be varied in the estimation procedure; and second, for a fixed step size in the evaluation, the total range over which x is varied (one unambiguous baseline lane width) is the same for any receiver position. This method of estimation necessarily yields all of the local maxima of the likelihood function. Thus a selected number of estimates of x which are less likely to be the correct estimate than x_{ml} can easily be retained. As discussed in Chapter IV, the ratio of the likelihood function evaluated at these alternate candidate values of x divided by the likelihood function evaluated at x_{ml} is a measure of the relative probability of the respective values of x being correct.

Figure 13 shows a block diagram of the estimation procedure. The collected Omega data is provided to a processor,

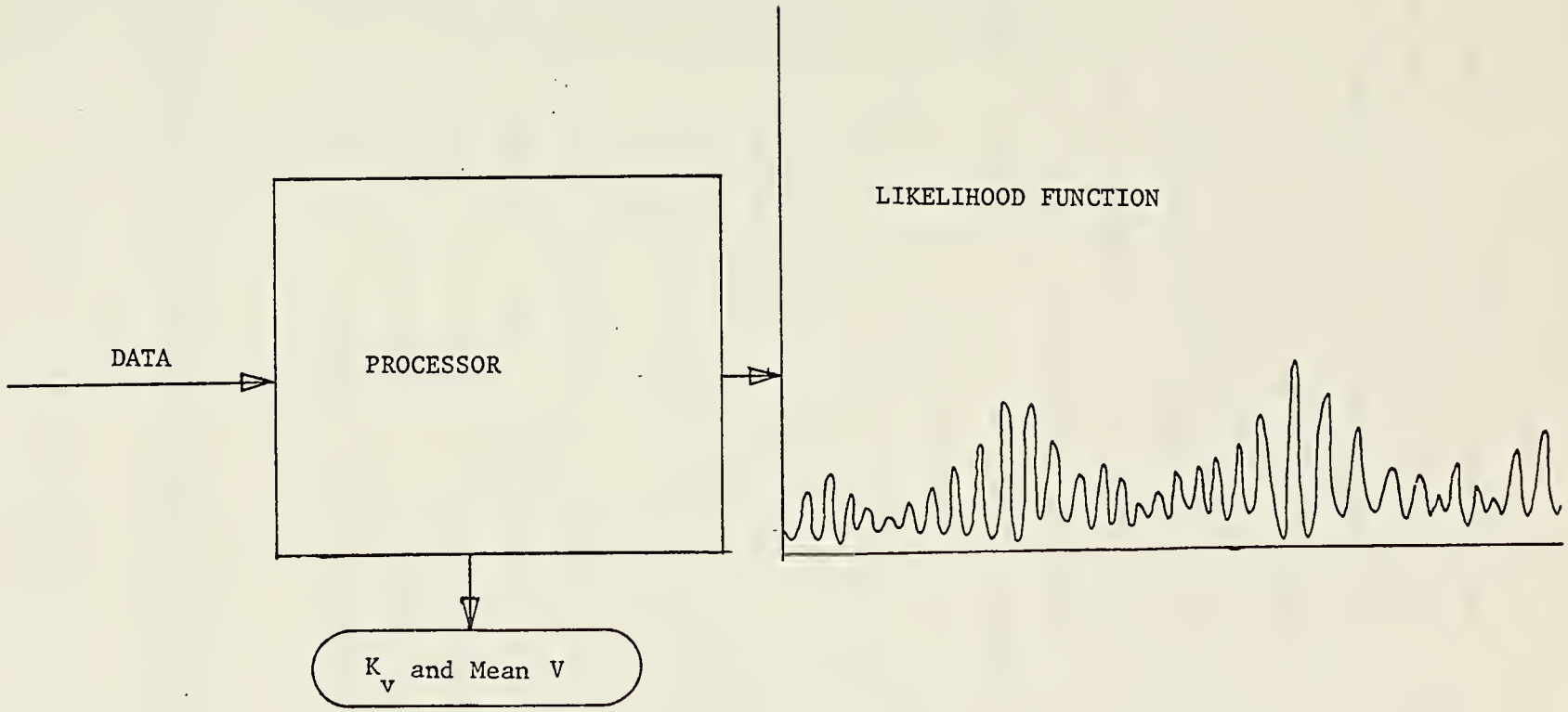

Figure 13. Block Diagram of the Estimation Process.

described in detail in Chapter IV, which evaluates a likelihood function over a prescribed range of values for x. Parameters which are provided to the processor are the mean values and covariance matrix for the phase velocities.

The IBM 360-67 at the Naval Postgraduate School was utilized for the processing of the Omega four-frequency data. A Fortran program (Appendix E), requiring 34K BYTES of core, was used to iteratively evaluate the likelihood function for x at 0.5 nmi increments from x = 855 nmi to x = 1540 nmi. The one nmi regions centered at the values of x which yielded the three[2] largest values for the likelihood function were then iteratively searched with 0.05 nmi increments to obtain a fine estimate. The values of the likelihood function for the second and third most likely values of x were then divided by the value of the likelihood function for x_{ml}, yielding a probability ratio discussed earlier. The time required to process one run (a data set corresponding to three minutes of collected data) was on the order of 15 seconds of computer time. The range of x for which the processing was done was nearly twice the nominal 360 nmi which would have been required had an ambiguity resolution technique provided the unambiguous lane over which x was to be

---

[2]Any number of values may be retained, however, three were found to be adequate to always contain the correct distance.

varied. This was considered the only fair way to process the data since the correct value of x (1197.53 nmi) was known a priori and was considered as the center of the unambiguous lane. In a finally implemented system, the a priori knowledge of x will consist of some probability density of x, across one or more unambiguous lane widths.

C. ESTIMATION USING PREDICTED FIRST MODE PHASE VELOCITIES

As an intermediate step, the optimum estimator must estimate the amplitudes, noise density heights and doppler frequencies of all eight signals. Appendices A and B give the derivation of these estimators. The doppler shift of the signals, which would result from physical motion or frequency drifts in the receiver, were found to be negligible since there was no SARCOM and thus no motion and were assumed to be zero for this experiment. In a finally implemented system, doppler effects must be estimated and removed. The signal amplitudes and noise density heights which were estimated as an integral part of the processing were used to form the signal power-to-noise density ratios in dB-Hz. The results of this estimation are presented in Appendix B.

The results of the LOP estimation utilizing the optimum estimator are presented in Table VI. The mean values of phase velocity shown in Table II, and the values for K_v given by (49) and (50) were used in the processing. Several values of σ, the standard deviation of the phase velocity to velocity of light (v/c) ratios, were used, but only $\sigma = 2 \times 10^{-4}$, $\sigma =$

TABLE VI

LOP ESTIMATION RESULTS
(Using TABLE II Phase Velocity Values)

Period		σ(x 10^{-4})	Total Runs	Minor Lane Errors	LOP Estimation Error mean (BL nmi)	Std dev (BL nmi)
1	D	2	144	0	.26	.13
1	N	2	137	36	-.12	.19
1	T	2	69	10	.12	.36
1	D	3	144	0	.25	.13
1	N	3	137	37	-.12	.19
1	T	3	69	10	.12	.36
1	D	4	144	0	.15	.14
1	N	4	137	48	-.10	.22
1	T	4	69	14	.10	.36
2	D	2	179	0	.46	.14
2	N	2	203	80	.23	.26
2	T	2	92	11	.32	.39
2	D	3	179	0	.45	.13
2	N	3	203	77	.21	.26
2	T	3	92	11	.33	.40
2	D	4	179	0	.40	.18
2	N	4	203	71	.31	.44
2	T	4	92	10	.30	.42

BL nmi = Baseline nmi

Spreading factor for Dallas receiver site = 1.88

3×10^{-4}, and $\sigma = 4 \times 10^{-4}$ are shown. The results of using other values of σ were significantly worse than for those shown. The minor lane errors which are referred to in Table VI are defined as runs for which one of the peaks of the likelihood function adjacent to the correct peak is the largest value of the function. This results in an LOP estimation error which is nominally 6-7 nmi from the correct LOP on the baseline. Major lane errors would be defined as lane errors greater than a minor lane error. However, in this experiment using the values of σ stated above, major lane errors did not occur. In Table VI, the column labeled "period" contains the numbers 1 or 2 and the letters D, N, or T. These refer to data collection periods 1 or 2 and Day, Night, or Transition condition paths, respectively.

The means and standard deviations of the LOP estimation error are in baseline measure. The hyperbolas which are formed by the isophase lines from a station pair in a phase comparison system diverge off the baseline (great circle passing through the two stations). The divergence occurs directly as csc $(\theta/2)$, the "spreading factor," where θ is the angle formed by the two great circles passing through the receiver location and the stations as discussed in Chapter I. Therefore, phase differences at points off the baseline correspond to greater distances than on the baseline. The spreading factor for the Dallas receiver location for this experiment was 1.88, thus the distances in Table VI must be multiplied by 1.88 to obtain the true measure for Dallas. The practice

of using baseline measure was selected so that the results can be more readily applied to the general case where a spreading factor of from 1 to perhaps 2 might result.

The values of σ which yielded the fewest errors were different for the two data collection periods. The value of $\sigma = 2 \times 10^{-4}$ resulted in the fewest minor lane errors for the first period and $\sigma = 4 \times 10^{-4}$ resulted in the fewest for the second period. Increasing the value of σ is equivalent to desensitizing the estimator to the mean values of phase velocity being used. It would thus appear that for the data obtained in the second period, the mean values or predicted values of phase velocity which were used were not as close to the actual phase velocities which were encountered.

It is believed, however, that the data was significantly disturbed by higher order modes of propagation for the night path from the Forestport station. Therefore, use of the first mode phase velocity values given in Table II would not be expected to yield error-free estimation results for night paths. This conclusion was reached after the following considerations. The mean values of the phase differences, $\Delta\phi$, for all four frequencies, f, for all lighted (day) transmission paths were utilized to estimate v/c from the data by using

$$(v/c)_i = \frac{f_i\ (L-2x)}{c(n_i + \Delta\phi_i/2\pi)} \qquad 1 \leq i \leq 4 \qquad (51)$$

to obtain Figure 14.[3] In (51) L is the (known) sum of the distances from the stations to the receiver, x is the (known) distance from the reference station to the receiver, c is the velocity of light in vacuum, and n_i is an integer equal to the number of whole cycles of phase difference at the receiver. Equation (51) assumes that the phase velocities for the same frequency signals were the same for both paths under day conditions. This is considered to be reasonable since the paths were both predominantly westerly and first mode propagation during day conditions apparently dominated. This latter assumption seems to be borne out by the fact that no day condition lane errors were experienced. The apparent parallel shift of the curves in Figure 14 from the predicted first mode values could be explained by timing errors between the two stations. Several 0.25 μs and 0.5 μs corrections in timing were inserted by Forestport during the data collection periods. This parallel shift in phase velocities will not cause lane errors to result, but will be seen as an estimation error or a bias in the estimation error mean value for this experiment.

The results of Figure 14 can now be used to obtain phase velocity values for dark paths (night) for all four frequencies from each station separately to determine if the phase

---

[3]The predicted phase velocity values shown in Figures 14, 15, 16, and 17 are taken from [11, 12, and 16] and private communication with Professor J. A. Pierce of Harvard University. The lines drawn between the plotted points serve only as aids for identification of points and should not be construed as portions of continuous curves.

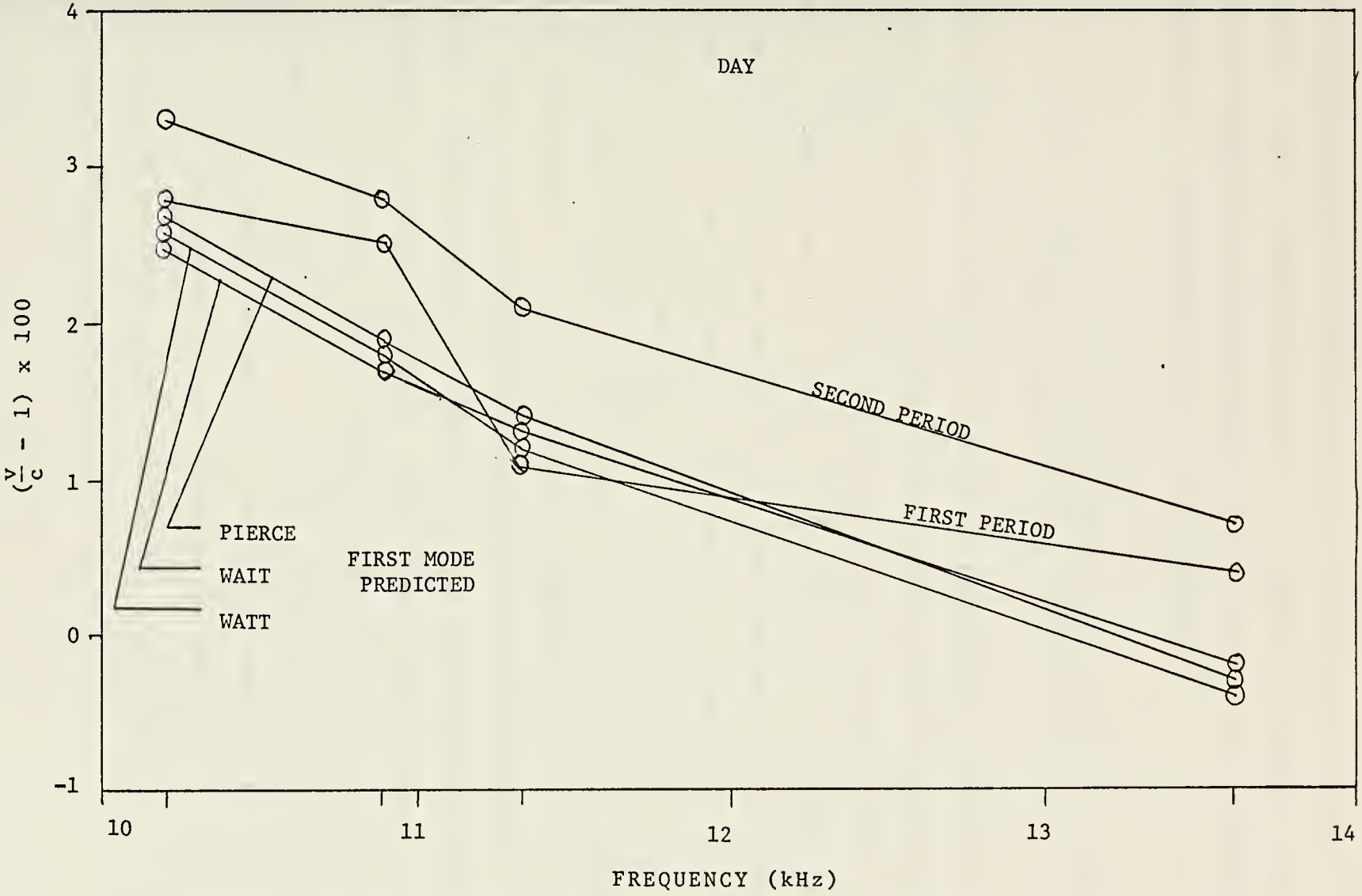

Figure 14. Day Path Phase Velocities, Considered Invariant with Station.

velocities from one station appear to be causing the lane errors. This was done by using the change in the mean values of the phase differences from day to night for each frequency from each station separately in the equation

$$(v/c)_{i,N} = \frac{2\pi f_i d\ (v/c)_{i,D}}{c(\phi_{i,N} - \phi_{i,D})(v/c)_{i,D} + 2\pi f_i d} \qquad 1 \leq i \leq 4 \ . \qquad (52)$$

In (52) d is the distance from the station under consideration to the receiver, $(v/c)_{i,D}$ are values taken from Figure 14, and $(\phi_{i,N} - \phi_{i,D})$ is the difference of the mean values of the night phase and the day phase for the ith frequency, treating the stations separately. The results of the night phase velocities obtained in this way are presented in Figures 15 and 16 for the first and second data collection periods respectively.[3] The phase velocities from the Forestport station are, by this analysis, apparently the cause of the lane errors which were experienced for the night conditions. The relatively parallel shift of the Trinidad phase velocities from the predicted first mode values indicates that the Trinidad data is probably dominated by first mode propagation. However, the erratic shifting of the Forestport phase velocity values from the first mode predictions indicates very probably that higher order propagation mode interference was experienced during the night conditions for both data collection periods.

---

[3] Ibid.

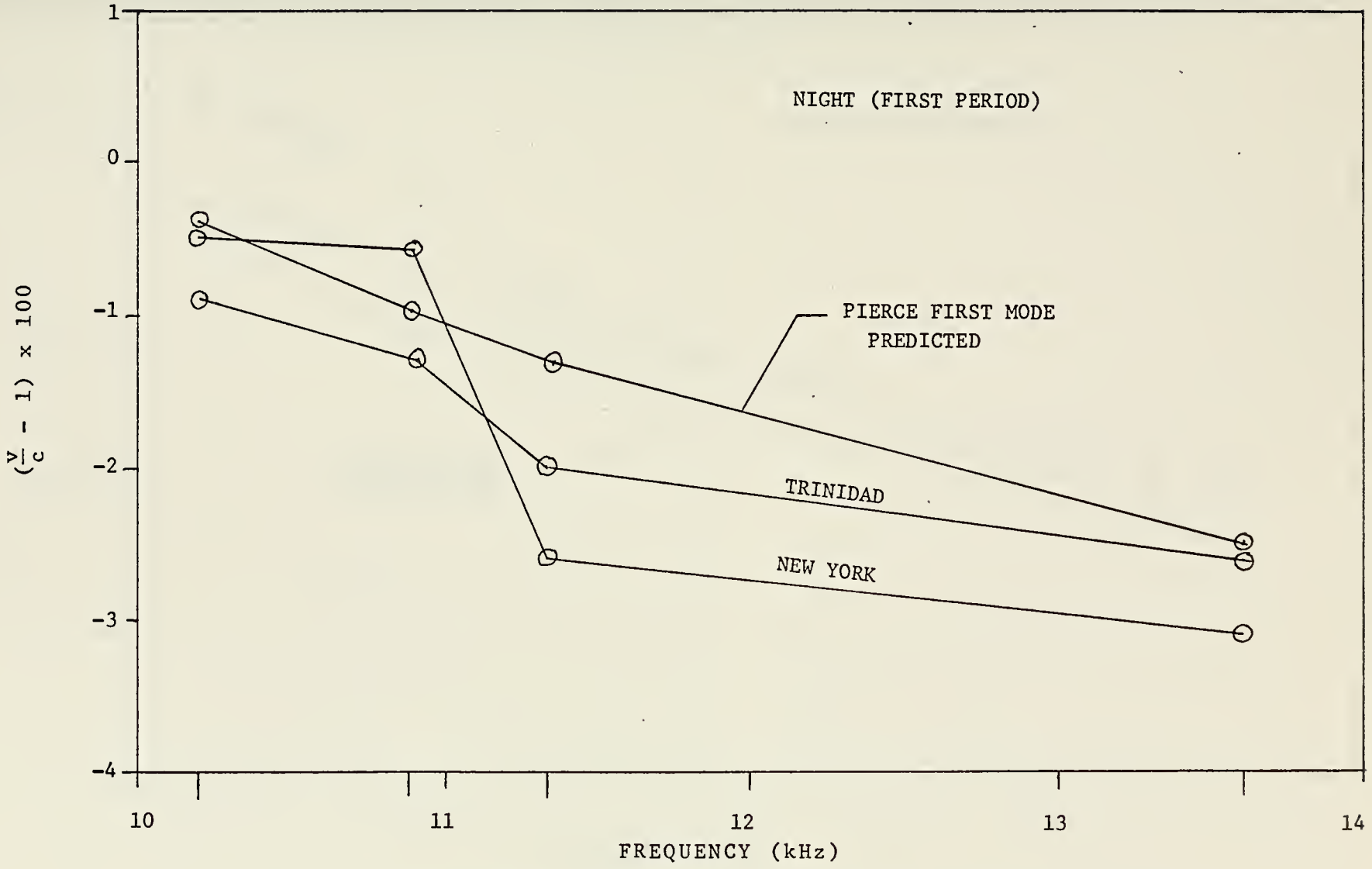

Figure 15. First Data Period, Night Path, Phase Velocities (Stations Separately).

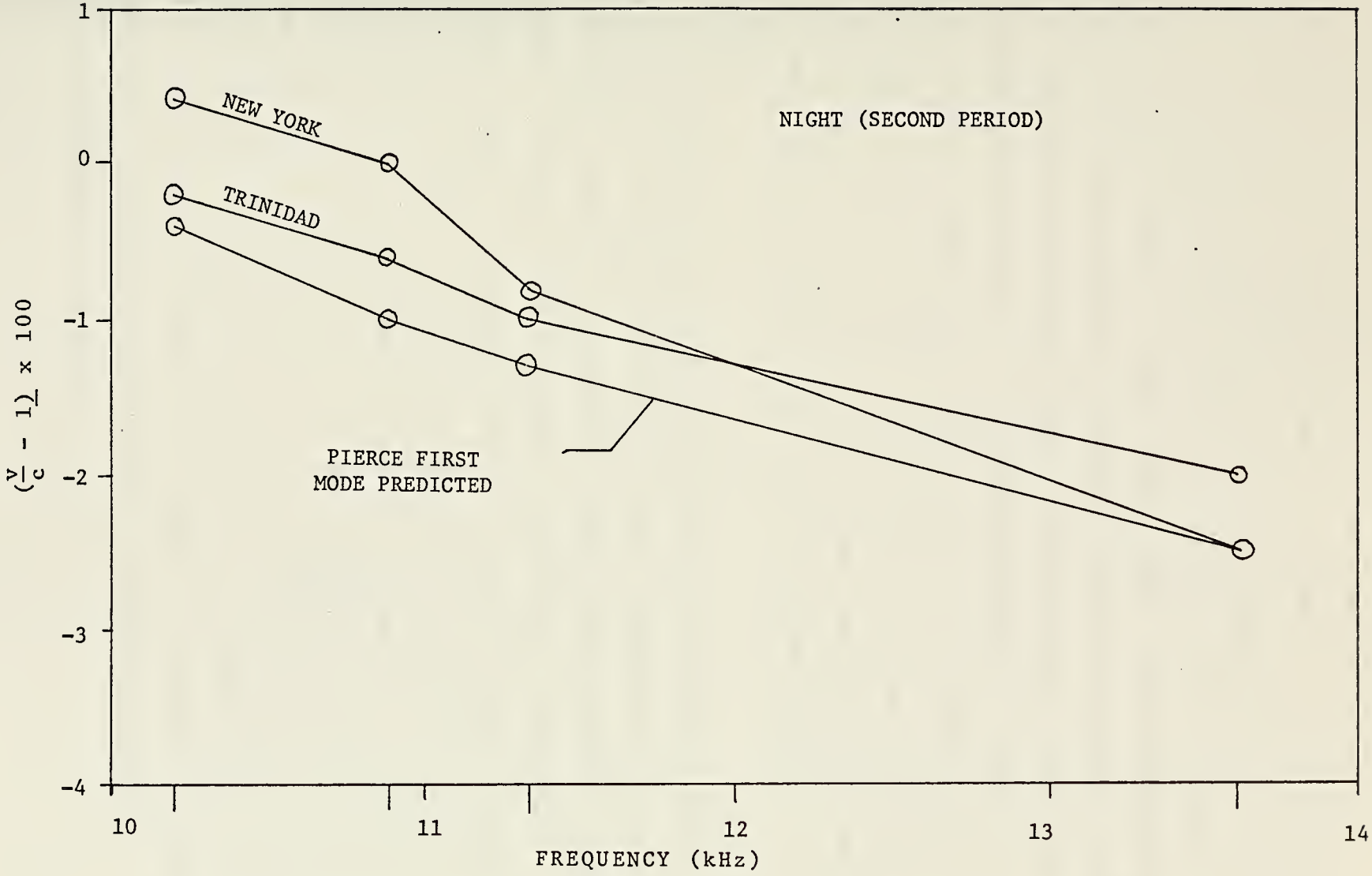

Figure 16. Second Data Period, Night Path, Phase Velocities (Stations Separately).

One further processing of the data was performed to demonstrate the consistency of the estimator. Phase velocity values for each frequency for lighted transmission paths and for each frequency for dark transmission paths were determined for each data set using (51). This method determines effective phase velocities, assumed the same from each station for the same frequency and path conditions. The phase velocities, normalized by c, thus determined are shown in Figure 14 for lighted paths and Figure 17 for dark paths.[3] The median values of phase velocities of the two collection periods were then taken from the curves and the entire data set was processed using this one set of phase velocity values.

The results of this processing were: three minor lane errors for the second period with night conditions and one minor lane error for the second period with transition conditions. All other data were lane error-free. This demonstrates that if reasonably accurate effective phase velocity values are known, extremely good estimation results can be expected from the maximum likelihood estimator. It further demonstrates that at least for the experiment conducted, the mean values of the effective phase velocities did not change significantly in more than one month. A single phase velocity value for each frequency for night and likewise for day conditions yielded excellent results for data collection periods separated by a month.

---

[3] Ibid.

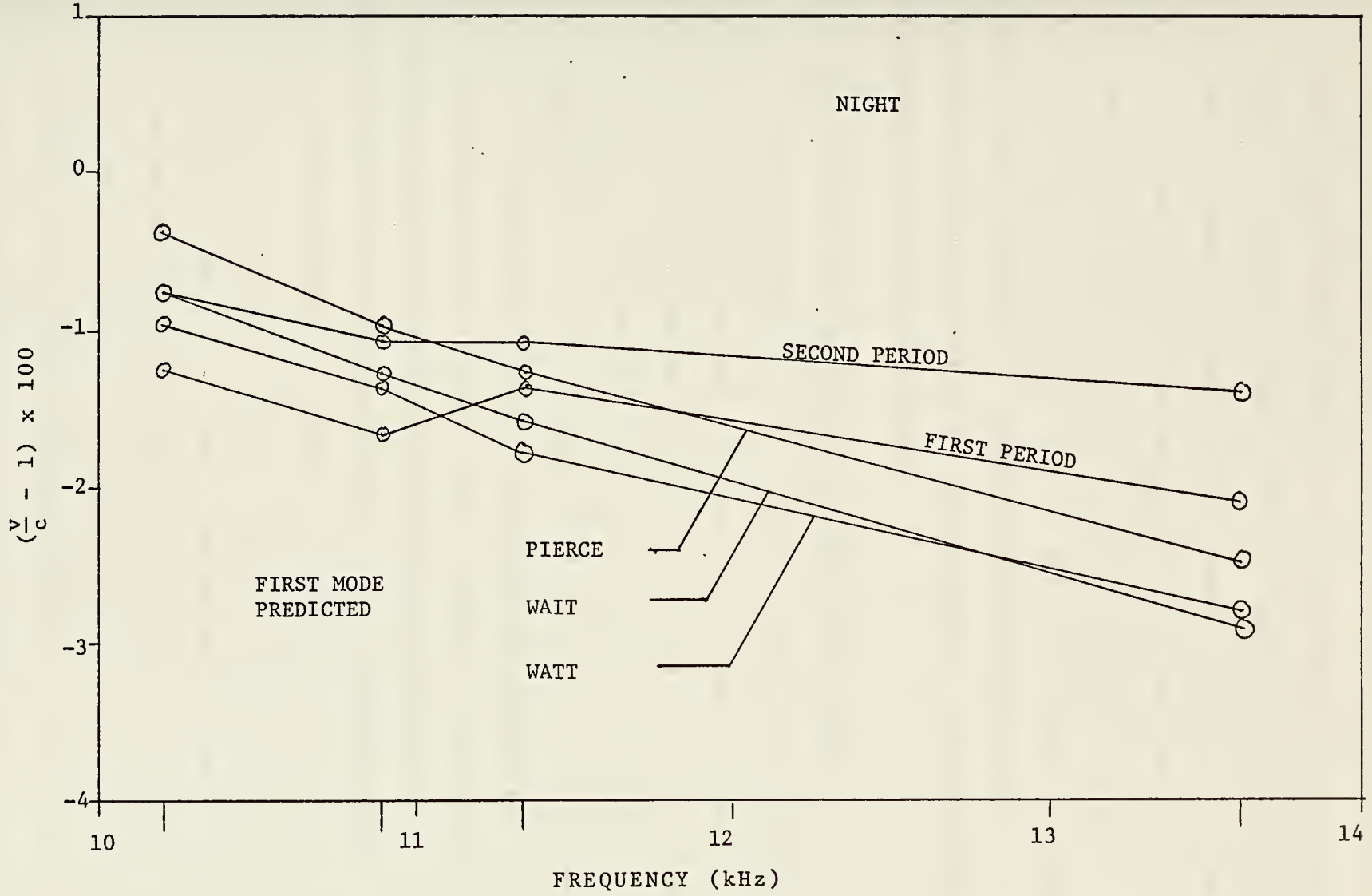

Figure 17. Night Path Phase Velocities, Considered Invariant with Station.

As stated before, higher order mode interference is the suspected cause of the lane errors experienced in processing the data utilizing the phase velocity values from Table II. This and the demonstrated relative insensitivity of the estimator to phase velocity values, along with the lane error-free day path condition results, indicate that very good estimation results can probably be expected from using single phase velocity values for a given receiver location. The sensitivity of these phase velocity values to receiver location remains to be determined.

D. ESTIMATION USING PROPAGATION CORRECTION TABLES

The Defense Mapping Agency publishes Omega Propagation Correction tables regularly for the active Omega stations in pairs for the two frequencies 10.2 kHz and 13.6 kHz. These corrections, when added to the observed phase difference of the appropriate frequency from a station pair, allow a mapping to be performed from the observed phase difference to an Omega navigational chart. These charts are plotted for an assumed value of $(v/c) = 1.00261$ for all frequencies. Many factors in addition to diurnal effects which affect phase, or equivalently the effective phase velocity, of the signals is accounted for by the computer program which generates these tables. In order to determine whether the predicted corrections would improve the results of the experiment, tables for the appropriate location, time, and station pair were obtained from Defense Mapping Agency. The corrections used for the 10.88 kHz and 11 1/3 kHz signals were obtained

by linear interpolation from the published corrections. Curves showing 24-hour plots of these correction factors are shown in Figures 18 and 19 for the second half of October 1973 and in Figures 20 and 21 for the second half of November 1973.

The results of the estimation when the data were corrected using the factors found as described above and using (v/c) = 1.00261, for all frequencies is presented in Table VII. The number of lane errors was decreased by utilizing the propagation correction factors; however, quite a large number of lane errors still occurred at night. It is believed that this helps to substantiate the higher order mode interference theory of the last section.

E. EXPERIMENT ESTIMATION SUMMARY

Because of the suspected higher order mode interference at night during this experiment, it cannot be considered conclusive that use of the Table II phase velocity values are inadequate for LOP estimation in a final SAR system. Further experiments at points an adequate distance from the stations to preclude higher order mode interference may show that propagation correction factors are helpful in reducing lane errors. If this results, the corrections can quite easily be implemented at the SARCEN and are not considered as a major hindrance in implementing a successful system.

One of the most important beneficial factors in using the maximum likelihood estimation procedure is the availability of multiple estimates along with their associated

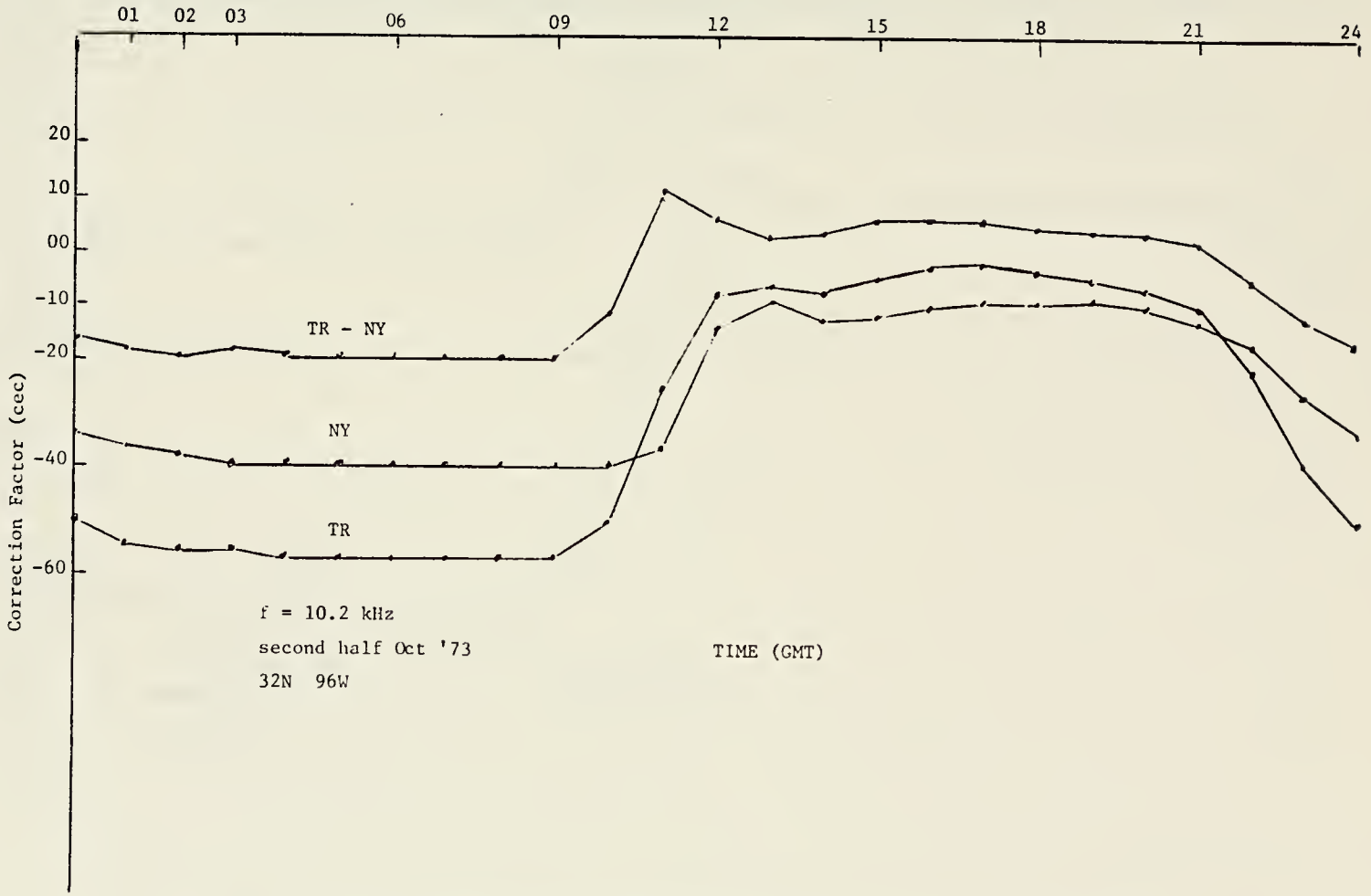

Figure 18. First Period Propagation Correction Factors for 10.2 kHz.

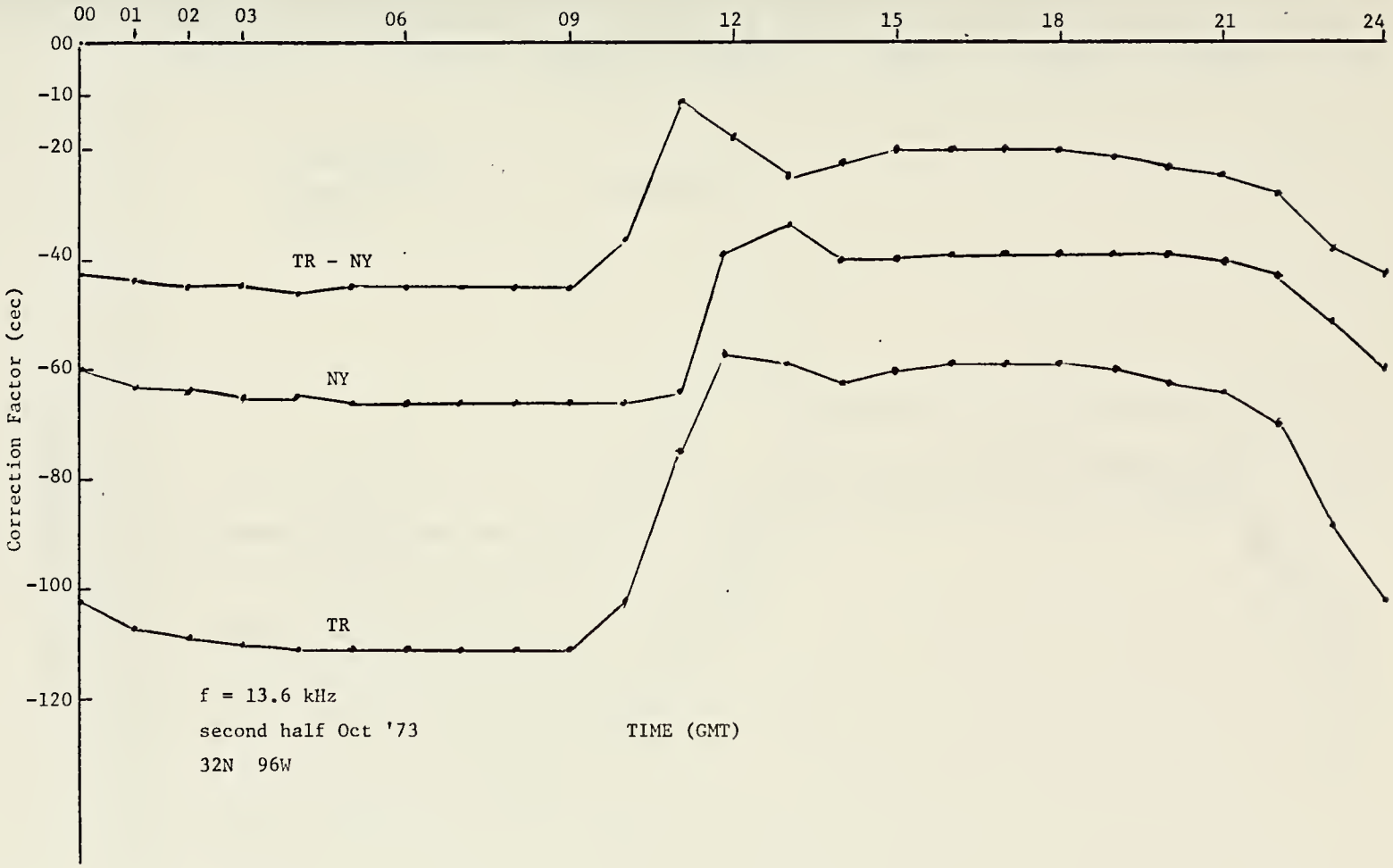

Figure 19. First Period Propagation Correction Factors for 13.6 kHz.

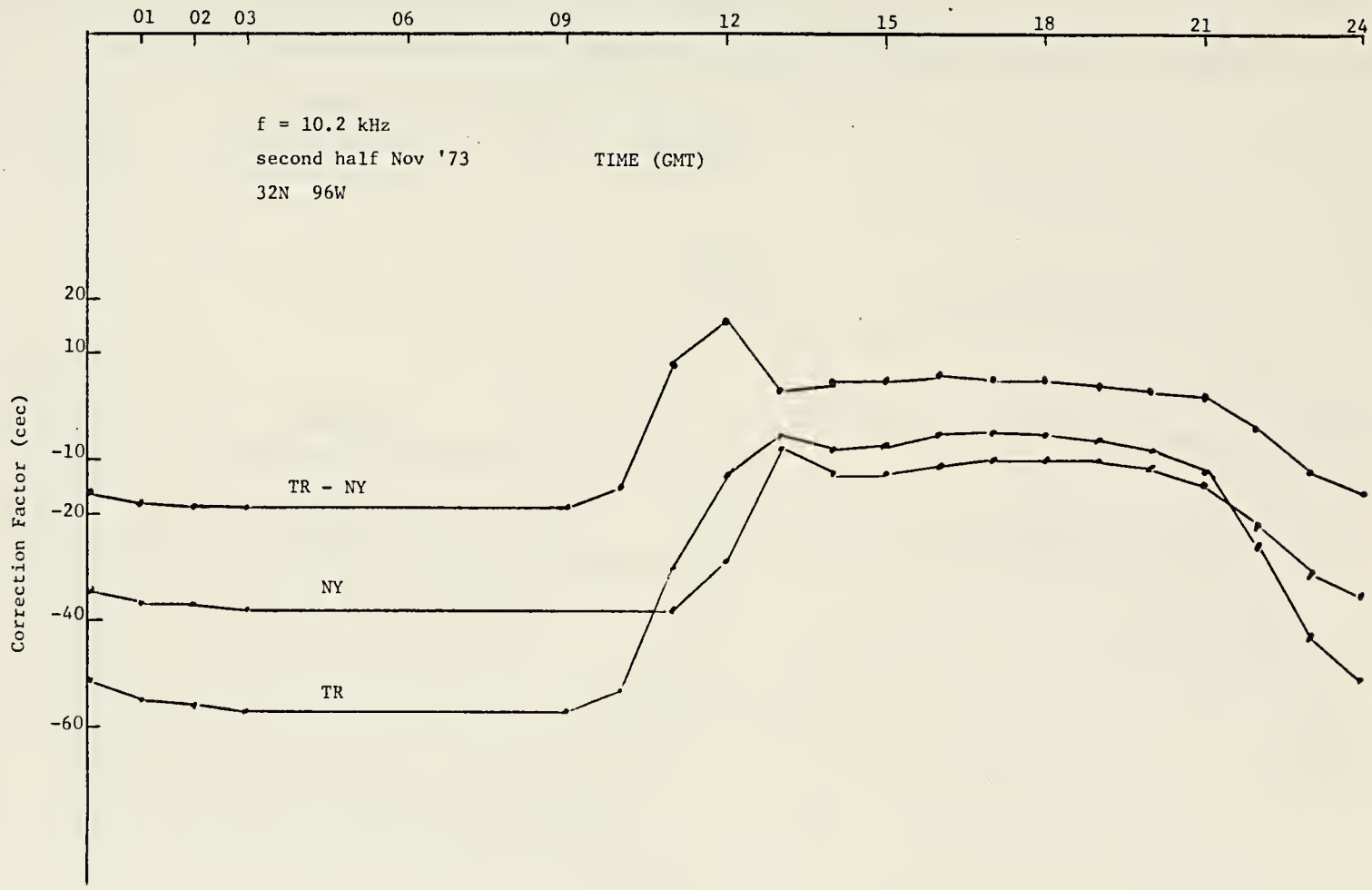

Figure 20. Second Period Propagation Correction Factors for 10.2 kHz.

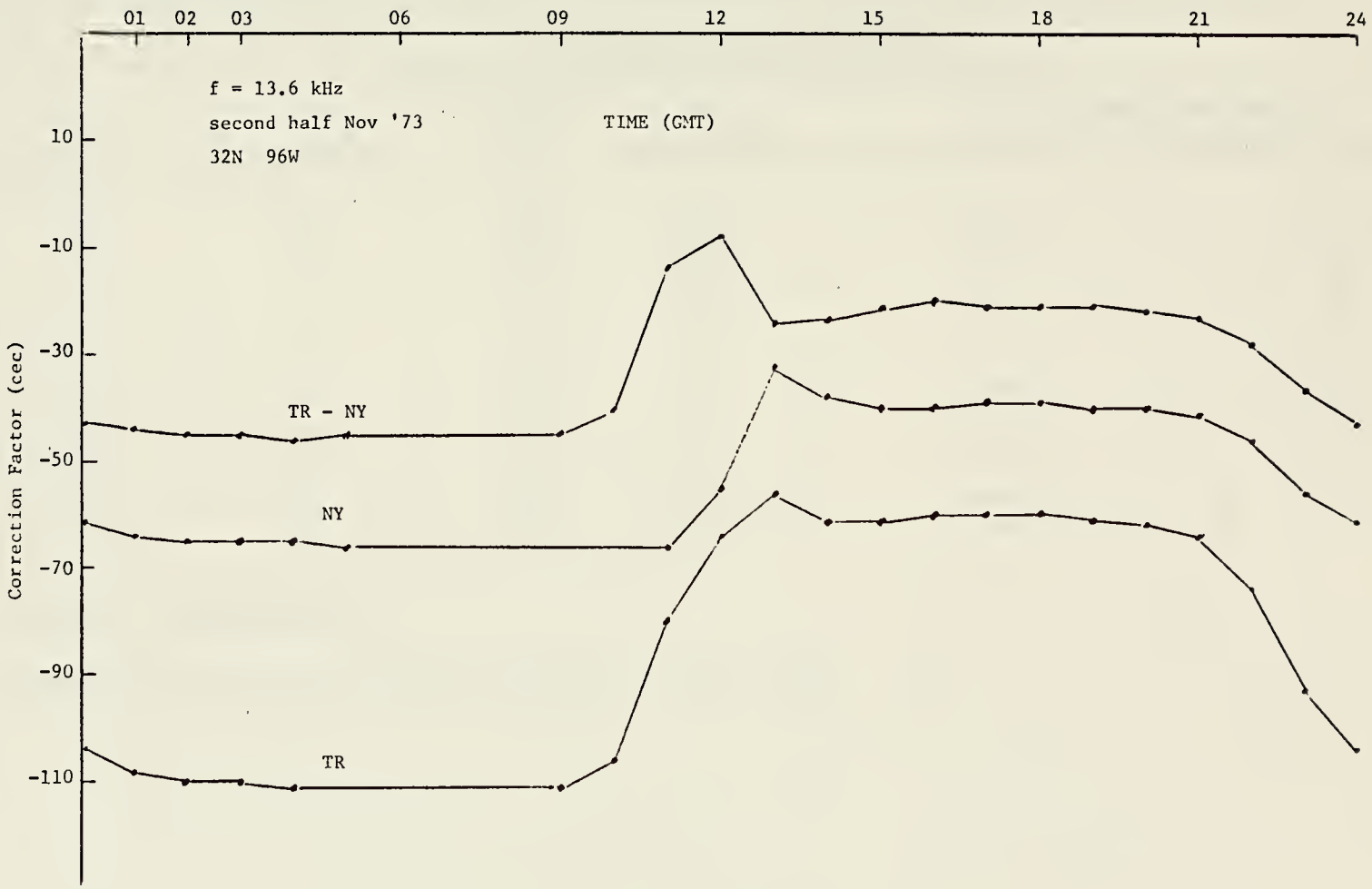

Figure 21. Second Period Propagation Correction Factors for 13.6 kHz.

TABLE VII

LOP ESTIMATION RESULTS
(Using Propagation Correction Factors)

Period		σ(x 10^{-4})	Total Runs	Minor Lane Errors	LOP Estimation Error mean (BL nmi)	Std dev (BL nmi)
1	D	2	144	0	-.11	.11
1	N	2	137	28	-.36	.19
1	T	2	69	10	-.43	.29
1	N	3	137	25	-.37	.19
1	T	3	69	10	-.43	.30
2	D	2	179	0	.09	.13
2	N	2	203	59	-.01	.26
2	T	2	92	7	-.29	.29
2	N	3	203	58	-.03	.26
2	T	3	92	7	-.29	.30

BL nmi = Baseline nmi

Spreading factor for Dallas receiver site = 1.88

relative probabilities of being correct which are obtained. When lane errors were made using the phase velocity values from Table II for the first period, the correct LOP was always the second most likely. For the second period, the correct LOP was second most likely for all but eight runs where lane errors occurred. For seven of the eight runs the correct LOP was third most likely and for one run it was fourth most likely. When propagation correction tables were used, the correct LOP was second most likely for all but one run where lane errors resulted. For this run the correct LOP was third most likely.

For the estimation performed with the Table II phase velocity values and $\sigma = 3 \times 10^{-4}$, the probability ratios discussed in Chapter IV were examined. As explained in Chapter IV, the ratios of the likelihood function evaluated for two values of x is equivalent to a ratio of the probabilities of these x being the correct x for the receiver location. Figures 22-25 give selected probability ratios for the first data collection period and Figures 26-31 give selected probability ratios for the second period. The symbol ⊛ denotes the probability ratio of the second most likely x when the correct x was the most likely. The symbol ⧋ denotes the probability ratio of the second most likely x when the correct x was second most likely. The symbol ⊡ denotes the probability ratio of the correct x when it was third or fourth most likely, the latter case occurring for only one run in the entire data set.

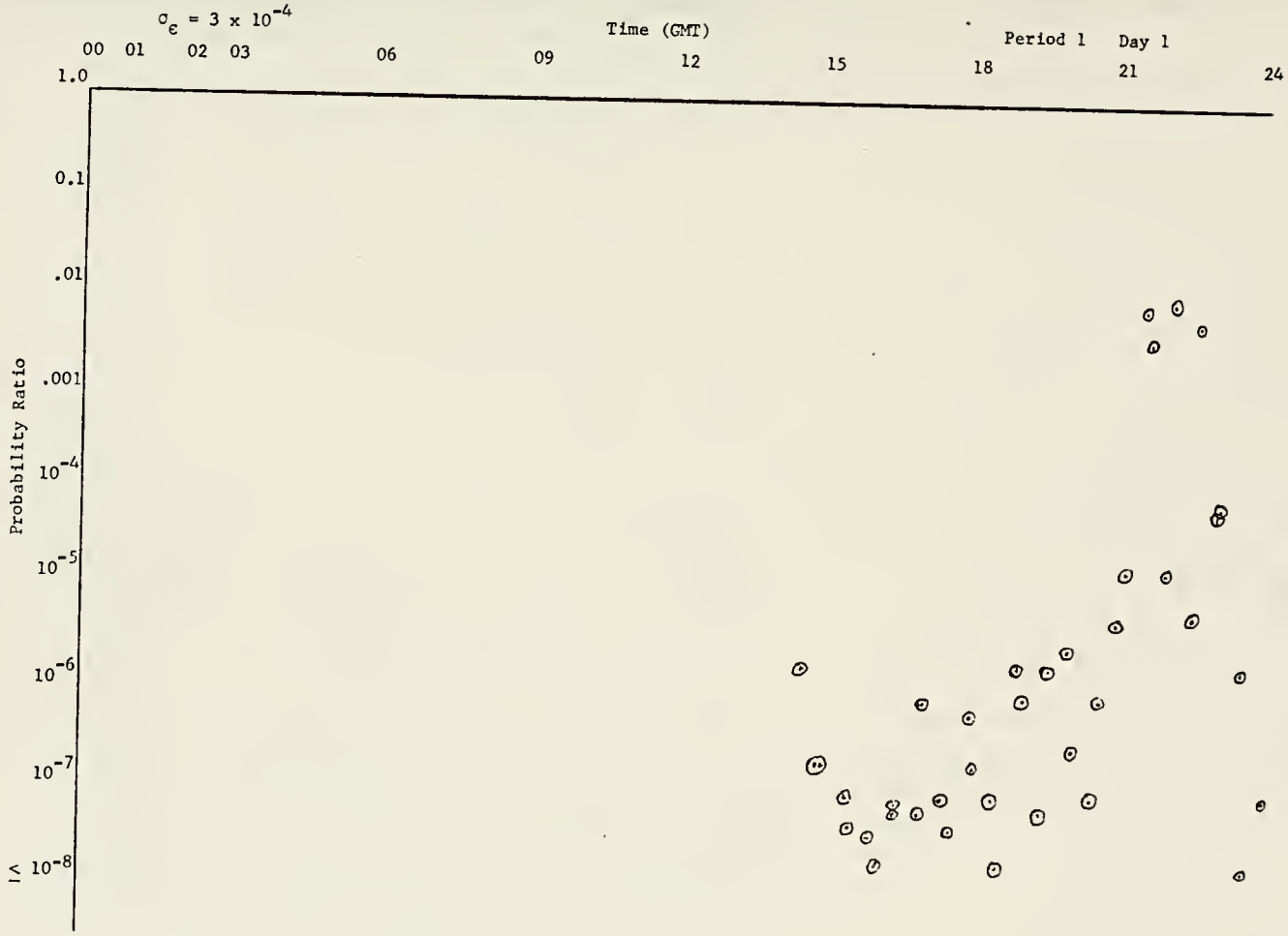

Figure 22. Probability Ratios, First Period Day One.

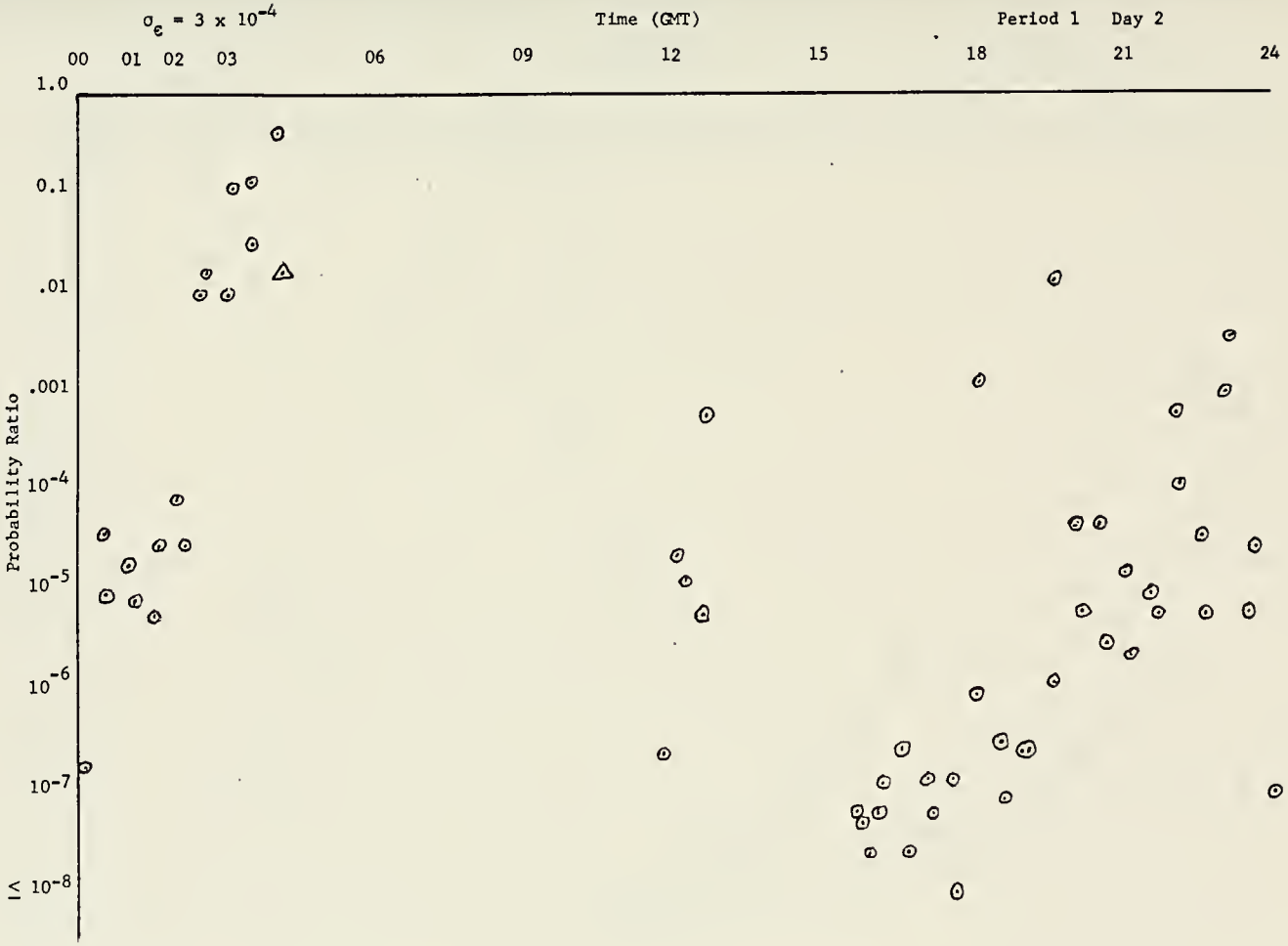

Figure 23. Probability Ratios, First Period Day Two.

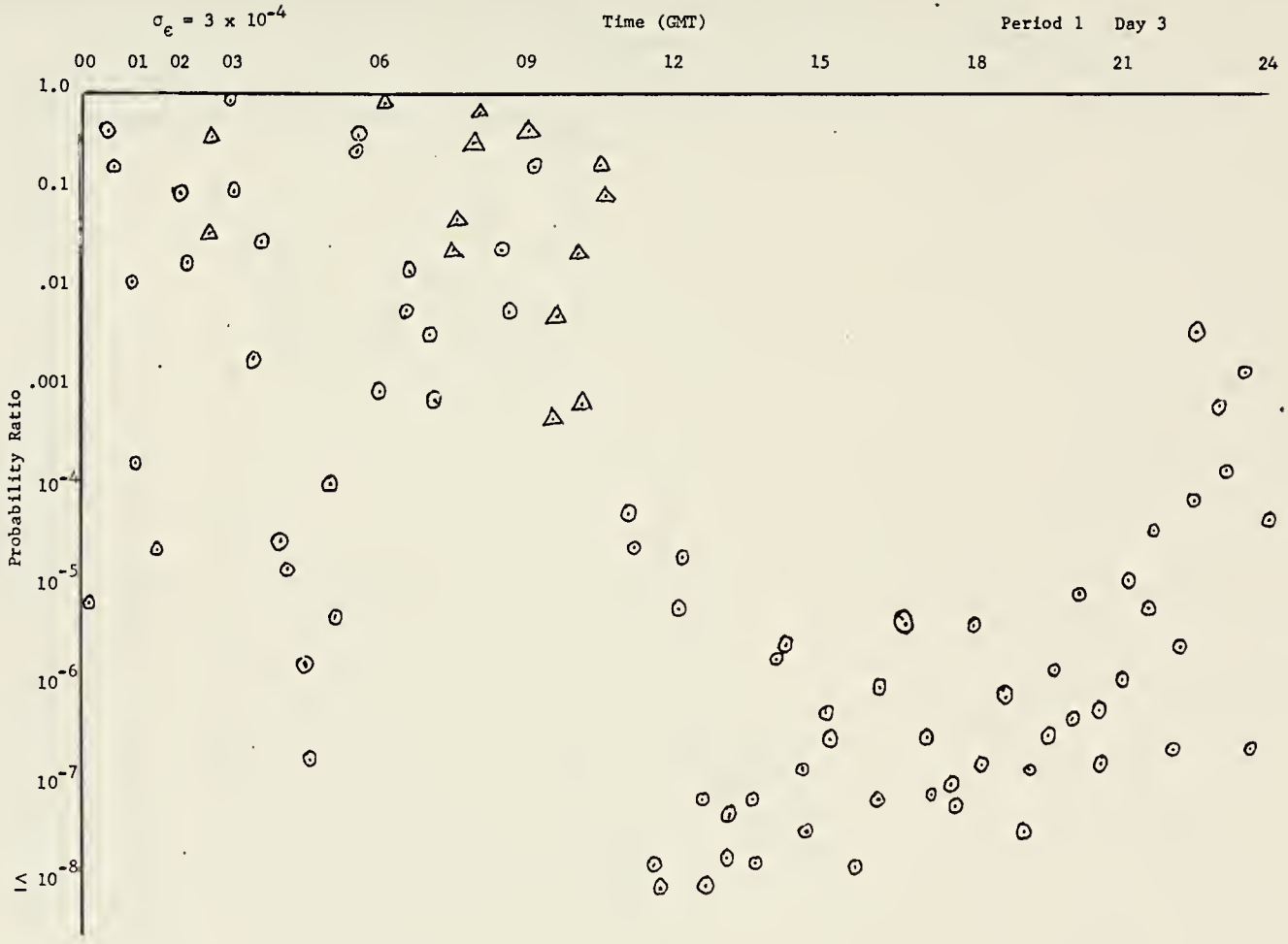

Figure 24. Probability Ratios, First Period Day Three

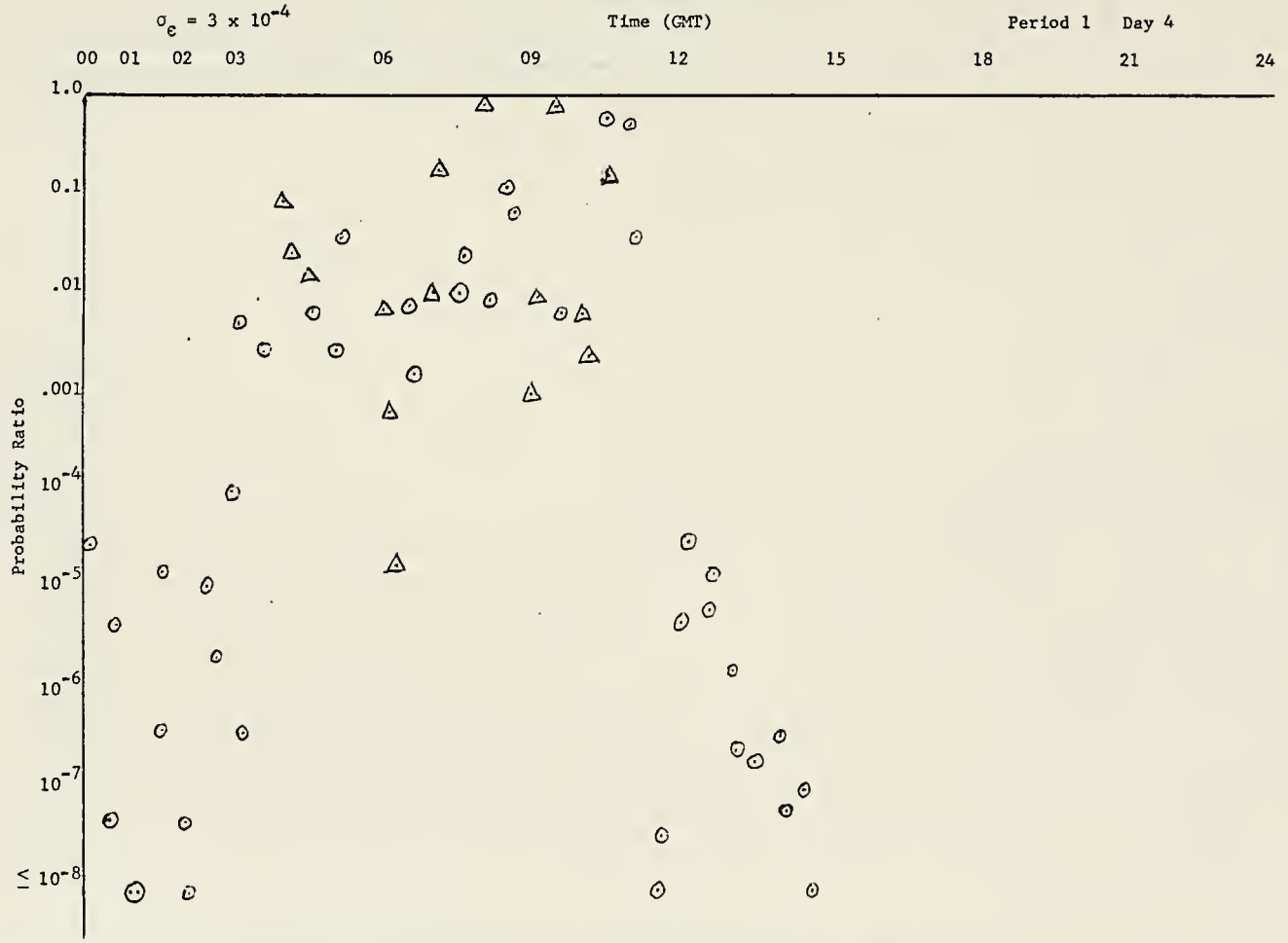

Figure 25. Probability Ratios, First Period Day Four.

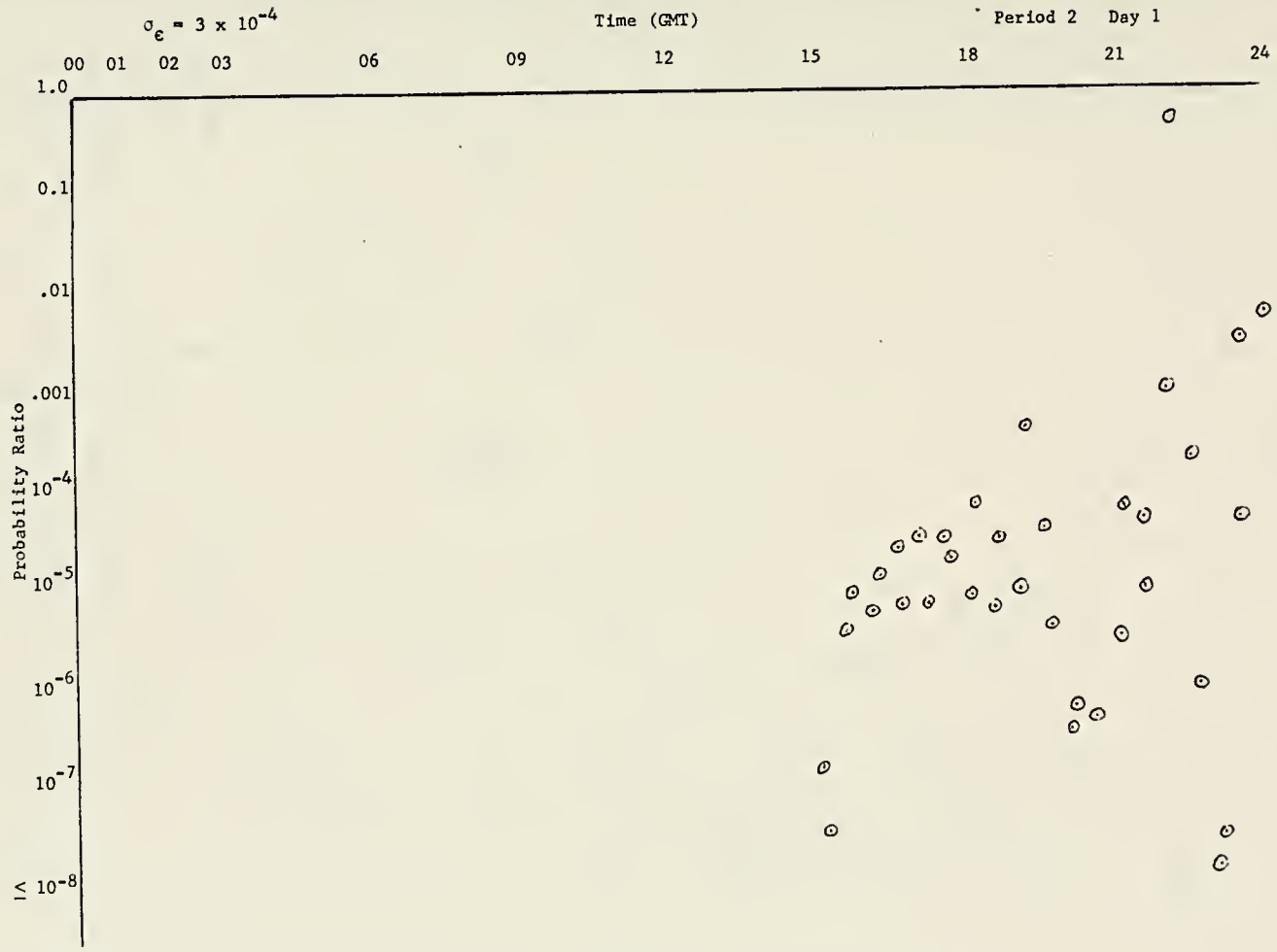

Figure 26. Probability Ratios, Second Period, Day One

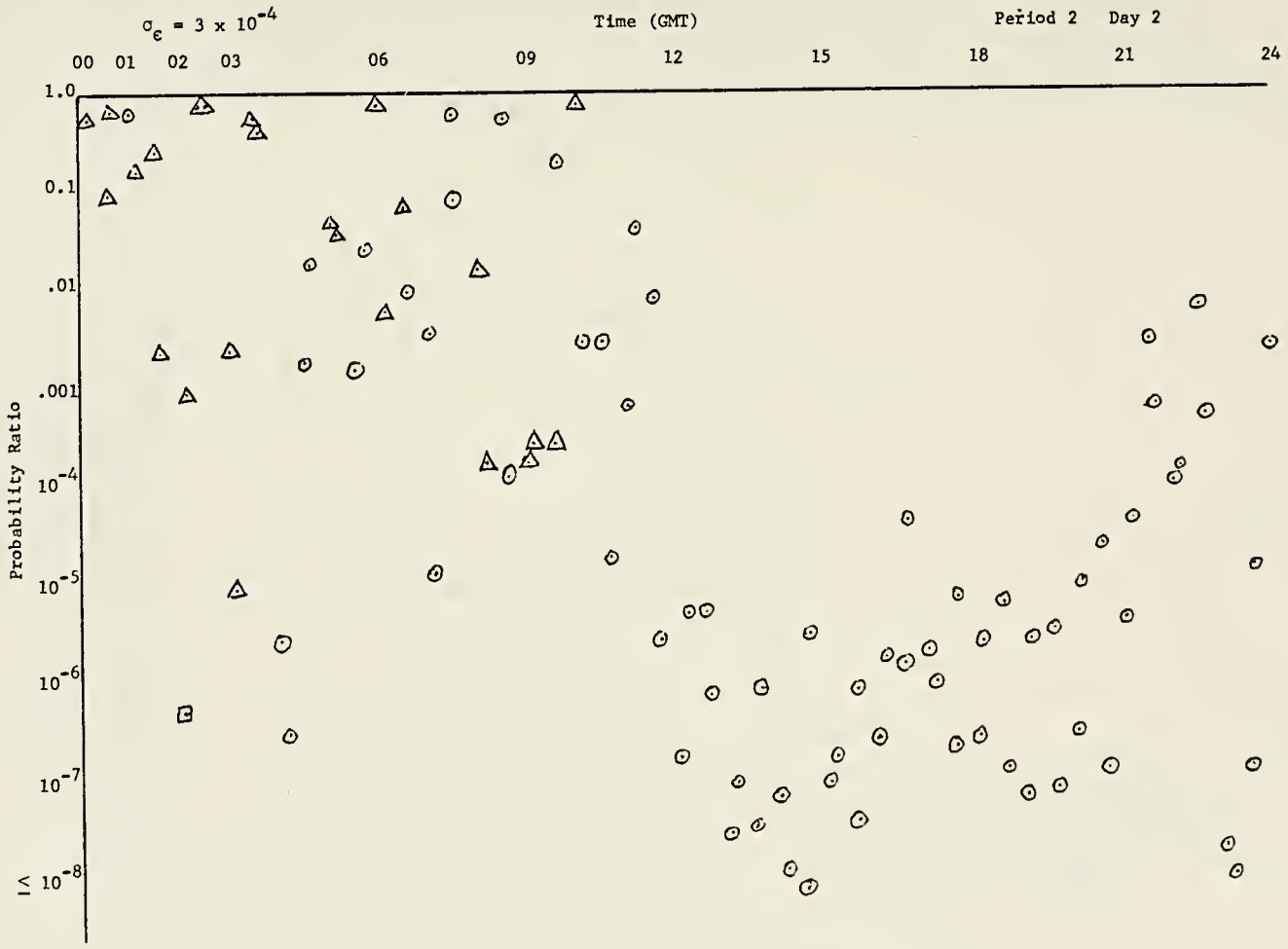

Figure 27. Probability Ratios, Second Period Day Two.

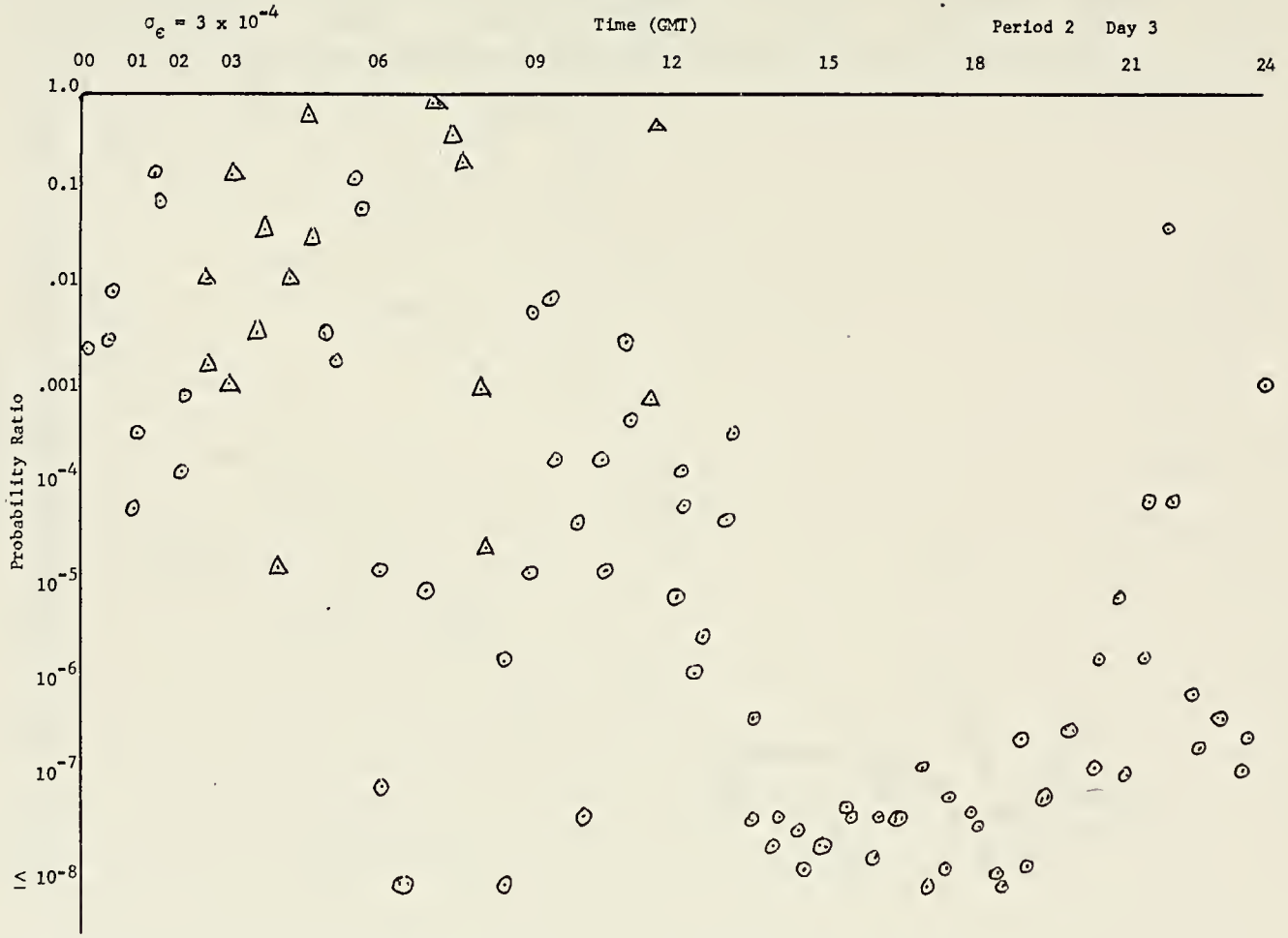

Figure 28. Probability Ratios, Second Period Day Three.

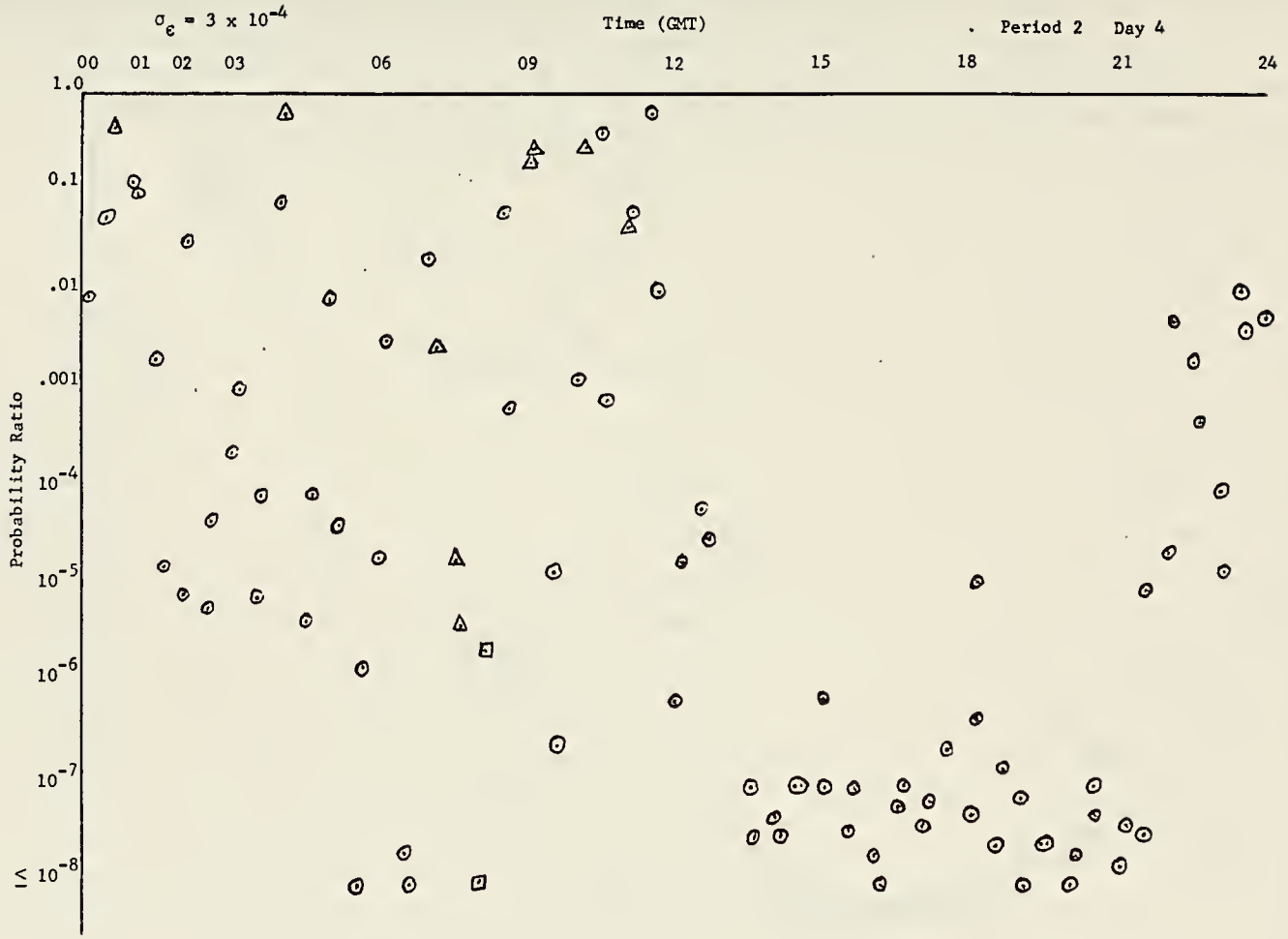

Figure 29. Probability Ratios, Second Period Day Four.

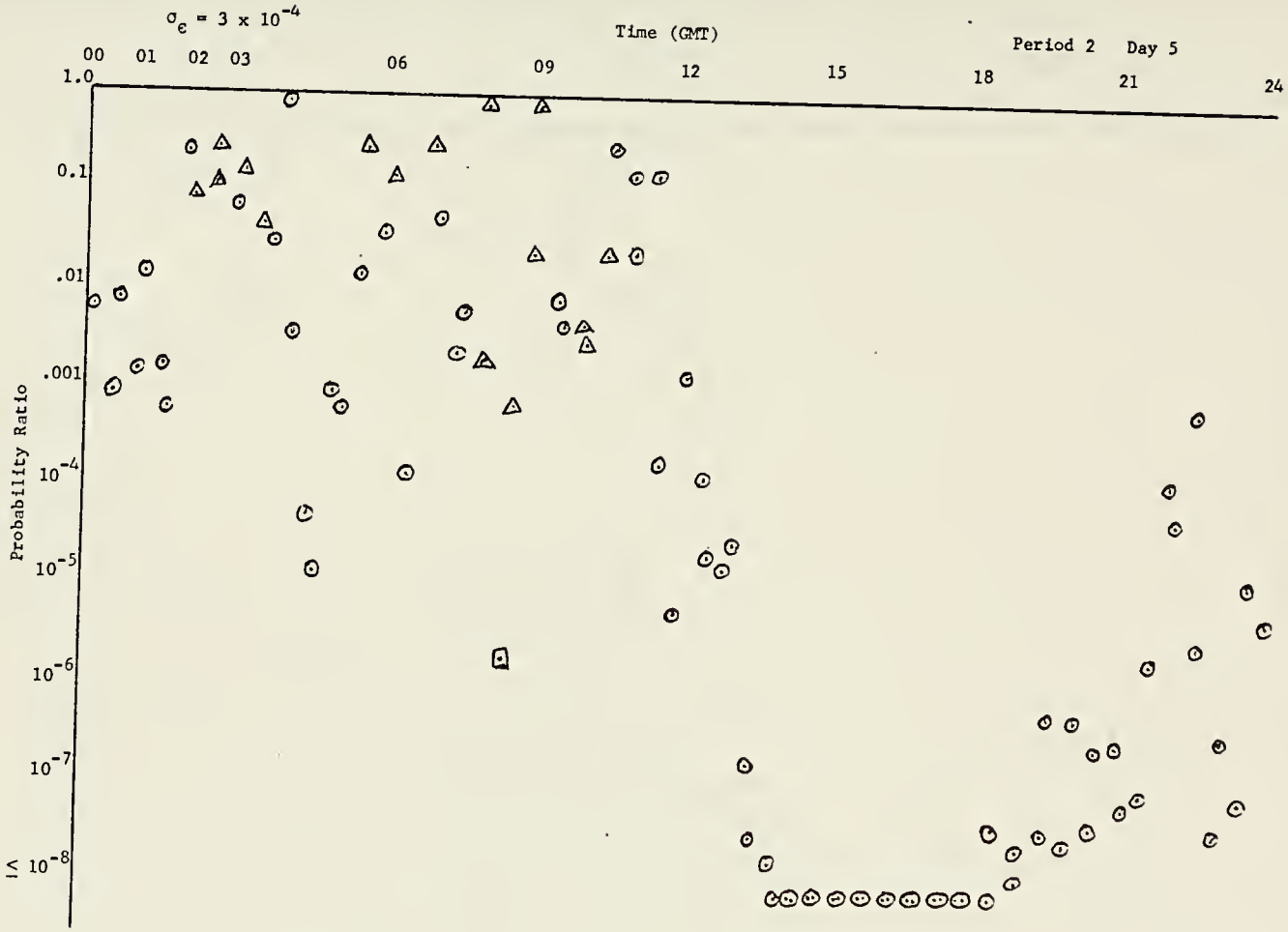

Figure 30. Probability Ratios, Second Period Day Five.

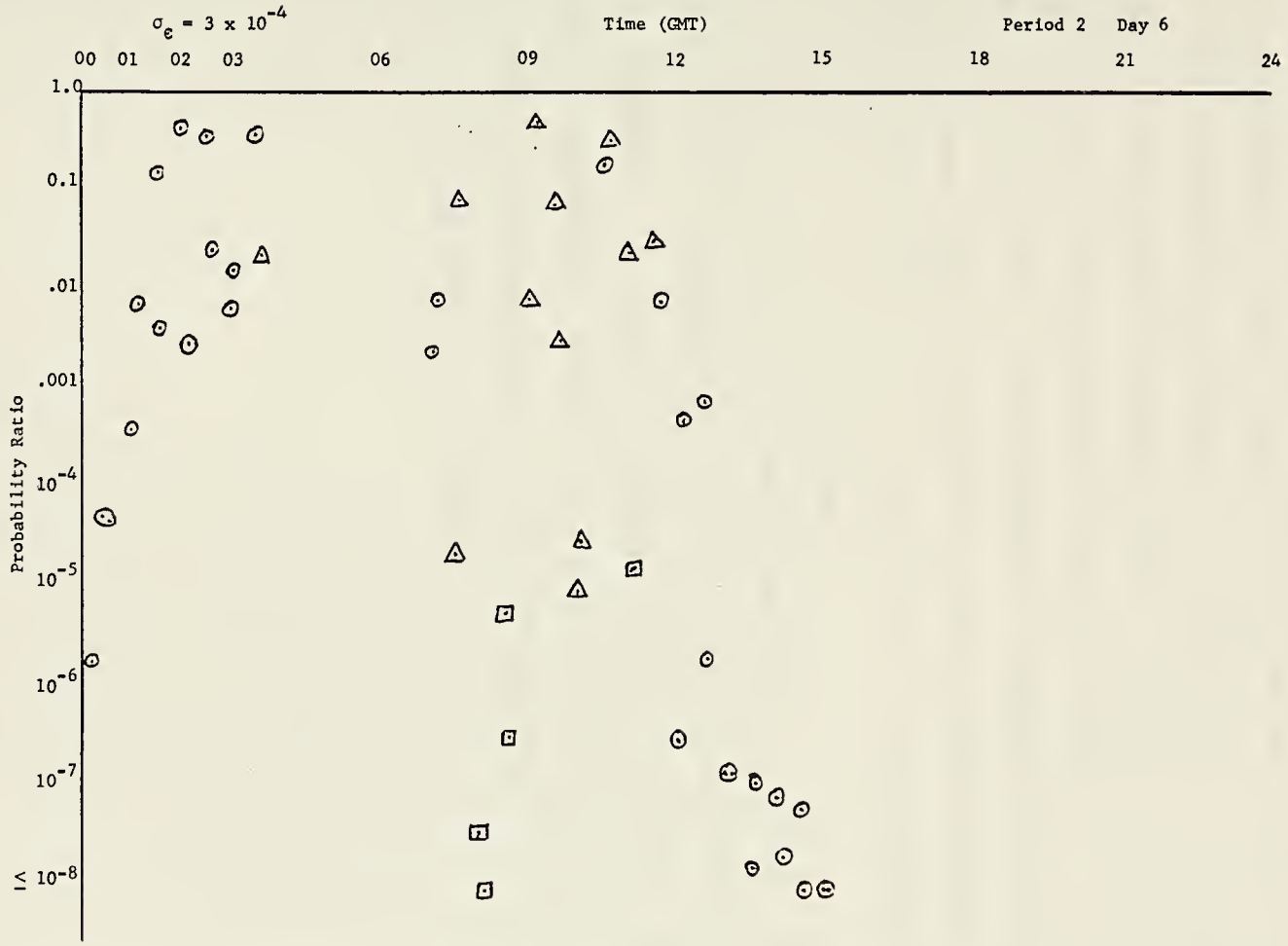

Figure 31. Probability Ratios, Second Period Day Six.

From these results, it appears that a threshold could be established such that when a probability ratio of an x was above a threshold, it would be considered as likely and SAR forces could be sent to the site. It is not suggested that the probability ratio values be treated as actually having meaningful numerical value. It appears that the maximum likelihood estimator places quite a lot more confidence in the data for this experiment than the results of the experiment would suggest is reasonable. Whether these values will be more meaningful as numerical values when receiver sites where higher order mode propagation is not a factor must be determined by future experiment.

The information of "ranked" position estimates which can be provided is considered to be of great importance for a SAR system. If the most likely position estimate does not yield a recovery, rather than spending hours or even days in an ever-widening search, the SAR forces can be vectored to the next most likely position.

VII. MULTIPLE STATION POSITION ESTIMATION

A. AN OPTIMUM POSITION ESTIMATOR

The mathematical model to be used for the multiple station problem will be the same as that for the two station problem presented in Chapter II except that the vectors will be of length PK instead of 2K where P is the number of Omega stations from which data is received. Arbitrarily ordering the stations as one through P, the first K components of the received column vector

$$Y(t) = S(t) + N(t) \tag{53}$$

will be from station one, the second K from station two, etc. Here again, K is the number of different frequencies common to all Omega stations for use in hyperbolic navigation. In (53), S(t) and N(t) will be PK dimensional column vectors as well. The components of S(t) will represent the signal portion of the received vector Y(t) and the components of N(t) will represent sample functions from white, Gaussian noise processes, the ith component $n_i(t)$ having two-sided noise density height $N_i/2$. The ith signal component can be written as

$$s_i(t) = A_i \cos [(\omega_i + \Delta_i)t - \phi_i + \theta_i] \tag{54}$$

as in Chapter II. The same arguments as followed in Chapter II allow the following observations

$$\omega_i = \omega_{K+i} = \omega_{2K+i} = \cdots\cdots = \omega_{(P-1)K+i} \qquad (55)$$

and

$$\theta_i = \theta_{K+i} = \theta_{2K+i} = \cdots\cdots = \theta_{(P-1)K+i} \qquad (56)$$

where θ_i $(1 \leq i \leq K)$ are independent random variables, uniformly distributed on $(-\pi, \pi]$.

It will not be possible to follow the convention in Chapter II for defining the propagation phase delays. Therefore, the following definition will be made

$$\phi_{pK+1} = \omega_i \int_o^{x_{p+1}} \frac{d\gamma}{v_{pK+1}(\gamma)} - 2\pi m_{pK+i} \quad \begin{matrix}(1 \leq i \leq K) \\ [o \leq p \leq (P-1)]\end{matrix} \qquad (57)$$

where v_k is the kth phase velocity and x_n is the great circle distance from the nth Omega station to the receiver location being estimated.

Similar to the presupposed unambiguous lane in Chapter IV, a presupposed area on the globe is required to begin the multiple station estimation process. This must be obtained by some ambiguity resolution technique using the data received from P stations. The estimation problem now consists of evaluating a likelihood function for all points on the presupposed area and determining the column vector x which

maximizes the function on this area. The likelihood function will appear as a rubber sheet spread over the presupposed area with many spikes under it causing many "hills" in the sheet. The value of the column vector x which corresponds to the "highest hill" will be the maximum likelihood estimate of x and the components of this x will uniquely determine the great circle distances from the Omega stations to the maximum likelihood estimate of the Omega receiver position.

Following the notation and arguments of Chapter IV, the likelihood function for the multiple station problem can be written as

$$\Lambda(X) = E_V \int f(\theta) \exp \{ \sum_{i=1}^{K} \sum_{p=0}^{P-1} [R_{pK+i} \cos(\phi_{pK+i} - \mu_{pK+i})] \cos \theta_i + \sum_{i=1}^{K} \sum_{p=0}^{P-1} [R_{pK+i} \sin (\phi_{pK+i} - \mu_{pK+i})] \sin \theta_i \} d\theta. \quad (58)$$

In (58),

$$R_i^2 = (C_i^2 + S_i^2) (2A_i/N_i)^2 \quad (1 \leq i \leq PK) \quad (59)$$

and

$$\mu_i = \tan^{-1} (S_i/C_i) \quad (1 \leq i \leq PK) \quad (60)$$

where S_i and C_i are the data from the ith signal as in Chapter IV. $E_V(\cdot)$ denotes the expected value with respect to the PK

dimensional phase velocity vector with jointly Gaussian components as described in Chapter II. Utilizing Equation (15) from Chapter IV, some algebra and some trigonometric identities, (58) can be written as

$$\Lambda(X) = E_V \prod_{i=1}^{K} I_o \{[\sum_{p=0}^{P-1} R_{pK+i}^2 + 2 \sum_{p=0}^{P-1} \sum_{q=p+1}^{P-1} R_{pK+i} R_{qK+i} \cos \psi_{i,p,q}]^{1/2}\} \quad (q \leq P-1) . \tag{61}$$

In (61),

$$\psi_{i,p,q} = \text{principal value of } (\mu_{qK+i} - \mu_{pK+i} - \phi_{qK+i} + \phi_{pK+i}) . \tag{62}$$

Arguments similar to those made in Chapter IV allow the high SNR maximum likelihood estimation equation for multiple stations to be written as

$$\Lambda(X) = E_\varepsilon \exp[\sum_{i=1}^{K} \sum_{p=0}^{P-1} \sum_{q=p+1}^{P-1} Q_{i,p,q} \psi_{i,p,q}^2] . \tag{63}$$

In (63) ε is the PK dimensional column vector with jointly Gaussian components just as defined in Chapter IV and

$$Q_{i,p,q} = - \frac{R_{pK+i} R_{qK+i}}{2(R_{pK+i} + R_{qK+i})} . \tag{64}$$

The matrix form of Equation (63) could be formed and the required expected value taken as in Chapter IV. The matrices involved will be quite large, however, since in general, four, five, or even more Omega station's signals are expected to be received. Since the solution to the estimation problem involves matrix inversions for each set of x_p $(1 \leq p \leq P)$ examined[4] in an iterative process, the processing time required for the implementation of the optimum position estimator will be prohibitive. Although non-optimum, the most reasonable multiple station position estimation processor to implement is considered to be a pairwise station processor.

B. MULTIPLE LOP POSITION ESTIMATION

Multiple LOP estimation will require the estimation of the set of most likely LOP for the (P-1) different pairs of the P received stations. Consideration must be given to the spreading factor (defined in Chapter I) when choosing the stations as pairs. The smallest spreading factors which can be achieved are desirable.

Frenkel in [23] presents a maximum likelihood position estimation procedure which finds the optimum position estimate when given multiple LOP estimates. Although presented

---

[4]Although some of the possible candidate components for X can be discarded before the matrix inversion is required by utilizing the "coarse check" procedure described in Appendix E, the processing time for the optimum multiple station estimation will still be prohibitively large for a SAR application as shown in Appendix E.

as an ambiguity resolution technique, the procedure applies directly to the multiple station position estimation problem when the stations are treated pairwise as proposed. The covariance matrix required for the position estimation procedure can be calculated as in [23] if the variance of the phase estimates corresponding to the LOP estimates are known. In order to approximate what these variances will be, we recall Equations (25a, 25b)

$$\phi_i \approx \bar{\phi}_i - \frac{\omega_i d}{c} \varepsilon_i - 2\pi m_i \qquad (1 \leq i \leq K) \qquad (65)$$

where d is the great circle distance of the receiver from the Omega transmitter generating the K signals. Since ε_i $(1 \leq i \leq 2K)$ were assumed to be jointly Gaussian random variables with known covariance, the variance of each ϕ_i due to phase velocity uncertainty only is

$$\sigma_{\phi_i}^2 \cong \left(\frac{\omega_i d}{c}\right)^2 \sigma_{\varepsilon_i}^2 \,. \qquad (66)$$

It has been shown as a result of [17, 21] that the noise disturbances to observed phase will in general be dominated by the phase disturbances due to phase velocity uncertainty. It is therefore a reasonable assumption to consider only phase velocity contributions in determining an idea of the variance of the 2K phases in the two station LOP estimation problem.

As a result of [17] and the experimental results reported on in Chapter VI, standard deviations of the phase velocity ratios (v/c) on the order of 3×10^{-4} are expected for the four frequencies 10.2 kHz, 11 1/3 kHz, 13.6 kHz, and 10.88 kHz. Thus, Table VIII can be created, where d is the great circle distance from the station generating the signals to the receiver in nmi. If the standard deviations of the four frequencies given by Table VIII and the correlation coefficients given by Equation (49) in Chapter VI are used and the phases are considered to be equally weighted by the estimator, it can be shown that

$$\sigma_\phi/d \approx .1253 \times 10^{-3} . \qquad (67)$$

The value of σ_ϕ in (67) corresponds to the standard deviation of the phase estimate for one station. The standard deviation corresponding to the LOP estimate resulting from a station pair would be the rms of the σ_ϕ associated with the two stations. The value of d required in (67) can be quite approximate and can be the great circle distance in nmi from the appropriate Omega station to the center of the presupposed area on the globe which was assumed given by an ambiguity resolution technique. The value of σ_ϕ given by (67) is approximate, since the optimum estimator actually accounts for the estimated SNR of the signals instead of weighting them equally. However, (67) yields a result which is most probably adequate to enter the multiple LOP position

TABLE VIII

STANDARD DEVIATION OF PHASE DIFFERENCES

i	f_i(kHz)	$\sigma_{\phi i}/d$ (d in nmi)
1,5	10.2	$.1188 \times 10^{-3}$
2,6	11 1/3	$.1320 \times 10^{-3}$
3,7	13.6	$.1584 \times 10^{-3}$
4,8	10.88	$.1267 \times 10^{-3}$

estimation procedure of [23]. Note that this σ_ϕ only applies for four-frequency Omega using the frequencies specified in Table VIII.

A final piece of information which must be provided to the multiple LOP position estimation procedure in [23] in order to obtain valid results is an effective phase velocity associated with the phase ϕ. This is required in order to do the mapping from phase to latitude/longitude on the earth. Although the phase velocities of the different signals have been modeled as having known mean values with additive disturbances, it is expected that an average of the mean values of phase velocity will be sufficient to provide the necessary phase velocity for the mapping. These mean values will already account for diurnal effects on the path being considered.

VIII. CONCLUSIONS

This dissertation has reported the results of research efforts applied to the problem of achieving an optimum position estimator to be utilized for the GRAN worldwide SAR system. The principal new results which it contains are discussed below. Areas into which future research is needed are discussed as well.

A. PRINCIPAL NEW RESULTS

The dissertation has presented a new way to model VLF phase uncertainties. As presented in Chapter II, these uncertainties have been modeled as effective phase velocities which are jointly Gaussian random variables. The propagation effects on phase which can be reasonably well predicted such as diurnal effects are accounted for by specifying the mean values of the phase velocities. All the remaining effects which cannot be so readily predicted are modeled as contributing to the uncertainty in phase through a randomness of effective phase velocity. This model allows for very conveniently incorporating any correlations in the phase uncertainties, either interfrequency or interstation. This is accomplished by means of treating the effective phase velocities as being jointly Gaussian with known covariance.

The maximum likelihood LOP estimator for an arbitrary number of Omega frequencies was derived for two stations in

Chapter IV. This estimator takes advantage of the model previously discussed. In particular, the correlation between frequencies which is known to be significant and is presently actively being researched is simply incorporated into the estimator. If the interfrequency correlation which is expected can be determined quite accurately, lane error occurrence can be very significantly reduced. Uncertainties in phase or equivalently in phase velocity would still cause errors in LOP estimation but much fewer lane errors would occur if correlation between frequencies from an Omega station were high and predictable.

As an integral part of the maximum likelihood estimator, doppler shift, signal amplitude, and noise density height estimation equations are derived in the appendices. The results of four-frequency experimental data processed by the signal amplitude and noise density estimators are presented in terms of SNR in one Hz in Appendix B.

Monte Carlo simulations were carried out utilizing the maximum likelihood estimator derived in Chapter IV. These simulations were carried out for four-frequency Omega with fourth frequencies chosen primarily on the basis of ease of implementation at the Omega stations, their separation from other known or planned frequencies and the resulting unambiguous lane size. As discussed in the previous chapters, it is nearly certain that for any of the known methods of ambiguity resolution which appear to have any hope of materializing for SAR systems, unambiguous lane size in

excess of the three-frequency, nominally 72 nmi lanes must be achieved. This fact prompted the simulations and it is now possible for the decision concerning the choice of a fourth frequency to be made in terms of lane error tradeoffs to achieve acceptable lane size. The fact that the simulations present results illustrating the extent to which lane errors can be expected as a function of SNR as well as phase velocity uncertainty and fourth frequency choice allow for observing the effect of SNR on lane errors.

The simulation results prompt the conclusion that with adequate knowledge of the effective phase velocity variance and correlation and with reasonable signal-to-noise ratios, the unambiguous lane size can be increased beyond the present baseline nominal 72 nmi obtained with three frequency Omega. The controlling factors in the selection of a fourth frequency for Omega to be used for SAR purposes are (1) the capability of ambiguity resolution techniques to resolve the lane ambiguity with restricted amounts of Omega data and (2) the accuracy with which the phase velocities of the Omege frequencies can be predicted.

The maximum likelihood estimator of a line-of-position for the two-station Omega problem as derived in Chapter IV was applied to experimental four-frequency Omega data. The results of this estimation (presented in Chapter VI) demonstrated that the maximum likelihood estimator was superior in terms of lane errors to the walk-up technique, [29], which is presently the only other method of processing the

experimental data. Of particular significance was the 20-25 percent fewer lane errors experienced using the maximum likelihood estimator for the second data period, night path conditions, over the walk-up technique employed in [29].

The experimental data processing using the maximum likelihood estimator was done utilizing the best available expected interfrequency effective phase velocity correlation coefficients (see Chapter VI) and various values of standard deviation for these phase velocities. The standard deviation values which yielded the best results in terms of minimizing lane errors were on the order of 2×10^{-4} to 4×10^{-4} as expected from previous study by other authors [17]. The relatively large number of lane errors which were experienced for night and transition periods are suspected to be the result of higher-order-mode propagation interference on the Forestport Omega station path. The basis for this argument is presented in Chapter VI. A four-frequency experiment planned by the Naval Air Test Center, Patuxent River, Maryland for late 1974 which is to relay the Omega data via satellite from various globe locations is expected to verify this argument. Retransmitter (SARCOM) positions far enough from the Omega stations to insure small contribution from higher-order-modes of propagation are planned.

B. FUTURE AREAS FOR INVESTIGATION

Several areas into which future research efforts could be made have been observed as a result of this work. Since this is the first known attempt at modeling the VLF phase

velocities as random variables, prior efforts by other researchers have not analyzed the VLF data they have collected in a fashion which readily yields the necessary parameters. The variances which can be expected as a function of distance for all the Omega frequencies need to be better determined.

There is presently some interest in investigating the correlation between phase uncertainties. Professor Pierce of Harvard has been examining the possibility of using the interfrequency correlation of Omega to advantage for some time. It is felt by this author that the determination of correlation, both interfrequency and interstation, if it can be determined to be significant even for some paths, is a most fruitful area for study. Interfrequency correlation could reduce lane error occurrence in Omega dramatically.

In terms of the GRAN application, one of the areas which appears to have been neglected is the study of methods to reduce doppler shift of the signals received at the SARCEN. Proper design of the SARCOM and processing at the SARCEN could eliminate some of the sources of doppler shift and thus allow for an estimate of the velocity of the SARCOM to be made. In the present advanced OPLE concept, this was not considered possible [28]. For a SAR system, particularly for processing a distress incident at sea, SARCOM motion during and after transmission is a very real possibility. It will be much easier to locate a drifting life raft minutes or hours after notification if some velocity estimate is available.

APPENDIX A

DOPPLER SHIFT ESTIMATION FOR THE TWO-STATION K-FREQUENCY CASE

Ideally, if we knew the frequency of the received Omega signals at the SARCEN precisely (both ω_i and Δ_i for all i), we could perform the necessary operations to obtain Equations (12a, 12b) in Chapter IV. They are

$$C_i = \sum_{j=1}^{M} \int_{10(j-1)}^{10(j-1)+T_i} y_i(t) \cos [(\omega_i + \Delta_i)t]dt \qquad \text{(A-1a)}$$

and

$$S_i = \sum_{j=1}^{M} \int_{10(j-1)}^{10(j-1)+T_i} y_i(t) \sin [(\omega_i + \Delta_i)t]dt \; . \qquad \text{(A-1b)}$$

The frequencies ω_i $(1 \leq i \leq K)$ are known quite well, however, because of the A/R tone which is created in the SARCOM and sent with the Omega data to the SARCEN and because the frequencies at the Omega stations are well controlled. Therefore, we can form

$$C_i' = \sum_{j=1}^{M} \int_{10(j-1)}^{10(j-1)+T_i} y_i(t) \cos \omega_i t dt \qquad \text{(A-2a)}$$

and

$$S_i' = \sum_{j=1}^{M} \int_{10(j-1)}^{10(j-1)+T_i} y_i(t) \sin \omega_i t dt \qquad \text{(A-2b)}$$

at the SARCEN from the received data.

In order to form the likelihood function for Δ_i ($1 \leq i \leq 2K$) the definitions

$$C'_{ij} = \int_{10(j-1)}^{10(j-1)+T_i} y_i(t) \cos \omega_i t dt \qquad \text{(A-3a)}$$

and

$$S'_{ij} = \int_{10(j-1)}^{10(j-1)+T_i} y_i(t) \sin \omega_i t dt \qquad \text{(A-3b)}$$

are made. Recalling that

$$y_i(t) = A_i \cos [(\omega_i + \Delta_i)t - \phi_i + \theta_i] + n_i(t), \qquad \text{(A-4)}$$

the probability density functions of C'_{ij} and S'_{ij} conditioned upon knowing θ_i and ϕ_i can be found as follows.

$$C'_{ij} = \int_{10(j-1)}^{10(j-1)+T_i} A_i \cos [(\omega_i + \Delta_i)t - \phi_i + \theta_i] \cos \omega_i t dt + \int_{10(j-1)}^{10(j-1)+T_i} n_i(t) \cos \omega_i t dt \qquad \text{(A-5)}$$

can be written as

$$C'_{ij} = \frac{A_i}{2} \int_{10(j-1)}^{10(j-1)+T_i} \cos(\Delta_i t - \phi_i + \theta_i) dt + N'_{cij} \qquad \text{(A-6)}$$

where the second order frequency term is disregarded as not being in the passband of the system and

$$N'_{cij} = \int_{10(j-1)}^{10(j-1)+T_i} n_i(t) \cos \omega_i t dt \ . \qquad \text{(A-7)}$$

The integration in Equation (A-6) can be carried out yielding

$$C'_{ij} = \frac{A_i}{2\Delta_i} \{\sin [10\ \Delta_i(j-1) + \Delta_i T_i - \phi_i + \theta_i] - \sin [10\ \Delta_i(j-1) - \phi_i + \theta_i]\} + N'_{cij} \qquad \text{(A-8)}$$

which can also be written as

$$C'_{ij} = \frac{A_i T_i}{2} \alpha_i \cos [\gamma_{ij} + \eta_i] + N'_{cij} \ . \qquad \text{(A-9)}$$

In (A-9)

$$\alpha_i = \frac{\sin (\Delta_i T_i/2)}{\Delta_i T_i/2} \ , \qquad \text{(A-10)}$$

$$\eta_i = - \phi_i + \theta_i \ , \qquad \text{(A-11)}$$

and

$$\gamma_{ij} = 10\ \Delta_i(j-1) + \frac{\Delta_i T_i}{2} \ . \qquad \text{(A-12)}$$

Recalling from Chapter II that $n_i(t)$ is a sample function from a white Gaussian random process with two-sided spectral density $N_i/2$, and since N'_{cij} is formed as a linear function of $n_i(t)$, N'_{cij} will be a Gaussian random variable. N'_{cij} will have mean value zero and variance

$$E[N_{cij}^2] = \int_{10(j-1)}^{10(j-1)+T_i} \frac{N_i}{2} \delta(\tau) \frac{1}{2} \cos \omega_i \tau d\tau = \frac{N_i T_i}{4} \qquad \text{(A-13)}$$

where the second order frequency term is again disregarded. Therefore, C'_{ij}, conditioned upon knowing ϕ_i and θ_i, is a Gaussian random variable with mean value

$$E[C'_{ij}] = \frac{A_i T_i}{2} \alpha_i \cos [\gamma_{ij} + \eta_i] \qquad \text{(A-14)}$$

and variance

$$\text{VAR} [C'_{ij}] = \frac{N_i T_i}{4} . \qquad \text{(A-15)}$$

It can similarly be shown that S'_{ij} is a Gaussian random variable with mean value

$$E[S'_{ij}] = - \frac{A_i T_i}{2} \sin [\gamma_{ij} + \eta_i] \qquad \text{(A-16)}$$

and variance

$$\text{VAR} [S'_{ij}] = \frac{N_i T_i}{4} . \qquad \text{(A-17)}$$

Using the conditional probability density functions found above and the fact that C'_{ij} and S'_{ij} can readily be shown to be uncorrelated, and thus, independent since they are Gaussian random variables, the joint conditional density function of C_{ij} and S_{ij} for the ith received signal can be written as

$$f(C'_{ij}, S'_{ij} | \Delta, \theta, x, V) = \prod_{j=1}^{M} \left(\frac{2}{\pi N_i T_i}\right) .$$

$$\exp \left\{ - \frac{2}{N_i T_i} \left[C'_{ij} - \frac{A_i T_i}{2} \alpha_i \cos (\gamma_{ij} + \eta_i) \right]^2 \right.$$

$$- \frac{2}{N_i T_i} \left[S'_{ij} + \frac{A_i T_i}{2} \alpha_i \sin (\gamma_{ij} + \eta_i) \right]^2 \} \ . \qquad \text{(A-18)}$$

This can be written as

$$f(C'_{ij}, S'_{ij} | \phi_i, \theta_i) = \prod_{j=1}^{M} \left(\frac{2}{\pi N_i T_i} \right) \exp\{ \frac{2A_i \alpha_i}{N_i} [C'_{ij} \cos (\gamma_{ij} + \eta_i)$$

$$- S'_{ij} \sin(\gamma_{ij} + \eta_i) - \frac{A_i T_i \alpha_i}{4}] - \frac{2}{N_i T_i} (C'^2_{ij} + S'^2_{ij}) \}$$

$$= \left(\frac{2}{\pi N_i T_i} \right)^M \exp\left[- \frac{M T_i A_i^2 \alpha_i^2}{2N_i} \right] \exp\{ \frac{2A_i \alpha_i}{N_i} [\cos \eta_i \sum_{j=1}^{M} (C'_{ij} \cos \gamma_{ij} -$$

$$S'_{ij} \sin \gamma_{ij}) - \sin \eta_i \sum_{j=1}^{M} (S'_{ij} \cos \gamma_{ij} + C'_{ij} \sin \gamma_{ij})] -$$

$$\frac{2}{N_i T_i} \sum_{j=1}^{M} (C'^2_{ij} + S'^2_{ij}) \} \ . \qquad \text{(A-19)}$$

Now utilizing the definition of the likelihood function as given in Equation (9) of Chapter IV and again following the practice of not redefining the likelihood function when a monotonic function of it is taken because of the equivalence of the likelihood functions,

$$\Lambda(\Delta_i) = \int \exp\left[- \frac{M T_i A_i^2 \alpha_i^2}{2N_i} \right] \exp\{ \frac{2A_i \alpha_i}{N_i} [\cos \eta_i \cdot \sum_{j=1}^{M} (C'_{ij} \cos \gamma_{ij} -$$

$$S'_{ij} \sin \gamma_{ij}) - \sin \eta_i \sum_{j=1}^{M} (S'_{ij} \cos \gamma_{ij} + C'_{ij} \sin \gamma_{ij})] \} f(\eta_i) d\eta_i \ .$$

$$\text{(A-20)}$$

In (A-20) $f(\eta_i)$ refers to the probability density function of η_i. The random variables η_i $(1 \leq i \leq 2K)$ are uniformly distributed on the interval $(-\pi, \pi]$. Therefore, Equation (15) in Chapter IV can be utilized to write (A-20) as

$$\Lambda(\Delta_i) \exp\left[-\frac{MT_i A_i^2 \alpha_i^2}{2N_i}\right] I_o\left[\frac{2A_i \alpha_i F_i}{N_i}\right] \qquad \text{(A-21)}$$

where

$$F_i = \left[\left(\sum_{j=1}^{M} C'_{ij} \cos \gamma_{ij} - \sum_{j=1}^{M} S'_{ij} \sin \gamma_{ij}\right)^2 + \left(\sum_{j=1}^{M} S'_{ij} \cos \gamma_{ij} + \sum_{j=1}^{M} C'_{ij} \sin \gamma_{ij}\right)^2\right]^{1/2}. \qquad \text{(A-22)}$$

The present OPLE ground station and the planned SARCEN call for processing the received signals at frequencies which result when the A/R tone is used for demodulating the folded or compacted spectrum. This will result in processing frequencies of less than 1 kHz. This method of processing results in doppler shifts due to the local oscillator in the SARCOM which will not be removed. Thus, although because of motion of the SARCOM relative to the stations, the elements of the first K and last K sets of signals will be highly correlated; this correlation is not taken advantage of and the doppler shifts are computed separately. Additionally, this method of processing, because of the reasonably unstable oscillator planned for the SARCOM units, will not allow velocity of the SARCOM to be predicted with any confidence [28].

Reference [28] also contains a doppler estimation procedure which is similar to the results of this appendix although nonoptimum.

Evaluation of (A-21) over an expected range of doppler shifts in increments for each signal will yield estimates of the doppler shift of each of the 2K signals. These values of Δ_i ($1 \leq i \leq 2K$) can be used to find the values of α_i ($1 \leq i \leq 2K$) and γ_{ij} ($1 \leq i \leq 2K$, $1 \leq j \leq M$). Substitutions of these values into the equations

$$C_{ij} = \frac{1}{\alpha_i} C'_{ij} \cos \gamma_{ij} - \frac{1}{\alpha_i} S'_{ij} \sin \gamma_{ij} , \qquad \text{(A-23a)}$$

$$S_{ij} = \frac{1}{\alpha_i} C'_{ij} \sin \gamma_{ij} + \frac{1}{\alpha_i} S'_{ij} \cos \gamma_{ij} , \qquad \text{(A-23b)}$$

$$C_i = \sum_{j=1}^{M} C_{ij} , \qquad \text{(A-24a)}$$

and

$$S_i = \sum_{j=1}^{M} S_{ij} \qquad \text{(A-24b)}$$

for all i ($1 \leq i \leq 2K$) yields the desired doppler corrected data. The data elements C_i and S_i can be shown, following the procedure in the first part of this appendix, to be Gaussian random variables with expected values

$$E(C_i \mid \theta_i, \phi_i) = \frac{A_i M T_i}{2} \cos(-\phi_i + \theta_i) \qquad \text{(A-25a)}$$

and

$$E(S_i \mid \theta_i, \phi_i) = -\frac{A_i M T_i}{2} \sin(-\phi_i + \theta_i) . \qquad \text{(A-25b)}$$

Their variance will be

$$\text{VAR}\ (C_i \mid \theta_i, \phi_i) = \text{VAR}\ (S_i \mid \theta_i, \phi_i) = \frac{N_i M T_i}{4\alpha_i^2} \qquad \text{(A-26)}$$

As the magnitude of the doppler shift of the ith signal increases causing $\Delta_i T_i \to \pm 2\pi$, α_i^2 will approach zero as seen by (A-10). The variance of the data will get very large and the data will have an extremely small SNR. A standard $\frac{\sin d}{d}$ curve will show that for $\Delta_i T_i = \pm \pi$, $\alpha_i^2 = 4/\pi^2 \approx 0.4$. In other words, since T_i is nominally one sec. for all i, doppler shifts of magnitude $\leq$ 0.5 Hz can be corrected with a deterioration in SNR of $\leq$ 4 dB. A doppler shift of 0.5 Hz corresponds to a relative velocity of in excess of 10,000 nmi/hr at the VLF frequencies, so with proper processing at the ground station utilizing the A/R tone, doppler shifts which are experienced in GRAN should be able to be estimated with little deterioration in SNR.

APPENDIX B

SIGNAL AMPLITUDE AND NOISE DENSITY ESTIMATION

The maximum likelihood estimator derived in Chapter IV requires an estimate of the signal amplitude and noise spectral density height. It will be assumed that the data available for this estimation is the received data corrected for doppler shift utilizing the estimation results of Appendix A. Therefore, the values of the Gaussian random variables C_{ij} and S_{ij} ($1 \leq i \leq 2K$, $1 \leq j \leq M$) given by Equation (A-23) will be the data. The value of K and M, as before, denote the number of frequencies and received Omega pulses respectively. The random variables C_{ij} and S_{ij} after correction for doppler shift will have conditional mean values and variance given by

$$E(C_{ij} \mid \theta_i, \phi_i) = \frac{A_i T_i}{2} \cos(-\phi_i + \theta_i) , \qquad \text{(B-1a)}$$

$$E(S_{ij} \mid \theta_i, \phi_i) = -\frac{A_i T_i}{2} \sin(-\phi_i + \theta_i) \qquad \text{(B-1b)}$$

and

$$VAR(C_{ij} \mid \theta_i, \phi_i) = VAR(S_{ij} \mid \theta_i, \phi_i) = \frac{N_i T_i}{4\alpha_i^2} . \qquad \text{(B-1c)}$$

In (B-1), A_i is the amplitude, T_i the pulse duration, ϕ_i the propagation phase delay, θ_i the random phase shift and $N_i/2$ the two-sided noise density height of the ith signal

$(1 \leq i \leq 2K)$. Also in (B-1)

$$\alpha_i = \frac{\sin(\frac{\Delta_i T_i}{2})}{\frac{\Delta_i T_i}{2}} \quad , \tag{B-2}$$

where Δ_i here is the estimated doppler shift of the ith signal. The estimate of the value of Δ_i and thus α_i will be considered known for this derivation since it was assumed as the first processing step.

The joint conditional probability density function of the data from the ith signal is

$$f(C_{ij}, S_{ij} \mid \theta_i, \phi_i) = (\frac{2\alpha_i^2}{\pi N_i T_i})^M \cdot$$

$$\exp\{-\frac{2\alpha_i^2}{N_i T_i}[\sum_{j=1}^{M}(C_{ij} - \frac{A_i T_i}{2}\cos\eta_i)^2 +$$

$$\sum_{j=1}^{M}(S_{ij} + \frac{A_i T_i}{2}\sin\eta_i)^2]\} \tag{B-3}$$

where

$$\eta_i = -\phi_i + \theta_i \cdot \tag{B-4}$$

This joint conditional density function can be written as

$$f(C_{ij}, S_{ij} \mid \theta_i, \phi_i) = (\frac{2\alpha_i^2}{\pi N_i T_i})^M \cdot$$

$$\exp\left\{-\frac{2\alpha_i^2}{N_i T_i}\left[\xi_i + \frac{A^2{}_i MT^2{}_i}{4} - A_i T_i C_i \cos\eta_i + A_i T_i \sin\eta_i\right]\right\} \qquad \text{(B-5)}$$

where

$$\xi_i = \sum_{j=1}^{M} (C_{ij}^2 + S_{ij}^2) , \qquad \text{(B-6a)}$$

$$C_i = \sum_{j=1}^{M} C_{ij} \qquad \text{(B-6b)}$$

and

$$S_i = \sum_{j=1}^{M} S_{ij} . \qquad \text{(B-6c)}$$

The definition of the likelihood function was given in Equation (9) of Chapter IV. Again, the practice of not re-defining the likelihood function when a monotonic function of it is taken will be followed because of the equivalence of the likelihood functions. The likelihood function for amplitude and noise density estimation can thus be written as

$$\Lambda(A_i,N_i) = \frac{1}{N_i{}^M}\int \exp\left[-\frac{2\alpha_i^2}{N_i T_i}\left(\xi_i + \frac{A_i{}^2 MT_i{}^2}{4}\right)\right] \cdot \exp\left[\frac{2\alpha_i{}^2 A_i}{N_i}\left(C_i \cos\eta_i - S_i \sin\eta_i\right)\right] \cdot f(\eta_i)\, d\eta_i . \qquad \text{(B-7)}$$

$f(\eta_i)$ in (B-7) is the probability density function of η_i. In Chapter II θ_i $(1 \leq i \leq K)$ were shown to be uniformly distributed on $(-\pi, \pi]$, so all the η_i will also have this density function. This and Equation (15) in Chapter IV allow the likelihood equation to be written as

$$\Lambda(A_i\ N_i) = \frac{1}{N_i^M} \exp\left[-\frac{2\alpha_i^2}{N_i T_i}\left(\xi_i + \frac{A_i^2 M T_i^2}{4}\right)\right].$$

$$I_o\left(\frac{2\alpha_i^2 A_i \beta_i}{N_i}\right) \tag{B-8}$$

where

$$\beta_i = (C_i^2 + S_i^2)^{1/2} . \tag{B-9}$$

$I_o(\cdot)$ in (B-8) is the zero order modified Bessel function of the first kind.

For estimation of A_i, the likelihood function is written as

$$\Lambda(A_i) = \exp\left(-\frac{A_i^2 M T_i \alpha_i^2}{2N_i}\right) \quad I_o\left(\frac{2\alpha_i^2 A_i \beta_i}{N_i}\right) . \tag{B-10}$$

Taking the partial derivative of (B-10) with respect to A_i and setting the result equal to zero yields

$$\hat{A}_i = \frac{2\beta_i}{MT_i} \frac{I_1\left(\frac{2\alpha_i^2 \hat{A}_i \beta_i}{N_i}\right)}{I_o\left(\frac{2\alpha_i^2 \hat{A}_i \beta_i}{N_i}\right)} \tag{B-11}$$

where $\hat{A}_i$ is the estimate of A_i and $I_1(\cdot)$ is the first order modified Bessel function of the first kind.

For estimation of N_i, the likelihood function is written as

$$\Lambda(N_i) = \frac{1}{N_i^M} \exp\left[-\frac{2\alpha_i^2}{N_i T_i}\left(\xi_i + \frac{A_i^2 M T_i^2}{4}\right)\right] \cdot$$

$$I_o\left(\frac{2\alpha_i^2 A_i \beta_i}{N_i}\right) . \qquad \text{(B-12)}$$

Taking the partial derivative of (B-12) with respect to N_i and setting the result equal to zero yields

$$\hat{N}_i = \frac{2\alpha_i^2 \xi_i}{M T_i} + \frac{\alpha_i^2 A_i^2 T_i}{2} - \frac{2\alpha_i^2 A_i \beta_i}{M} \frac{I_1\left(\frac{2\alpha_i^2 A_i \beta_i}{N_i}\right)}{I_o\left(\frac{2\alpha_i^2 A_i \beta_i}{N_i}\right)} \qquad \text{(B-13)}$$

where $\hat{N}$ is the estimate of N_i.

Equations (B-11) and (B-13) do not have the values to be estimated isolated and further, they must be jointly estimated since each estimate is dependent upon the result of the other. A convenient method of jointly solving the equations is to isolate the ratio $I_1(\cdot)/I_o(\cdot)$ in each equation and equate them. This yields

$$\hat{N}_i = \frac{2\alpha_i^2 \xi_i}{M T_i} - \frac{\hat{A}_i^2 T_i \alpha_i^2}{2} . \qquad \text{(B-14)}$$

Substitution of this value of $\hat{N}_i$ into (B-11) yields

$$\hat{A}_i = \frac{2\beta_i}{MT_i} \frac{I_1\left(\frac{4\hat{A}_i\beta_i MT_i}{4\xi_i - M\hat{A}_i^2 T_i^2}\right)}{I_o\left(\frac{4\hat{A}_i\beta_i MT_i}{4\xi_i - M\hat{A}_i^2 T_i^2}\right)} \quad . \tag{B-15}$$

Equation (B-15) can be iteratively solved for $\hat{A}_i$ now and using the resultant value of $\hat{A}_i$ in (B-14) yields an estimated value for $\hat{N}_i$.

In order to discover a method convenient to solve (B-15) iteratively, the following was done. For relatively small $\hat{N}_i$, in other words high SNR, from (B-14)

$$\frac{2\alpha_i^2\xi_i}{MT_i} \rightarrow \frac{A_i^2 T_i \alpha_i^2}{2} \quad . \tag{B-16}$$

Or

$$\xi_i \rightarrow \frac{MA_i^2 T_i^2}{4} \quad , \tag{B-17}$$

which implies the argument of the Bessel functions in (B-15) are large. For large arguments, $I_o(\cdot)$ and $I_1(\cdot)$ are approximately equal [27]; therefore, for high SNR

$$\hat{A}_i \approx \frac{2\beta_i}{MT_i} \quad . \tag{B-18}$$

If this value is formed from the data for each i ($1 \leq i \leq 2K$) and defined as an initial condition for an iterative process

$$\hat{A}_{i,o} = \frac{2\beta_i}{MT_i} , \tag{B-19}$$

the (N+1)st iteration value for $\hat{A}_i$ can be shown to be

$$\hat{A}_{i,N+1} = (\hat{A}_{i,o}) \frac{I_1 \left(\frac{2\hat{A}_{i,N}^2 \, M^2 T_i^2}{4\xi_i - \hat{A}_{i,N}^2 \, MT_i^2} \right)}{I_o \left(\frac{2\hat{A}_{i,N}^2 \, M^2 T_i^2}{4\xi_i - \hat{A}_{i,N}^2 \, MT_i^2} \right)} . \tag{B-20}$$

A computer program was written to do the iterative processing in (B-20). By substituting the resulting estimate of A_i into (B-14) an estimate of N_i was obtained. The flow chart of the computer program is contained in Appendix E. From these estimates, the signal-to-noise ratios in one Hz which the Omega signals have at the front end of the SARCOM receiver can be estimated from

$$SNR = \frac{\hat{A}_i^2}{2\hat{N}_i} . \tag{B-21}$$

The results of evaluating (B-21) with the four-frequency data obtained from the experiment discussed in Chapter VI are presented in Figures B1 - B24. Because of the significant diurnal effects on phase velocity, as discussed in

Chapter II, the data has been divided into three major categories. Both transmission paths in daylight is referred to as "Day" condition, both paths dark is referred to as "Night" condition and partially lighted paths is referred to as "Transition" condition. The SNR estimation results of the first five-day data period were so little different from the second five-day period that the two periods have been combined. The power radiated by the Forestport Omega station for the data collection periods was varied over quite a wide range as weather conditions varied. Radiated powers on the order of 100-200 watts for the lower three frequencies and 200-400 watts for 13.6 kHz were typical. The radiated power from the Trinidad station was on the order of 1 kW for all frequencies. The finally implemented Omega stations are expected to radiate 10 kW at all frequencies consistently.

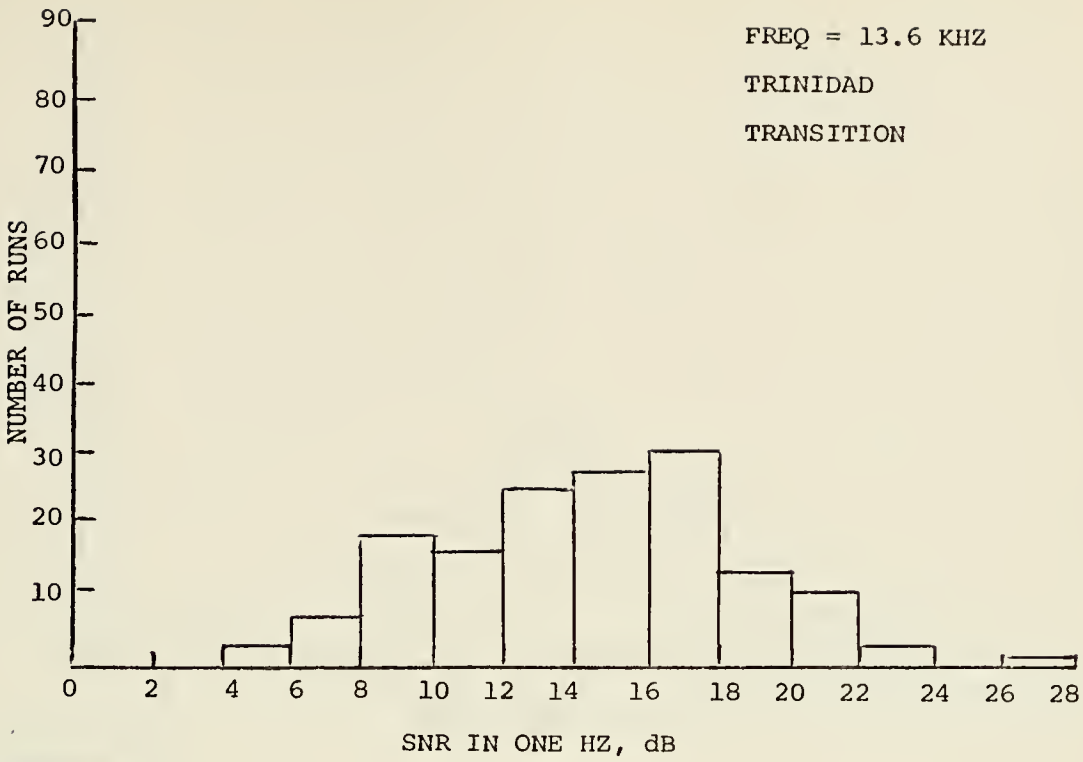

Figure B1.

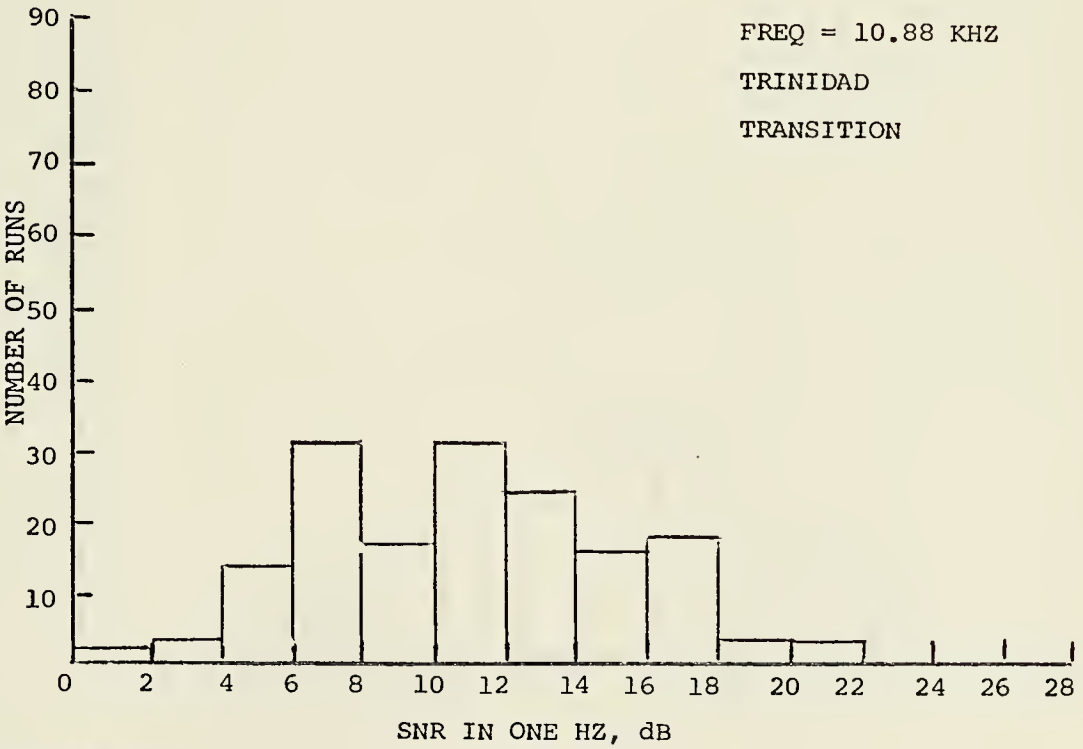

Figure B2.

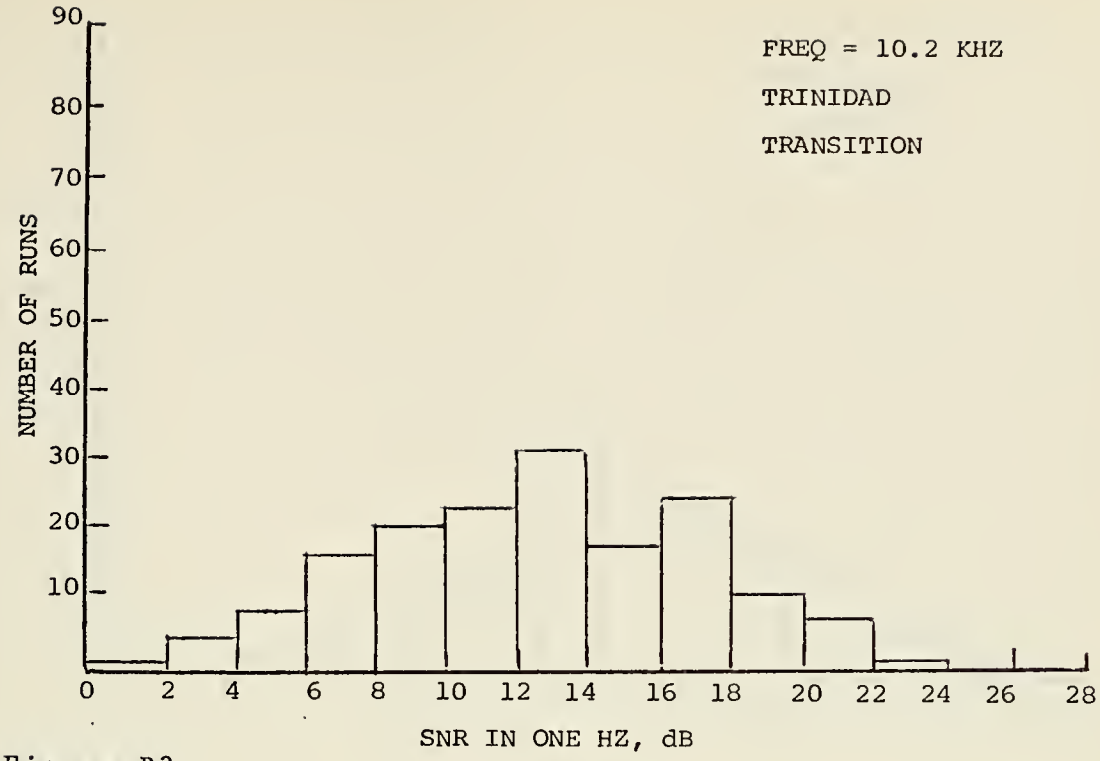

Figure B3.

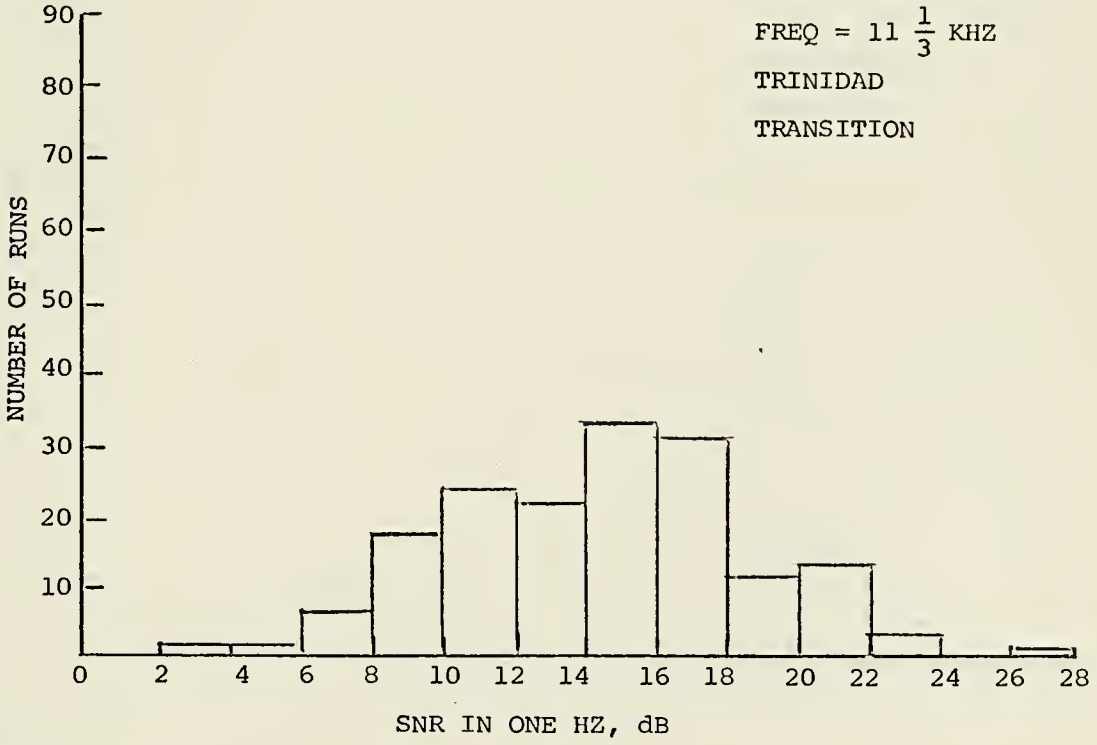

Figure B4.

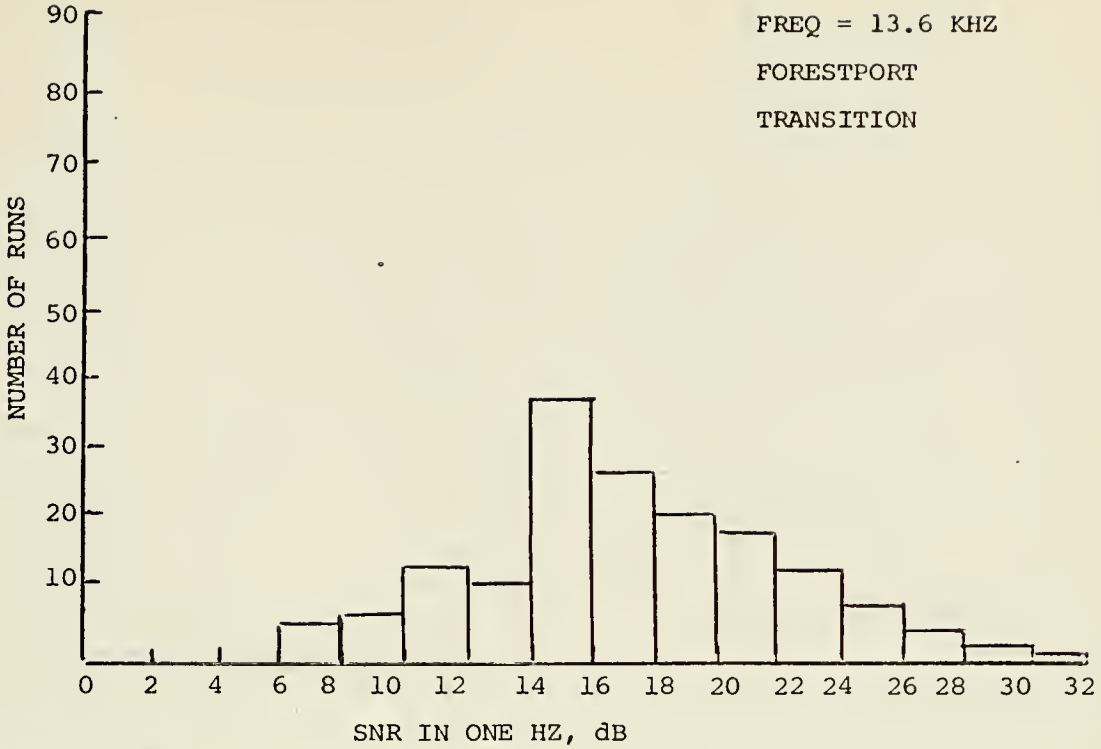

Figure B5.

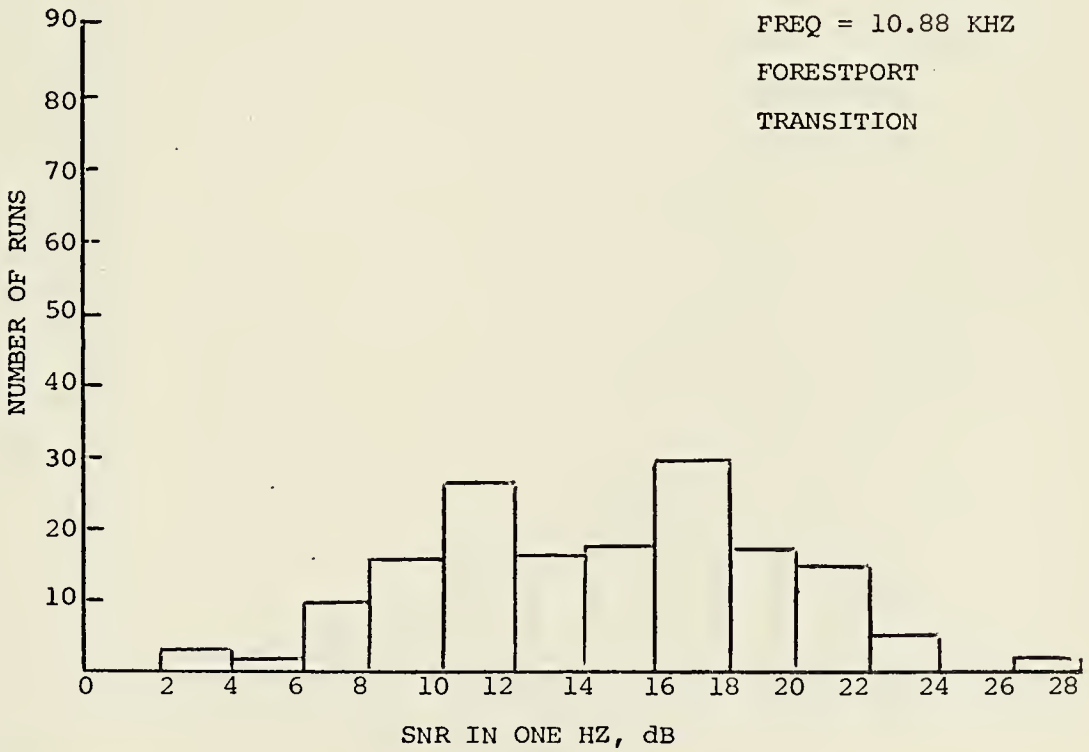

Figure B6.

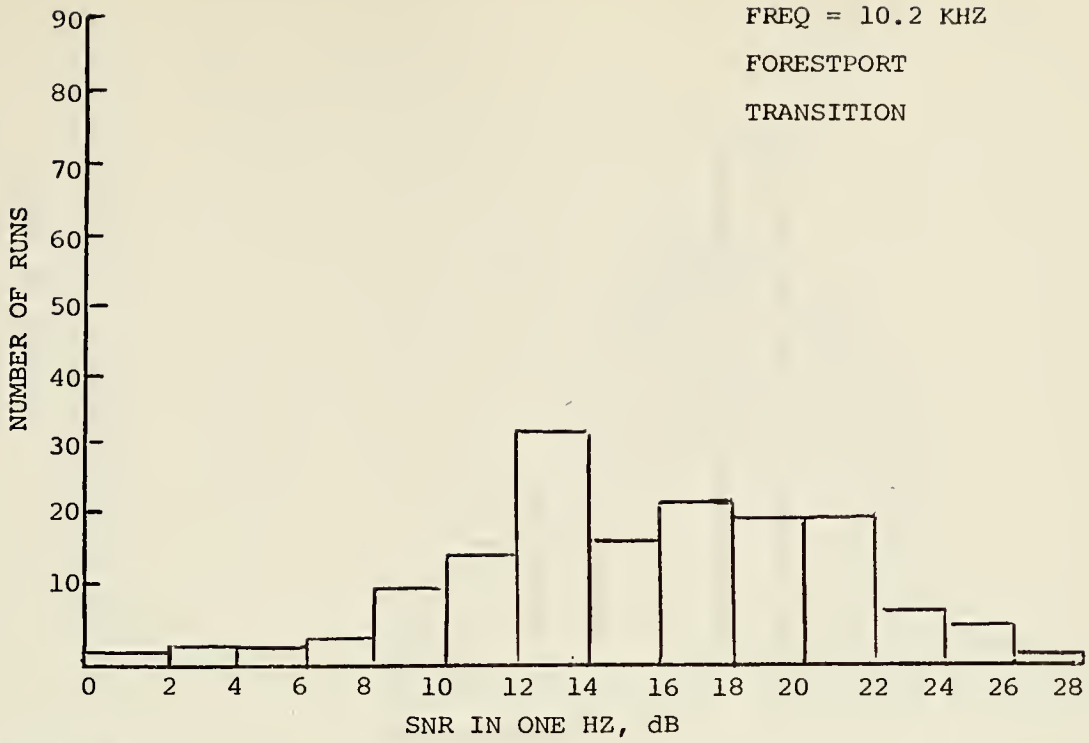

Figure B7.

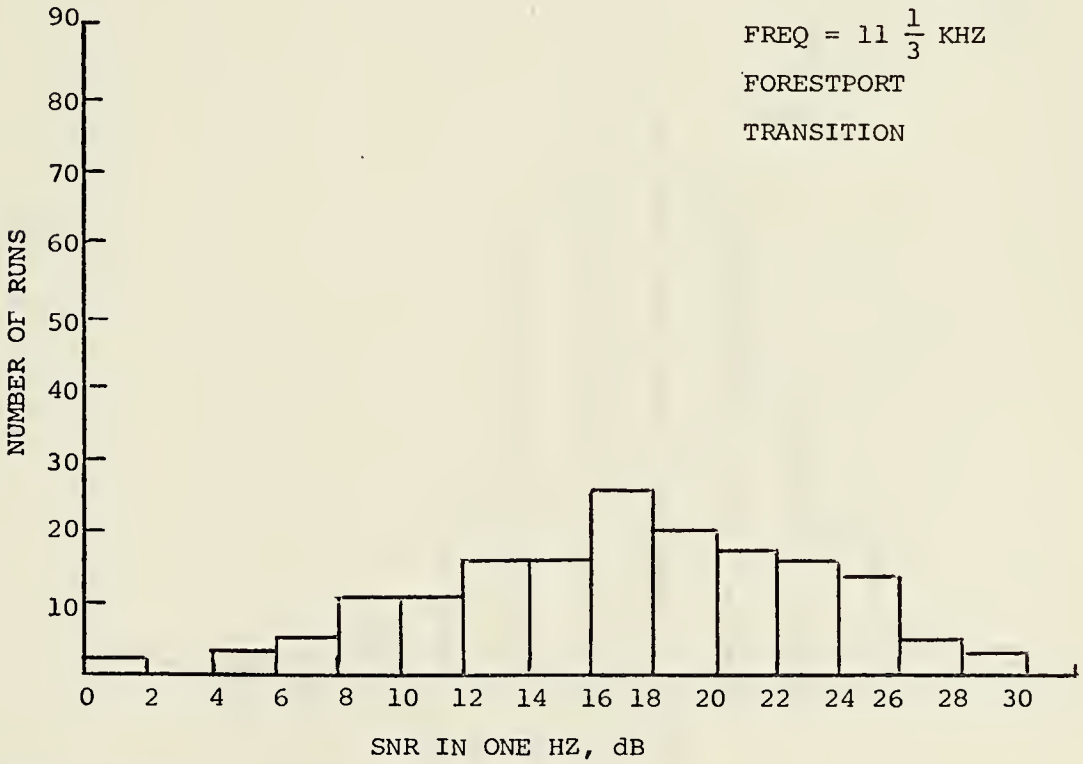

Figure B8.

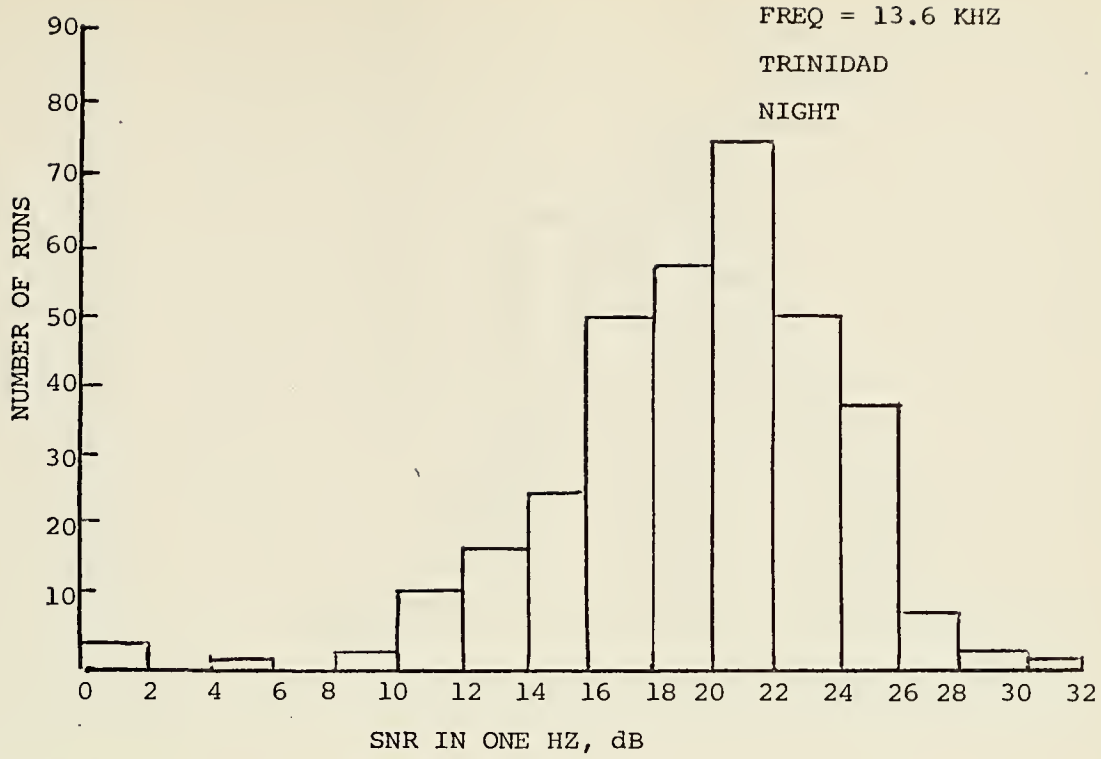

Figure B9.

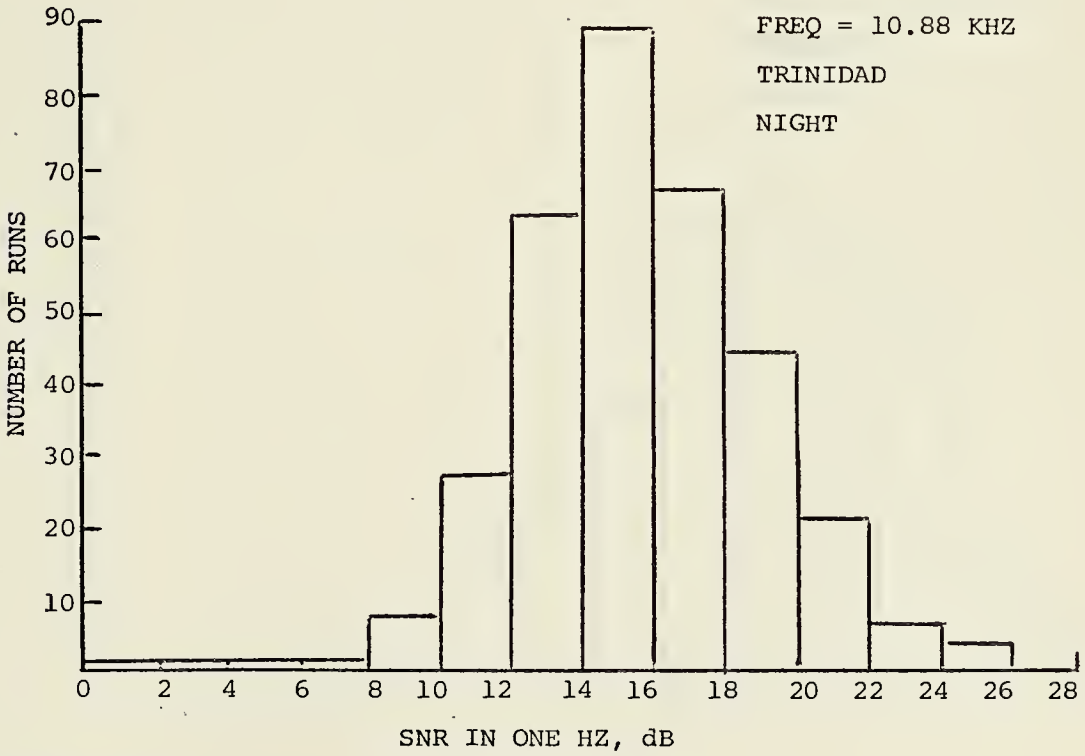

Figure B10.

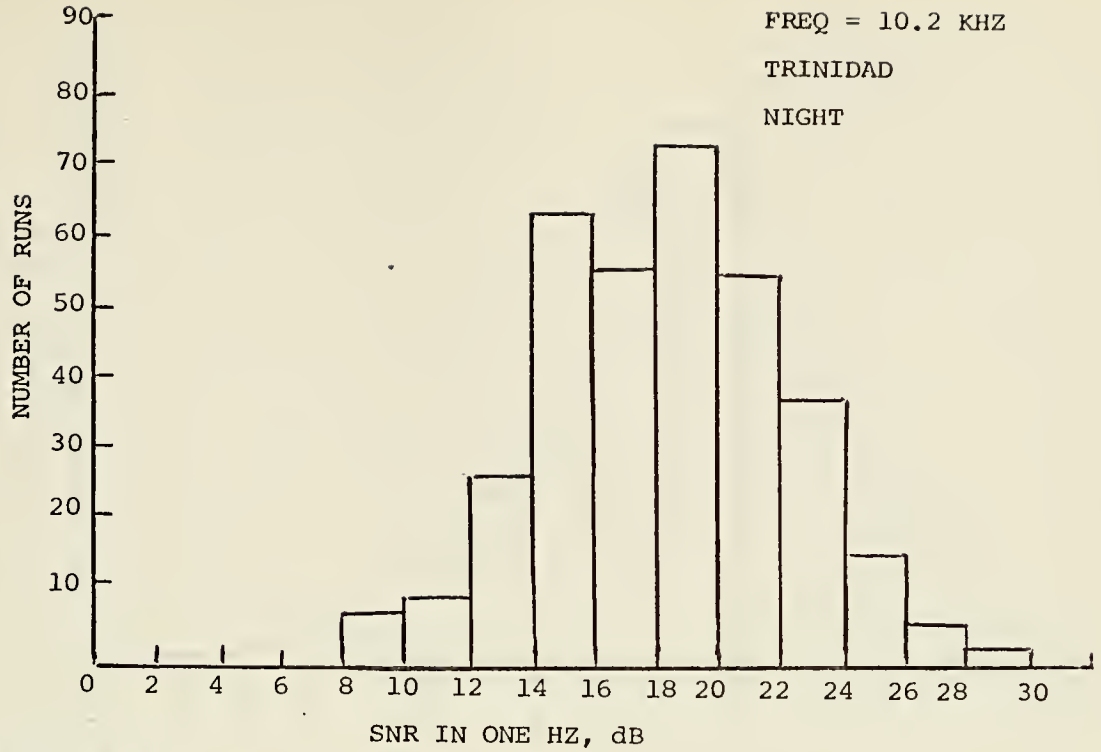

Figure B11.

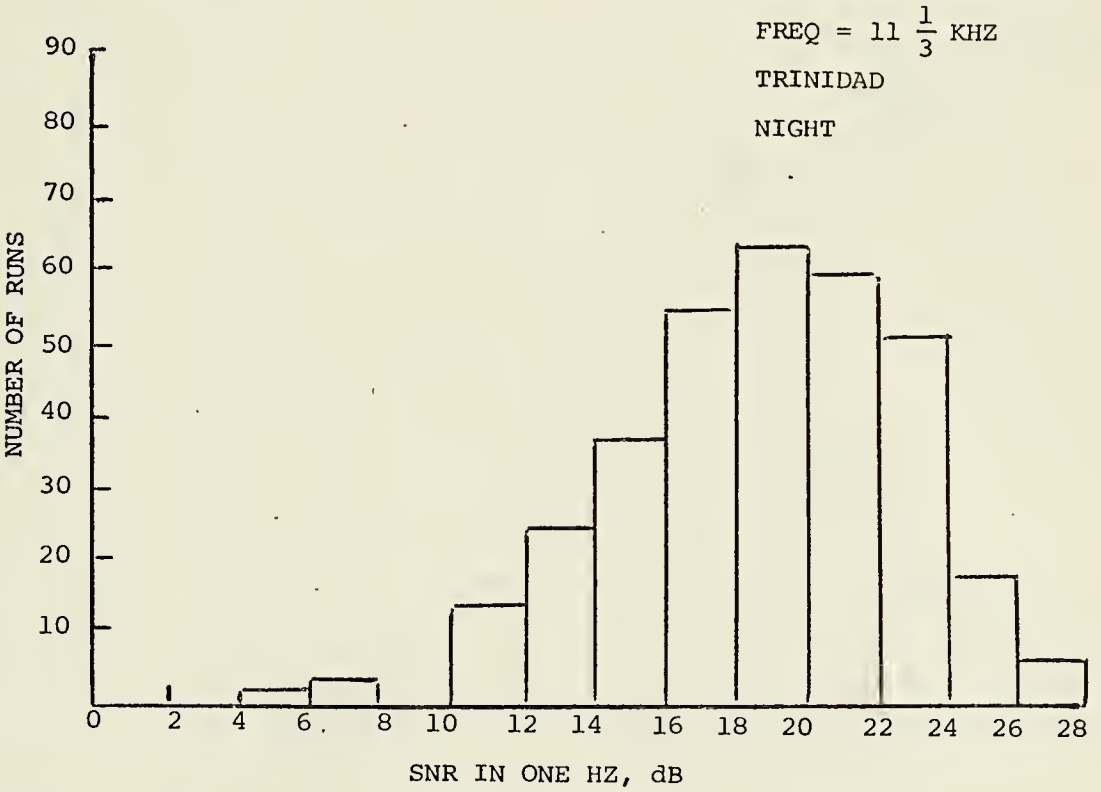

Figure B12.

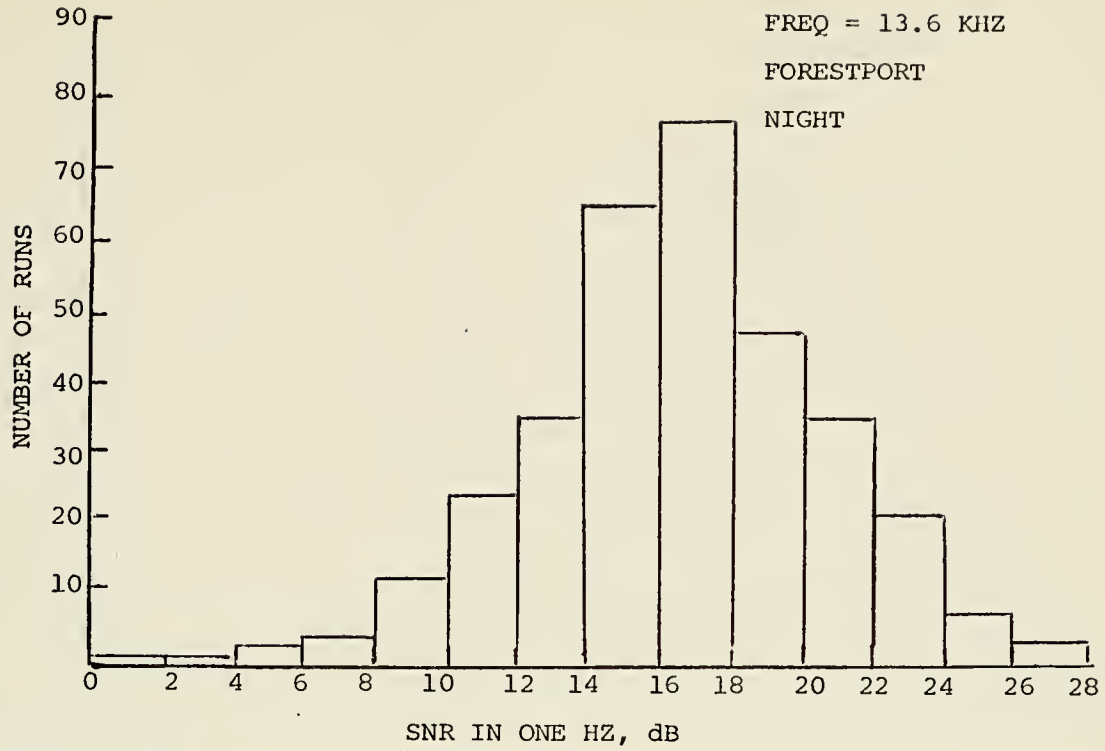

Figure B13.

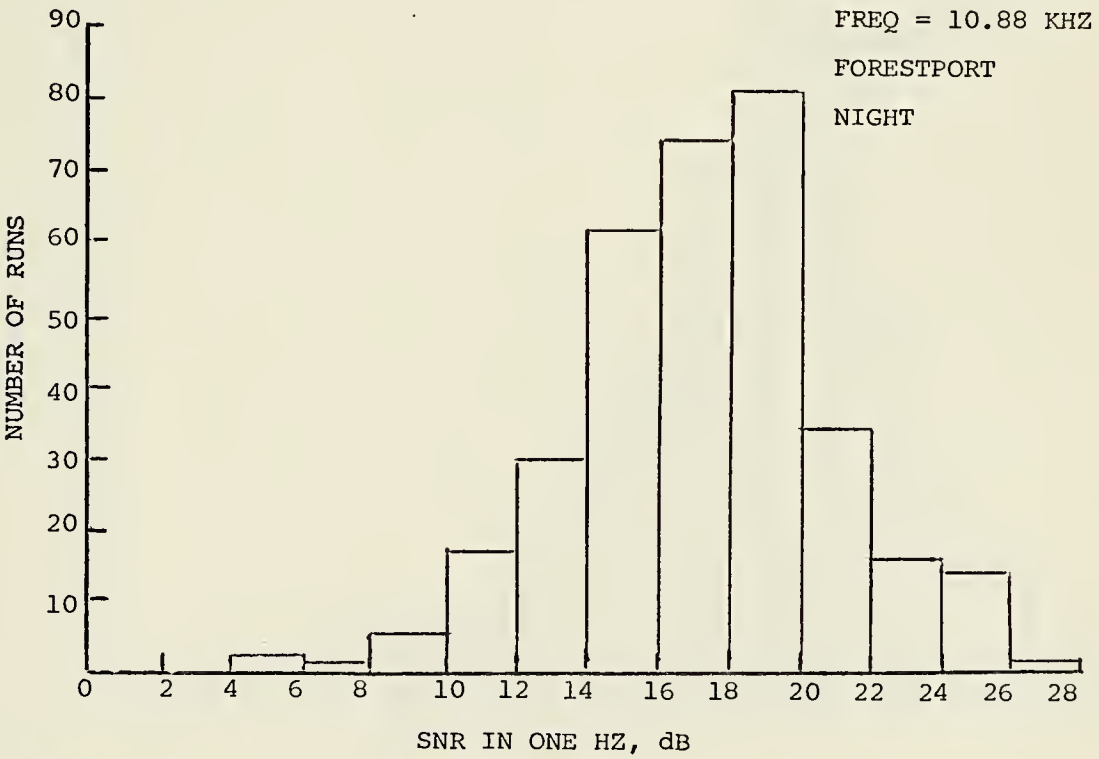

Figure B14.

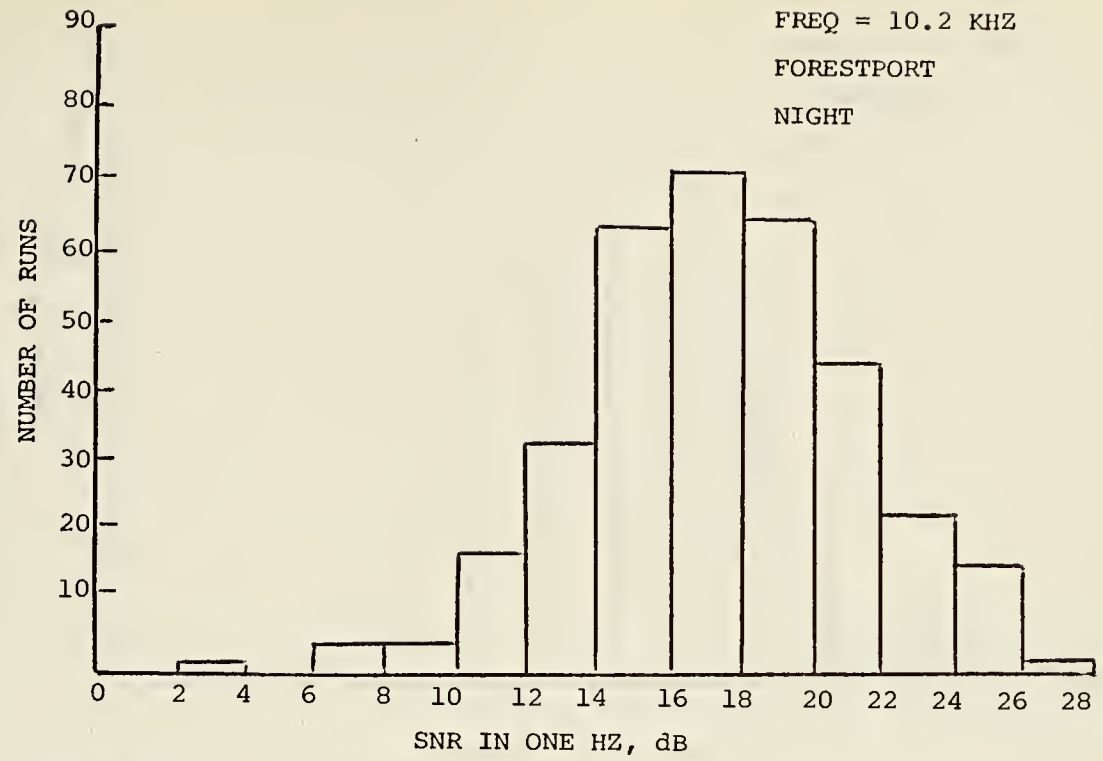

Figure B15.

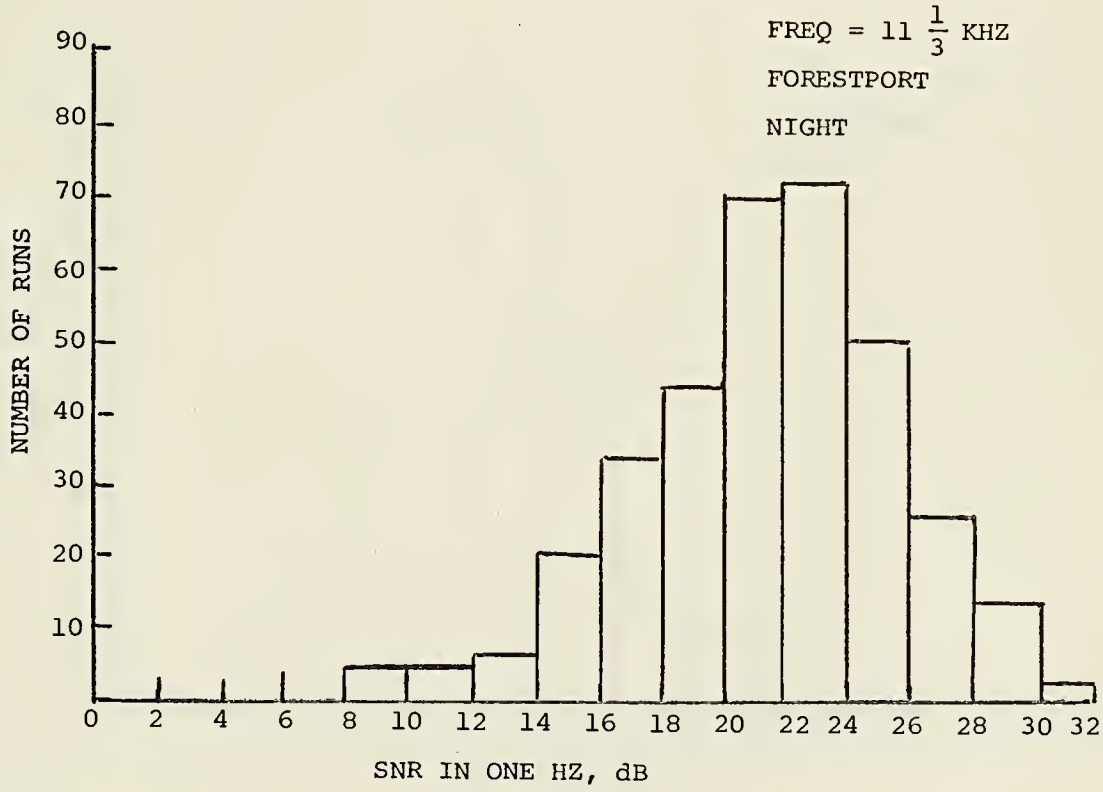

Figure B16.

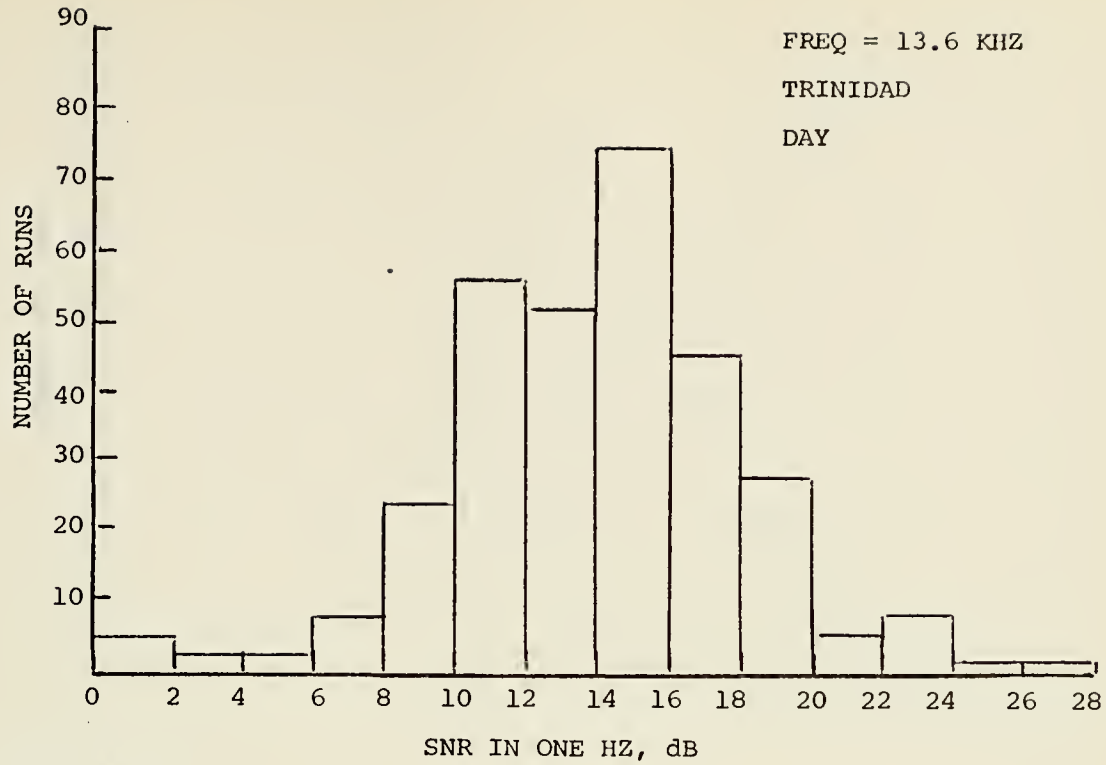

Figure B17.

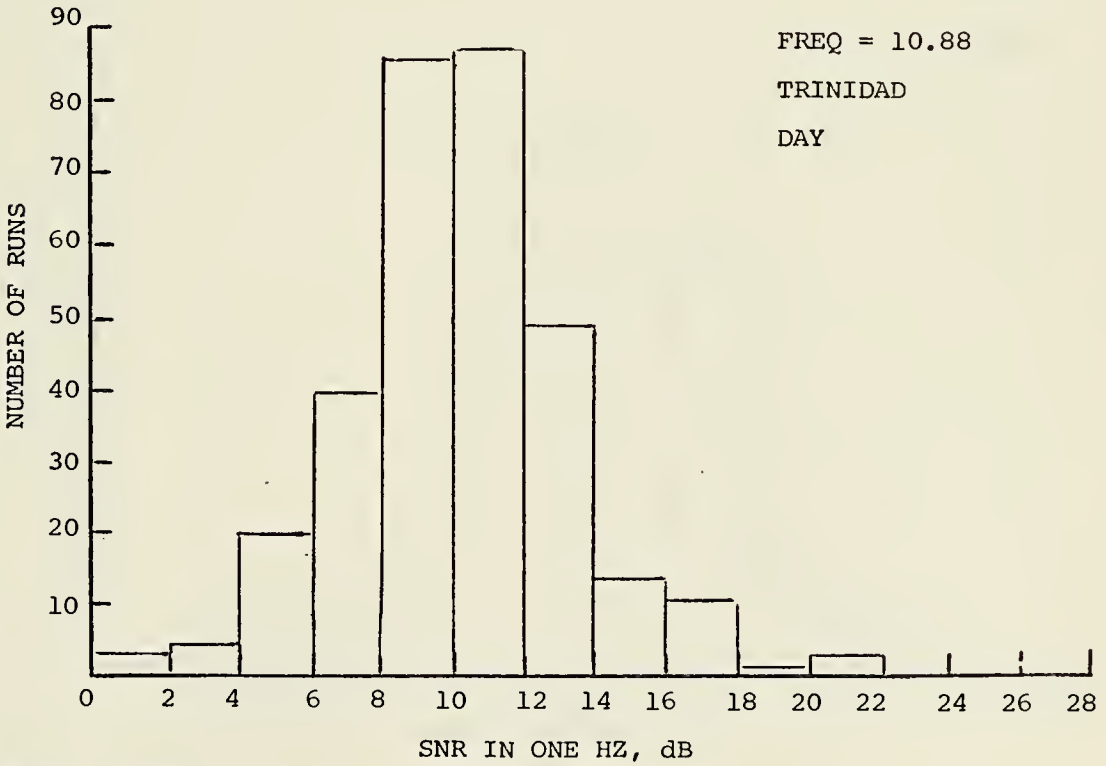

Figure B18.

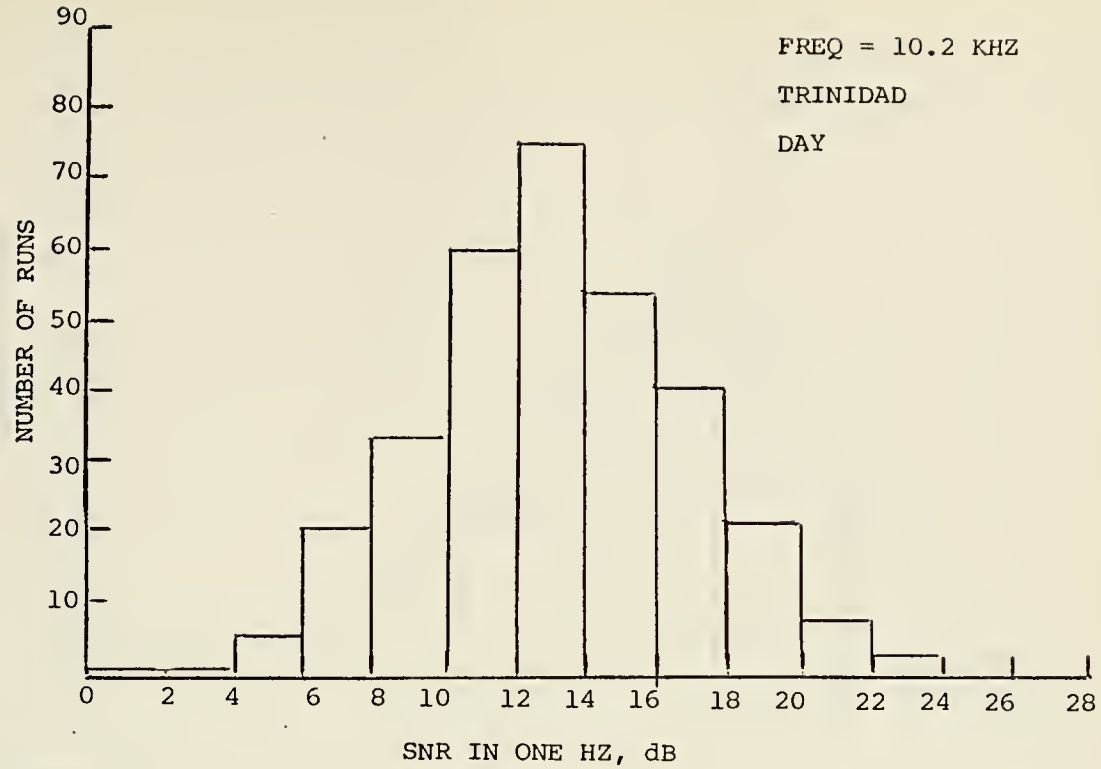

Figure B19.

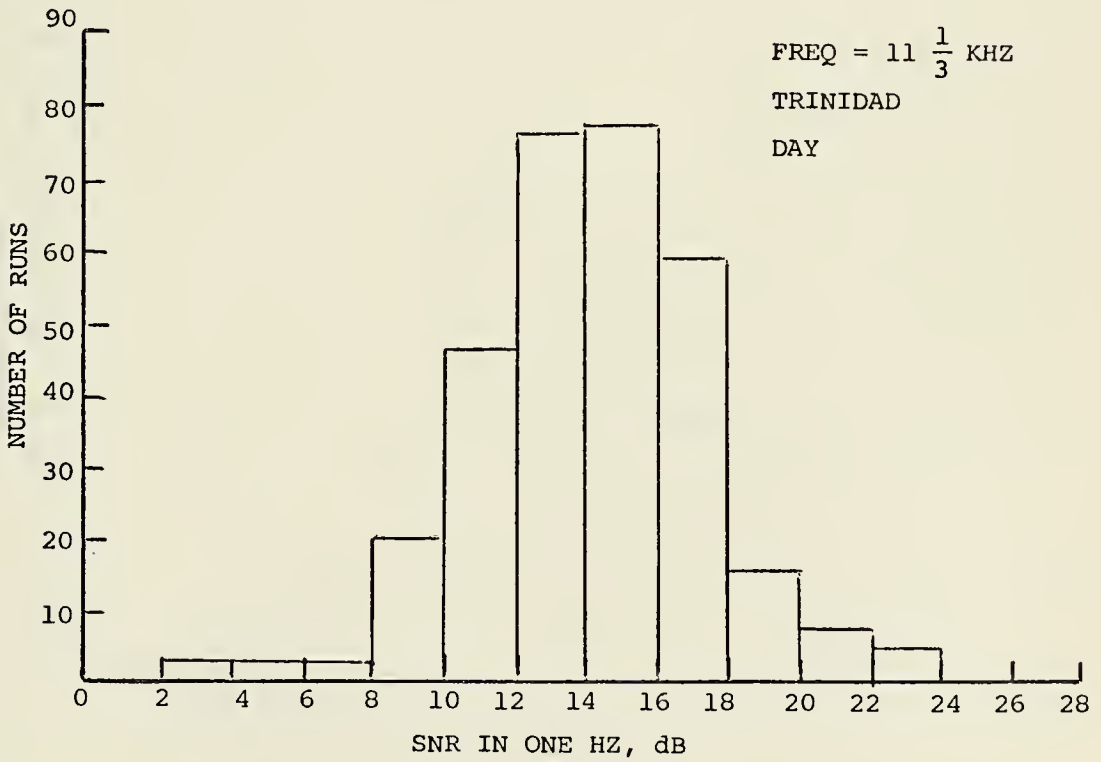

Figure B20.

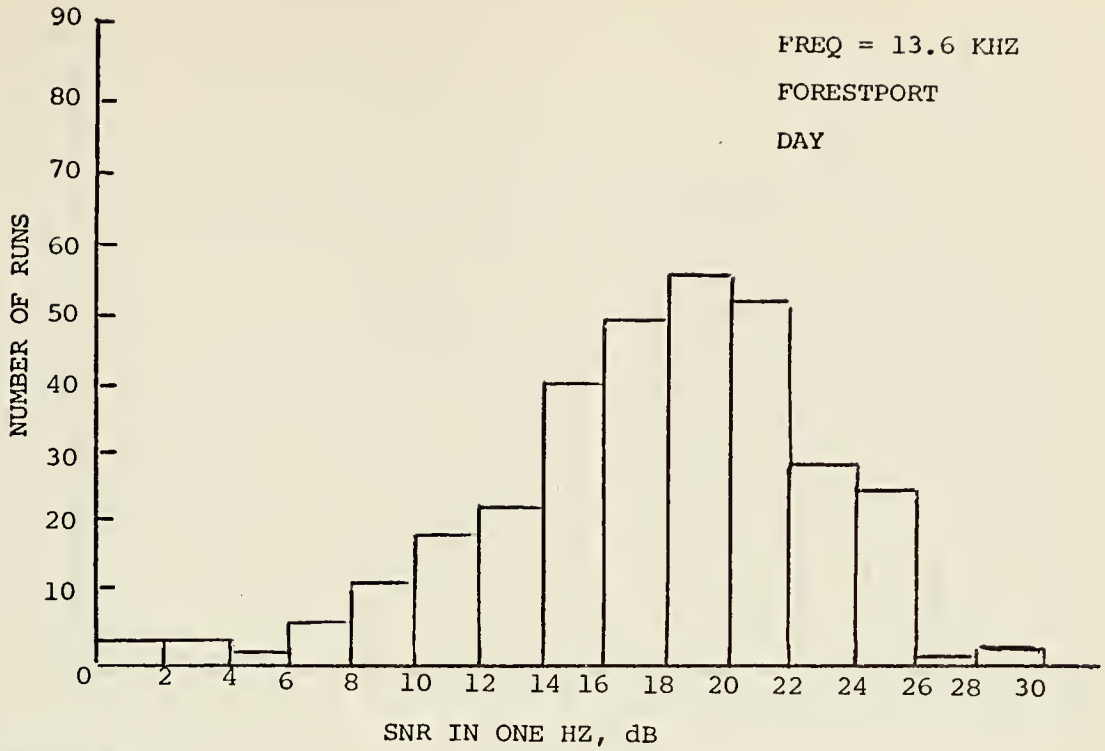

Figure B21.

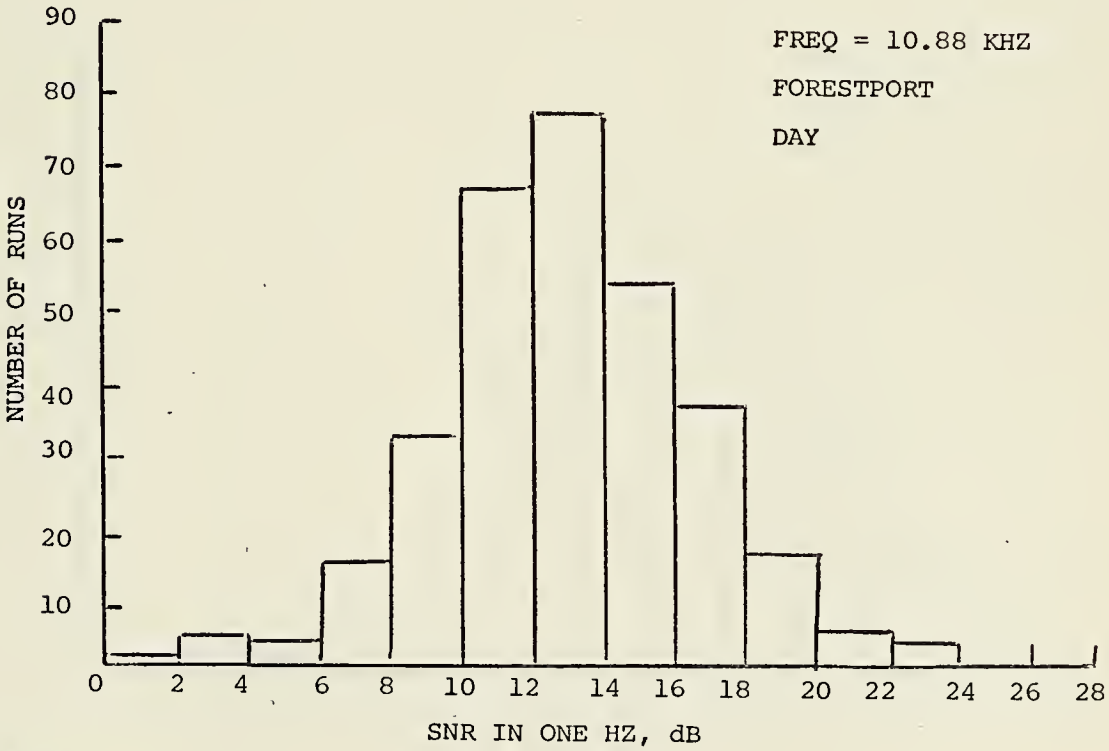

Figure B22.

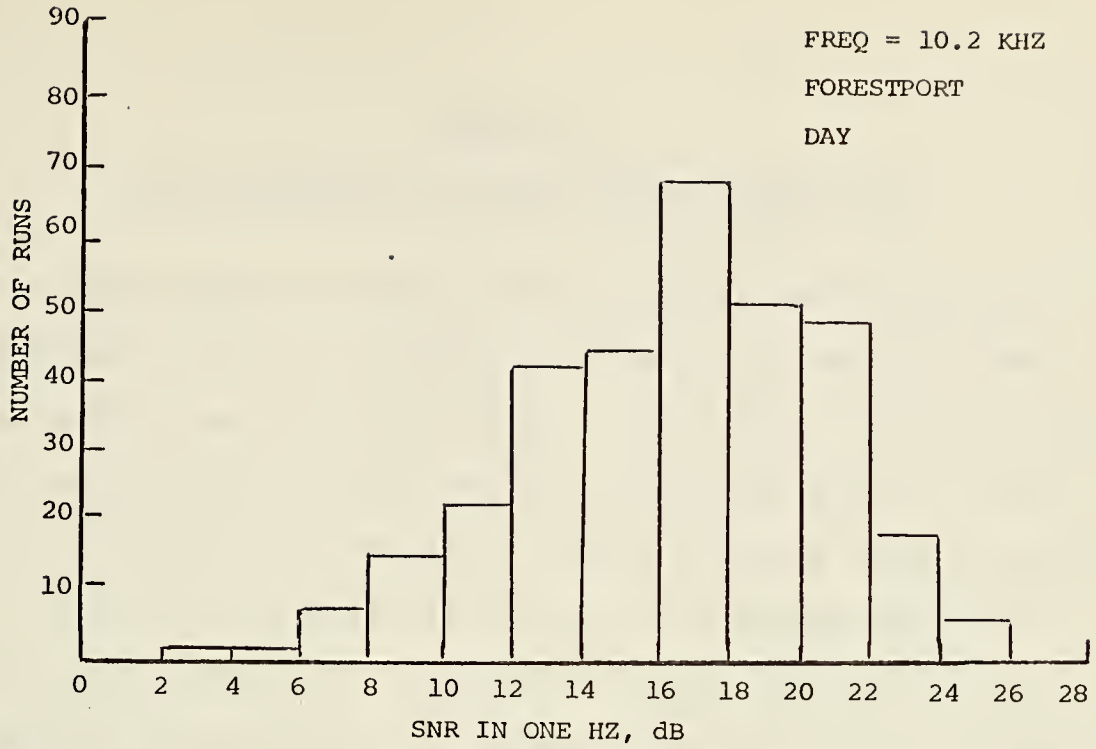

Figure B23.

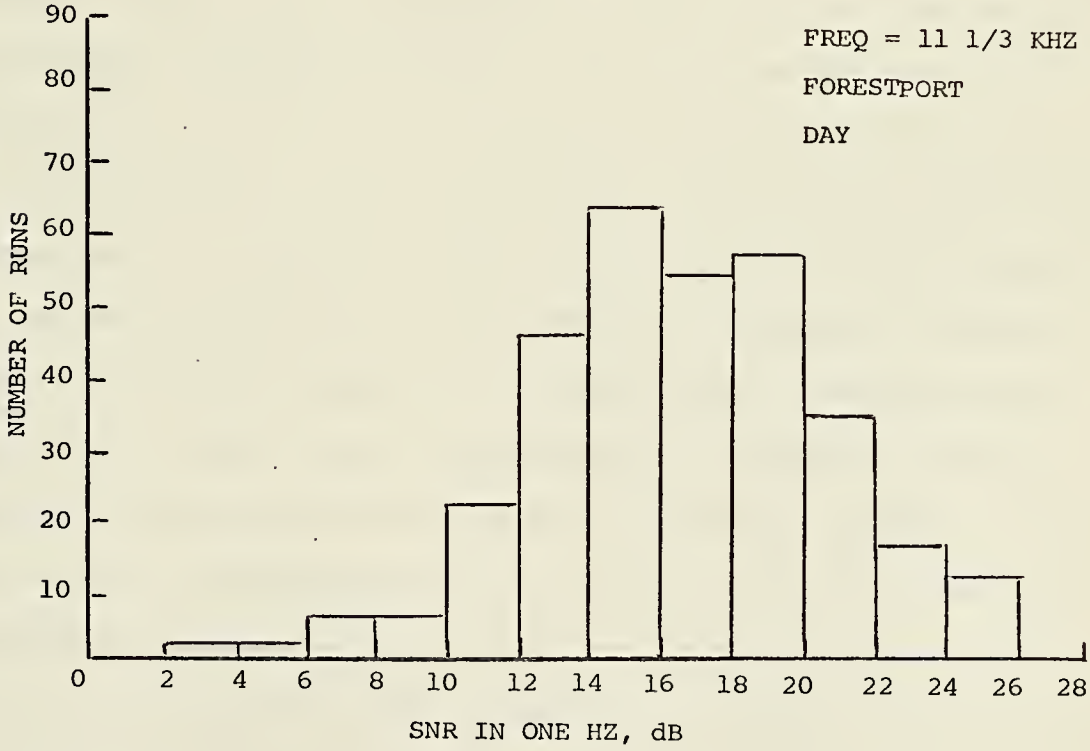

Figure B24.

APPENDIX C

LOP ESTIMATION FOR KNOWN PHASE VELOCITIES

In developing the model for the estimation problem to be solved, the first approach which was used was to assume the phase velocities were well known. The values of phase velocities which were intended for use were those given in Table II, the first mode propagation values obtained from Professor J. A. Pierce of Harvard University. The derivation of the likelihood function for this model is carried out in this appendix. Simulations with several possible fourth frequencies were carried out and they are presented here to serve as an upper bound for the performance which can be expected from the maximum likelihood estimator when the uncertainties in the phase velocities are accounted for in the derivation.

The difficulty with assuming well known phase velocities is that as the signal-to-noise ratio gets reasonably large, the estimator places great confidence in the data received. Since the additive noise is the only factor disturbing the data in the known phase velocity model, as SNR increases, very good data would be expected. Literature search and some preliminary experimental data processing revealed that the assumption of known phase velocities is not justifiable in a model and thus the model described in Chapter II was created. Because of its value in bounding the performance of the estimator and in obtaining a feel for the problem, the known

phase velocity estimator is derived herein.

As was pointed out in Chapter IV, Equation (16) can be used as a starting point for the known phase velocity estimator derivation since no approximations or operations involving the phase velocities' randomness have been performed. Therefore we have as a likelihood function

$$\Lambda(x) = \prod_{i=1}^{K} I_o \{[R_i^2 + R_{K+i}^2 + 2R_i R_{K+i} \cos \psi_i]^{1/2}\} \quad \text{(C-1)}$$

where the variables in (C-1) are defined as in Chapter IV. For high SNR, the same arguments as applied in Chapter IV can be applied. The likelihood equation can thus be written as in Chapter IV, Equation (30) as

$$\Lambda(x) = \exp \left[\sum_{i=1}^{K} Q_i \psi_i^2 \right] \quad \text{(C-2)}$$

since no application of the randomness of the phase velocities was made to that point. In (C-2) Q_i and ψ_i are defined as in Chapter IV, Equations (17) and (31). The log-likelihood function, an equivalent likelihood function to maximize, is convenient to form here, particularly for computer evaluation to avoid overflow problems. Therefore,

$$\Lambda(x) = \sum_{i=1}^{K} Q_i \psi_i^2 \, . \quad \text{(C-3)}$$

Monte Carlo simulation for several fourth frequencies which could easily be added to the Omega format was carried out

utilizing the estimation Equation (C-3). The results of the simulation in terms of the probability of lane error occurrence are presented in Figure C1. The definition of lane error here is as defined in Chapters IV & V.

Two general conclusions can be drawn from the simulation assuming known phase velocities. First, since there is a degradation in probability of lane error on the order of .1 to .2 in going from unambiguous lane size of a nominal 500 nmi to approximately 1000 nmi, the latter size can serve as a soft upper bound in selecting fourth frequencies to do simulations when jointly Gaussian distributed phase velocities are assumed. Second, a fourth frequency of 12.364 kHz which results in a nominal 785 nmi unambiguous lane appears to be worse in terms of lane error probability than either 10.462 kHz or 10.737 kHz which result in nominal 927 nmi and 1356 nmi unambiguous lane sizes respectively. This implies that frequencies chosen from the lower part of the 10-14 kHz spectrum can be expected to yield better estimation results than those chosen from the upper part of the spectrum in terms of lane error probability. This can be explained by the fact that the ith frequency being higher yields adjacent maxima of the ith component of the likelihood function which are closer together and thus the chances of small perturbations in the phase of the ith signal caused by noise will more readily cause the peak of the likelihood function associated with the incorrect LOP to be larger than the correct peak.

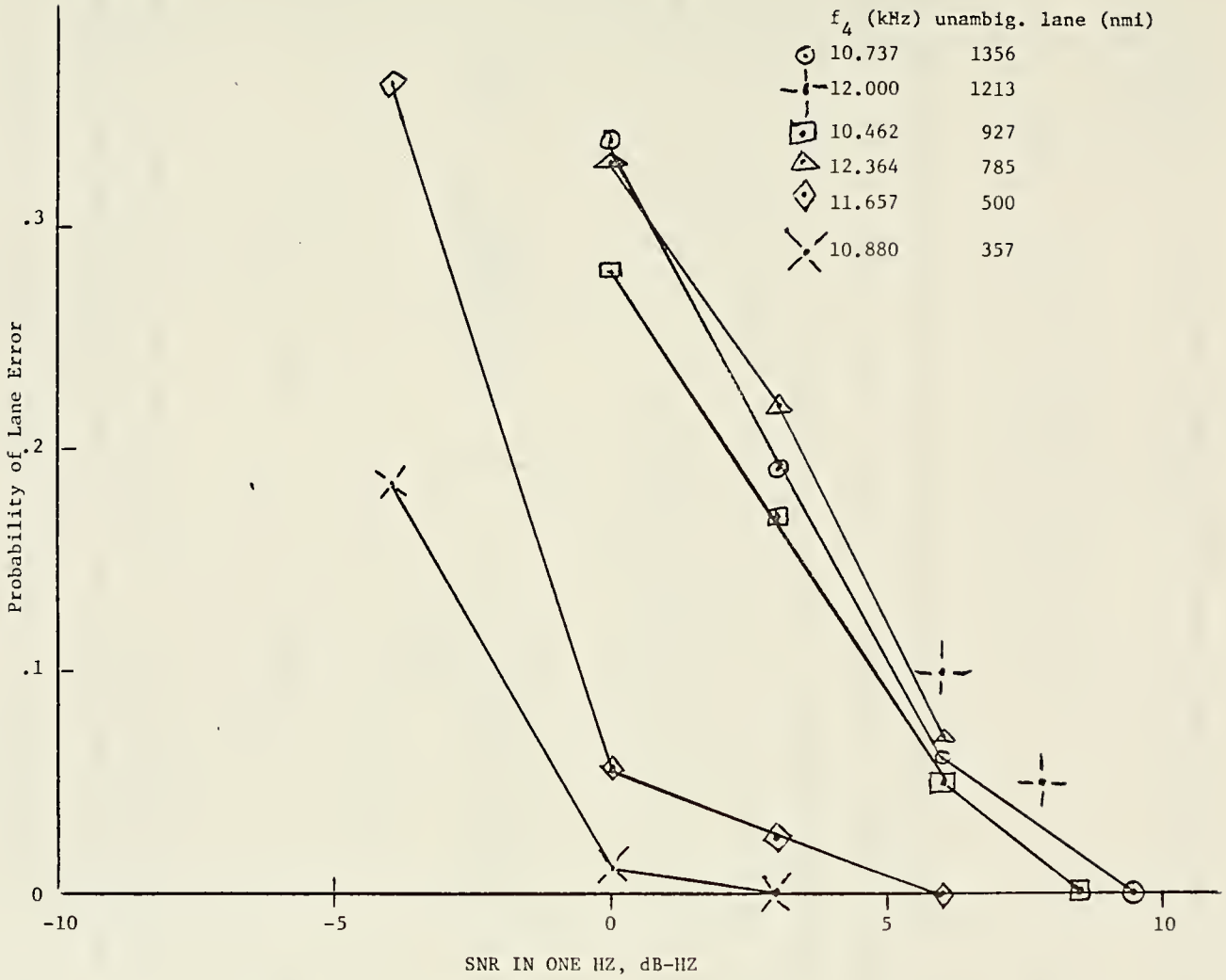

Figure C1. Simulation Results for Known Phase Velocities.

APPENDIX D

EXPECTED VALUE OF A SPECIAL FUNCTION

Chapter IV derived the likelihood equation given by Equation (32) as

$$\Lambda(x) = E_{\varepsilon} \exp\ [\varepsilon^T A\varepsilon + B^T\varepsilon + D] \ . \qquad \text{(D-1)}$$

In (D-1) $E_{\varepsilon}(\cdot)$ denotes the expected value with respect to ε where ε is a column vector with 2K elements jointly Gaussian distributed with zero mean values and covariance matrix K_{ε}. A is a 2K square matrix, B is a column vector with 2K elements, and D is a scalar. The expected value in (D-1) can be written as

$$\Lambda(x) = \frac{\exp(D)}{(2\pi)^K |K_{\varepsilon}|^{1/2}} \int_{\varepsilon_1} \cdots \int_{\varepsilon_{2K}} \exp\{-\frac{1}{2}[\varepsilon^T K_{\varepsilon}^{-1}\varepsilon$$

$$- 2\varepsilon^T A\varepsilon - 2B^T\varepsilon]\}\ d\varepsilon_1, \ldots\ldots\ d\varepsilon_{2K} \qquad \text{(D-2)}$$

where $|\cdot|$ denotes the determinant. The argument of the exponential in the integral defined as G can be written as

$$G = \varepsilon^T K_{\varepsilon}^{-1}\ \varepsilon - 2\varepsilon^T A\varepsilon - 2B^T\varepsilon = \varepsilon^T(K_{\varepsilon}^{-1} - 2A)\varepsilon - B^T\varepsilon - \varepsilon^T B, \quad \text{(D-3)}$$

which can then be written as

$$G = \varepsilon^T(K_\varepsilon^{-1} - 2A)\varepsilon - U^T(K_\varepsilon^{-1} - 2A)\varepsilon - \varepsilon^T(K_\varepsilon^{-1} - 2A)U \qquad (D\text{-}4)$$

where

$$U^T = B^T (K_\varepsilon^{-1} - 2A)^{-1} \qquad (D\text{-}5a)$$

and thus

$$U = (K_\varepsilon^{-1} - 2A)^{-1} B \; . \qquad (D\text{-}5b)$$

Equation (D-4) can now be written as

$$G = (\varepsilon - U)^T (K_\varepsilon^{-1} - 2A) (\varepsilon - U) - U^T(K_\varepsilon^{-1} - 2A) U \qquad (D\text{-}6)$$

by completing the square.

These manipulations allow (D-2) to be written as

$$\Lambda(x) = \frac{\exp\left[D + \frac{1}{2}U^T(K_\varepsilon^{-1} - 2A)\, U\right]}{(2\pi)^K \mid K_\varepsilon \mid^{1/2}} \; .$$

$$\int_{\varepsilon_1} \cdots\cdots \int_{\varepsilon_{2K}} \exp\{-\tfrac{1}{2}\left[(\varepsilon-U)^T(K_\varepsilon^{-1} - 2A)(\varepsilon-U)\right]\} d\varepsilon_1 \ldots d\varepsilon_{2K} \; . \qquad (D\text{-}7)$$

The integral is over all values of the jointly Gaussian random vector ε and thus equals

$$(2\pi)^K \mid (K_\varepsilon^{-1} - 2A)^{-1} \mid^{1/2} \; .$$

The desired expected value is then

$$\Lambda(x) = \frac{\left| (K_\varepsilon^{-1} - 2A)^{-1} \right|^{1/2}}{|K_\varepsilon|^{1/2}} \exp\left[D + \frac{1}{2}U^T(K_\varepsilon^{-1} - 2A)U\right] \quad \text{(D-8)}$$

Matrix manipulation of this equation allows the final simpler result

$$\Lambda(x) = \frac{\exp\left[D + B^T K_\varepsilon (I - 2AK_\varepsilon)^{-1} B\right]}{\left|(I - 2AK_\varepsilon)\right|^{1/2}} \quad \text{(D-9)}$$

to be written.

APPENDIX E

COMPUTER IMPLEMENTATION OF TWO-STATION LOP ESTIMATION

In order to solve the estimation equation given by Equation (38) in Chapter IV for the two-station, four-frequency experimental data discussed in Chapter VI, a computer program was written. A flow chart of that program is contained in this appendix. On the IBM 360-67, the program occupied 34K BYTES of core. The time required to process one "run" of data was on the order of 15 seconds. A run, as defined previously, consisted of nominally three minutes of Omega data. The range of values over which x was allowed to vary, as discussed in Chapter VI was twice that which would be required in an operational system.

A "coarse" processing which was performed to save computer time was the following. The values of $\psi_i (1 \leq i \leq 4)$ as given by Equation (17) in Chapter IV were examined with the value of x being tried in the iterative procedure before entering the actual matrix manipulation portion of the program. The magnitude of each value of ψ_i was required to be less than 1.5 rad. before the entire estimation process was carried out. This is equivalent to saying that noise and phase velocity uncertainties will not disturb the phases by more than $\pm$ 1.5 rad. for the Dallas, Texas receiver location.

The value which is used for this "coarse" processing can be determined for the ith frequency by examining the amount

of phase shift which two standard deviations of phase velocity disturbance from each station in opposite senses will cause. To determine the effect of a phase velocity disturbance on phase the equation

$$\phi_{K+i} - \phi_i = \omega_i \left(\frac{L-x}{v_{K+i}} - \frac{x}{v_i}\right) - 2\pi m_i \qquad \text{(E-1)}$$

is written. The values of ϕ are the propagation phase delays for the ith frequency signals, ω_i is the ith angular frequency, v_i are the phase velocities, m_i is the number of whole cycles in the phase difference and (L-x) and x are defined as in Chapters IV and VI. To see the maximum effect of perturbing phase velocities, let Δv be added to v_{K+i} and subtracted from v_i and for simplicity, assume $v_i = v_{K+i} = v$. Thus,

$$\phi_{K+i} - \phi_i - \Delta\phi_i = \omega_i \left(\frac{L-x}{v + \Delta v} - \frac{x}{v - \Delta v}\right) - 2\pi m_i$$

$$= \frac{\omega_i}{v} \left(\frac{L-x}{1 + \frac{\Delta v}{v}} - \frac{x}{1 - \frac{\Delta v}{v}}\right) - 2\pi m_i \qquad \text{(E-2)}$$

where $\Delta\phi_i$ is the perturbation in the phase difference caused by Δv. This can be written as

$$\phi_{K+i} - \phi_i - \Delta\phi_i \cong \frac{\omega_i}{v}\left[(L-x)\left(1 - \frac{\Delta v}{v}\right) - x\left(1 + \frac{\Delta v}{v}\right)\right] - 2\pi m_i$$

$$= \frac{\omega_i}{v}(L-2x) - 2\pi m_i - \frac{\omega_i L}{v}\left(\frac{\Delta v}{v}\right) \qquad \text{(E-3)}$$

since $\left(\frac{\Delta v}{v}\right)$ will be small. Or,

$$|\Delta\phi_i| = \frac{\omega_i L}{v}\left|\frac{\Delta v}{v}\right| \approx \frac{\omega_i L}{c}\left|\frac{\Delta v}{c}\right| . \qquad \text{(E-4)}$$

For L = 3547.15, which is the Forestport-Dallas-Trinidad distance, $\omega_i = 2\pi \cdot 13.6$ kHz and $\left|\frac{\Delta v}{c}\right| = 8 \times 10^{-4}$; the magnitude of the maximum expected phase perturbation is found to be

$$|\Delta\phi| \cong \frac{2\pi \cdot 13.6 \cdot 3547.15 \cdot 8 \cdot 10^{-1}}{161875.2} = 1.5 \text{ rad} . \qquad \text{(E-5)}$$

Since the $|\Delta\phi|$ for lower frequencies will be smaller, this was considered a reasonable upper bound to use for all frequencies of the four-frequency experimental data.

The amount of savings in terms of the number of values of x which must be considered when a coarse search such as this is used can be determined as follows. Consider the ith frequency phase difference as x is varied through a lane. Only one half the values of x will meet the coarse criterion if $|\psi_i|$ is required to be less than $\frac{\pi}{2}$. Since there are four frequencies, only 1/16 of the possible x will meet the coarse criterion. As discussed in Chapter VI, $\pm$ 350 nmi (nominally) were used in processing the four-frequency experimental data with increments of x = 0.5 nmi. Thus, only about 90 values of x vice about 1400 had to be processed through the entire estimation procedure.

For a generally implemented system such as GRAN, it would not be unusual to have values for L = 7000 nmi or greater, so it is not expected that this processing advantage can be generally implemented. Because of the significant time savings it affords, it may well be worth using a variable value which is determined after a rough estimate of L is known. In the final GRAN system, if 10.88 kHz is added as a fourth frequency, 360 nmi unambiguous lanes will result. If Δx of 0.5 nmi are used, 720 values of x must be processed. If no coarse estimate procedure is used, using the $\approx$ 15-second processing time for twice the number of values of x as a guide, about two minutes will be required to estimate an LOP for a station pair using a program similar to the one in this appendix.

Preferable methods of search for the values of x which maximize the likelihood function may exist, such as [30]. Methods other than the exhaustive search method discussed in previous chapters of this dissertation and implemented in the following computer program were not considered. The exhaustive search technique was chosen because of its simplicity and ease of implementation.

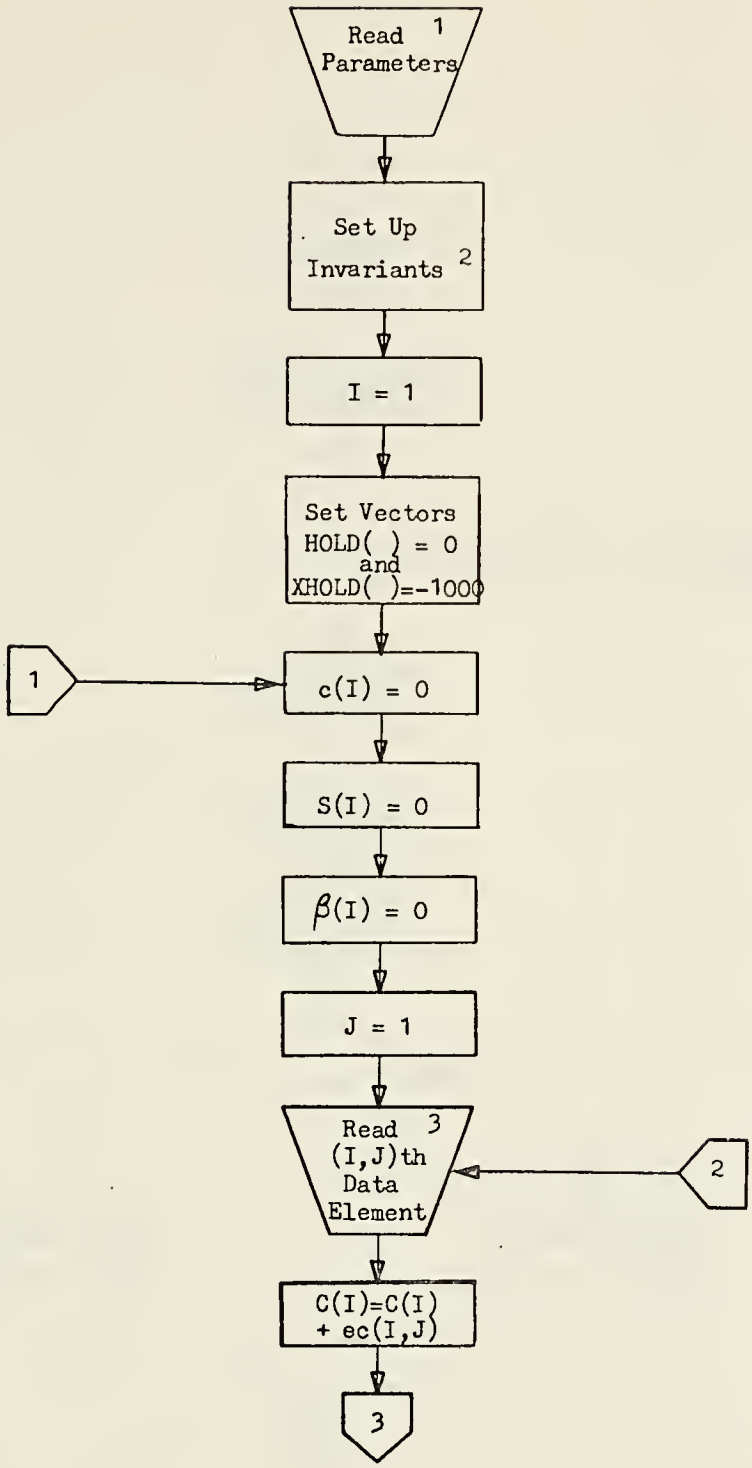
Read Parameters 1
Set Up Invariants 2
I = 1
Set Vectors HOLD( ) = 0 and XHOLD( )=-1000
1
c(I) = 0
S(I) = 0
β(I) = 0
J = 1
Read (I,J)th Data Element 3
2
C(I)=C(I) + ec(I,J)
3

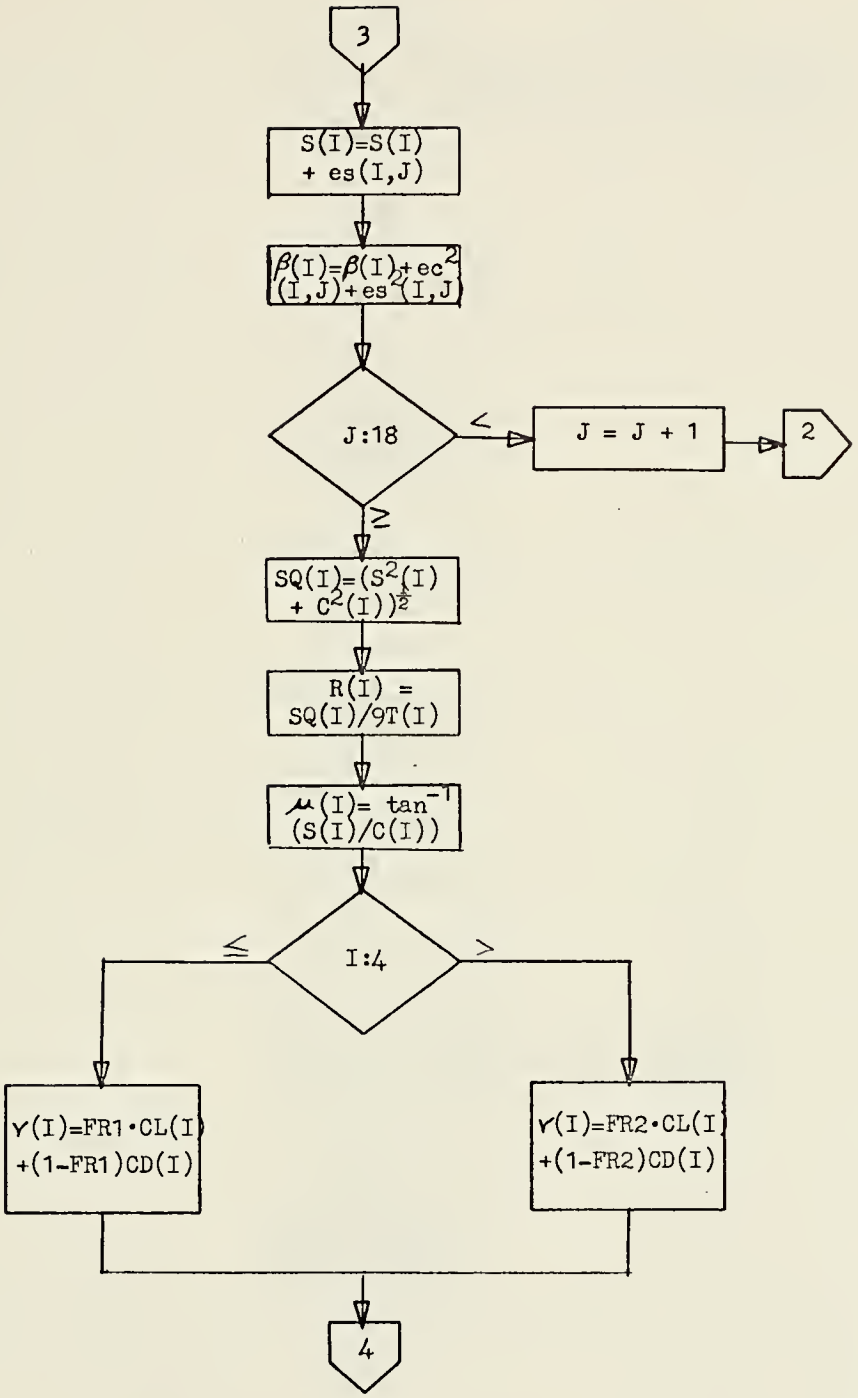
3
S(I)=S(I)
+ es(I,J)
β(I)=β(I)+ec²
(I,J)+es²(I,J)
J:18
<
J = J + 1
2
≥
SQ(I)=(S²(I)
+ C²(I))^½
R(I) =
SQ(I)/9T(I)
μ(I)= tan⁻¹
(S(I)/C(I))
I:4
≤
>
Y(I)=FR1·CL(I)
+(1-FR1)CD(I)
Y(I)=FR2·CL(I)
+(1-FR2)CD(I)
4

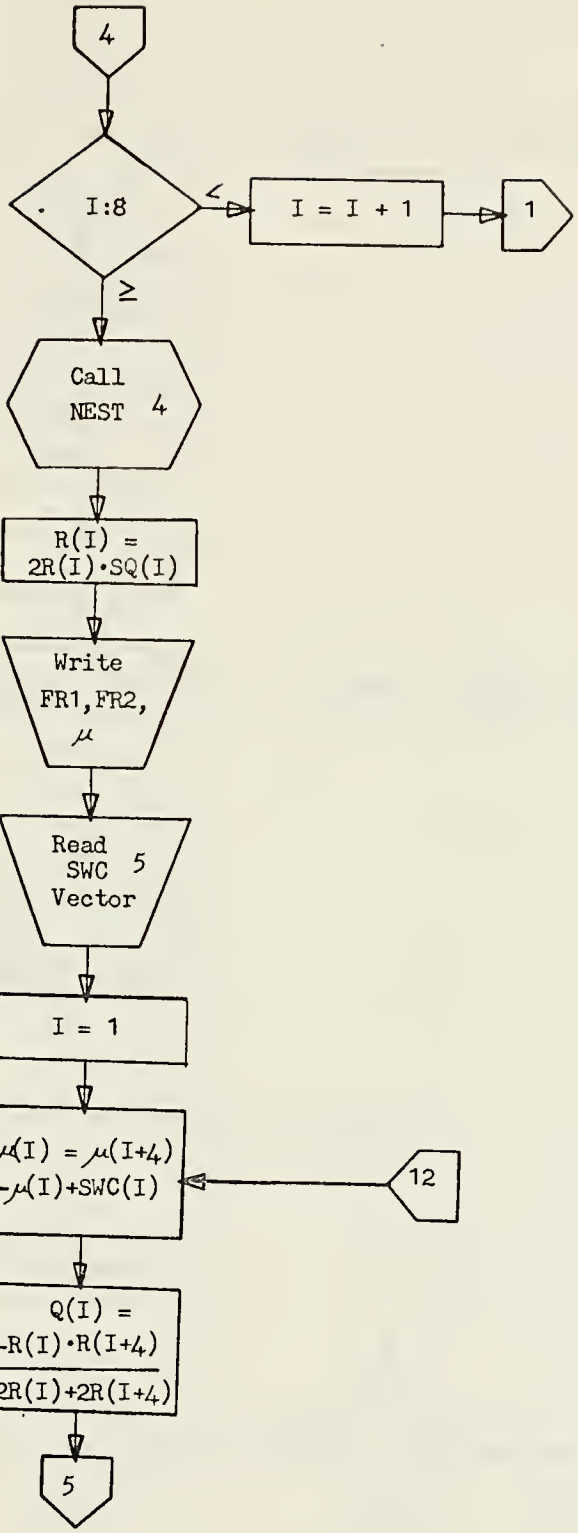
4
I:8
<
I = I + 1
1
≥
Call
NEST 4
R(I) =
2R(I)·SQ(I)
Write
FR1, FR2,
μ
Read
SWC 5
Vector
I = 1
μ(I) = μ(I+4)
-μ(I)+SWC(I)
12
Q(I) =
-R(I)·R(I+4)
2R(I)+2R(I+4)
5

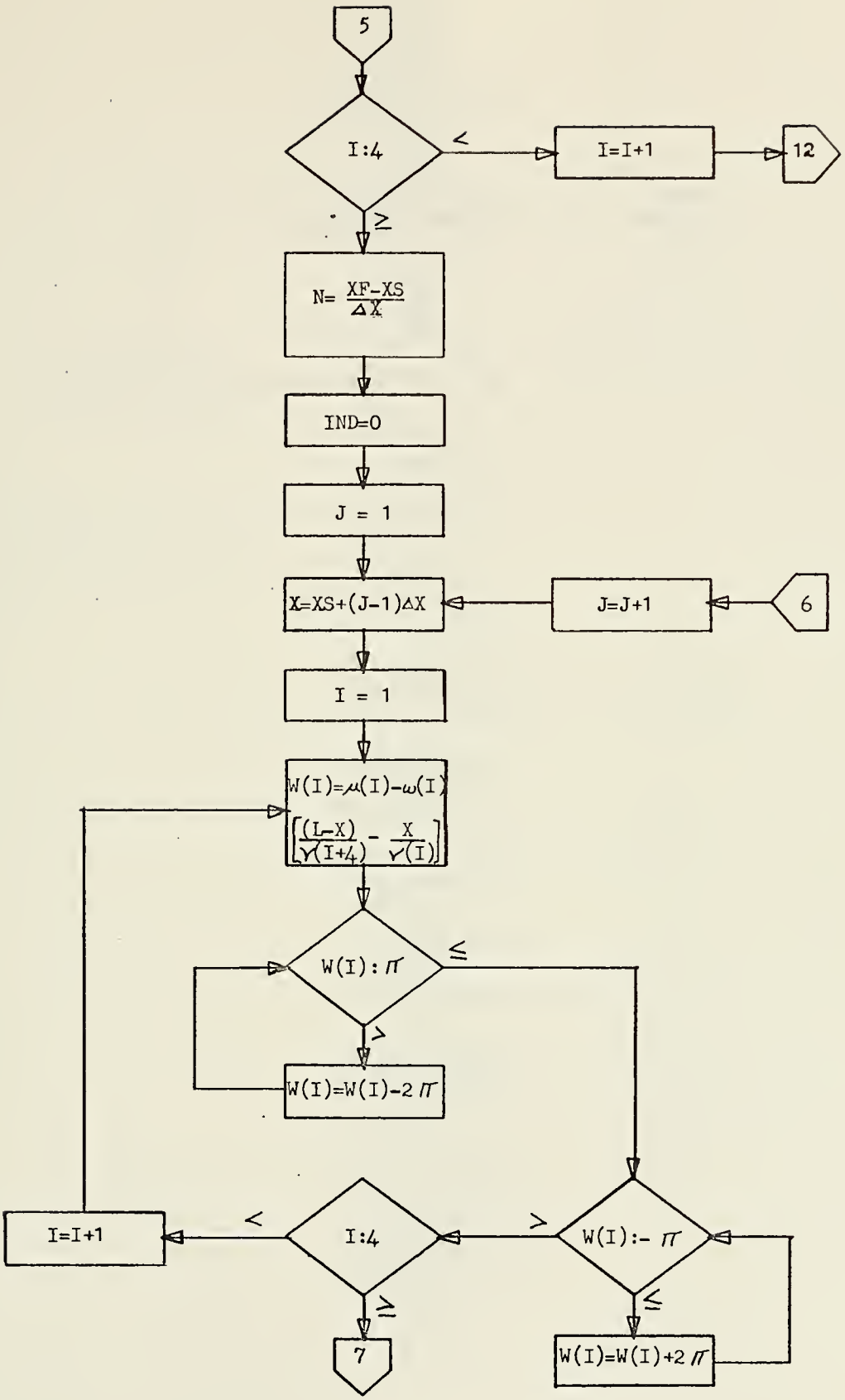
5
I:4
<
I=I+1
12
≥
N= XF-XS / ΔX
IND=0
J = 1
X=XS+(J-1)ΔX
J=J+1
6
I = 1
W(I)=μ(I)-ω(I)
[(L-X)/γ(I+4) - X/γ(I)]
W(I):π
≤
>
W(I)=W(I)-2π
I=I+1
<
I:4
>
W(I):- π
≤
≥
7
W(I)=W(I)+2π

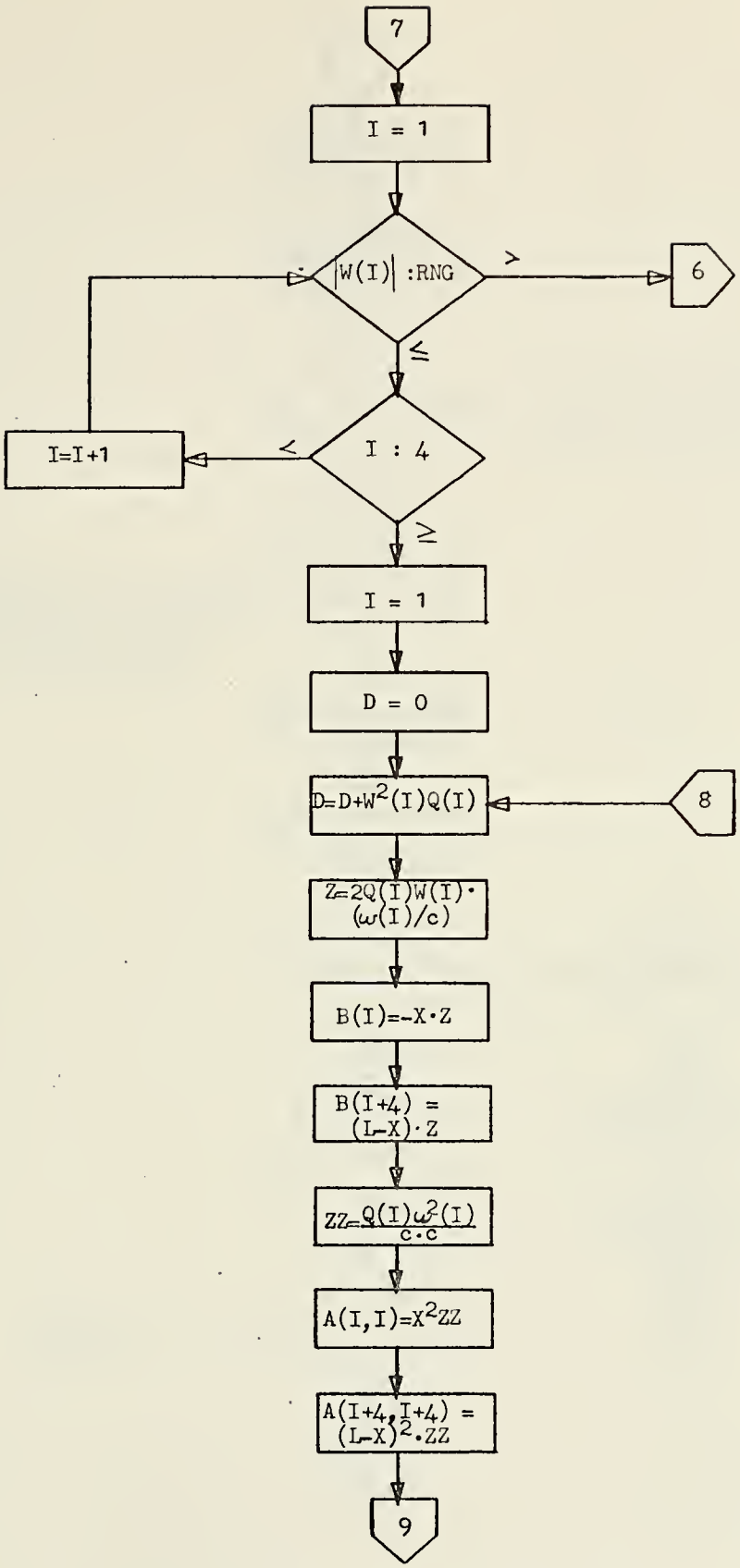
7
I = 1
|W(I)| :RNG
>
6
≤
I : 4
<
I=I+1
≥
I = 1
D = 0
D=D+W²(I)Q(I)
8
Z=2Q(I)W(I)·(ω(I)/c)
B(I)=-X·Z
B(I+4) = (L-X)·Z
ZZ=Q(I)ω²(I)/c·c
A(I,I)=X²ZZ
A(I+4,I+4) = (L-X)²·ZZ
9

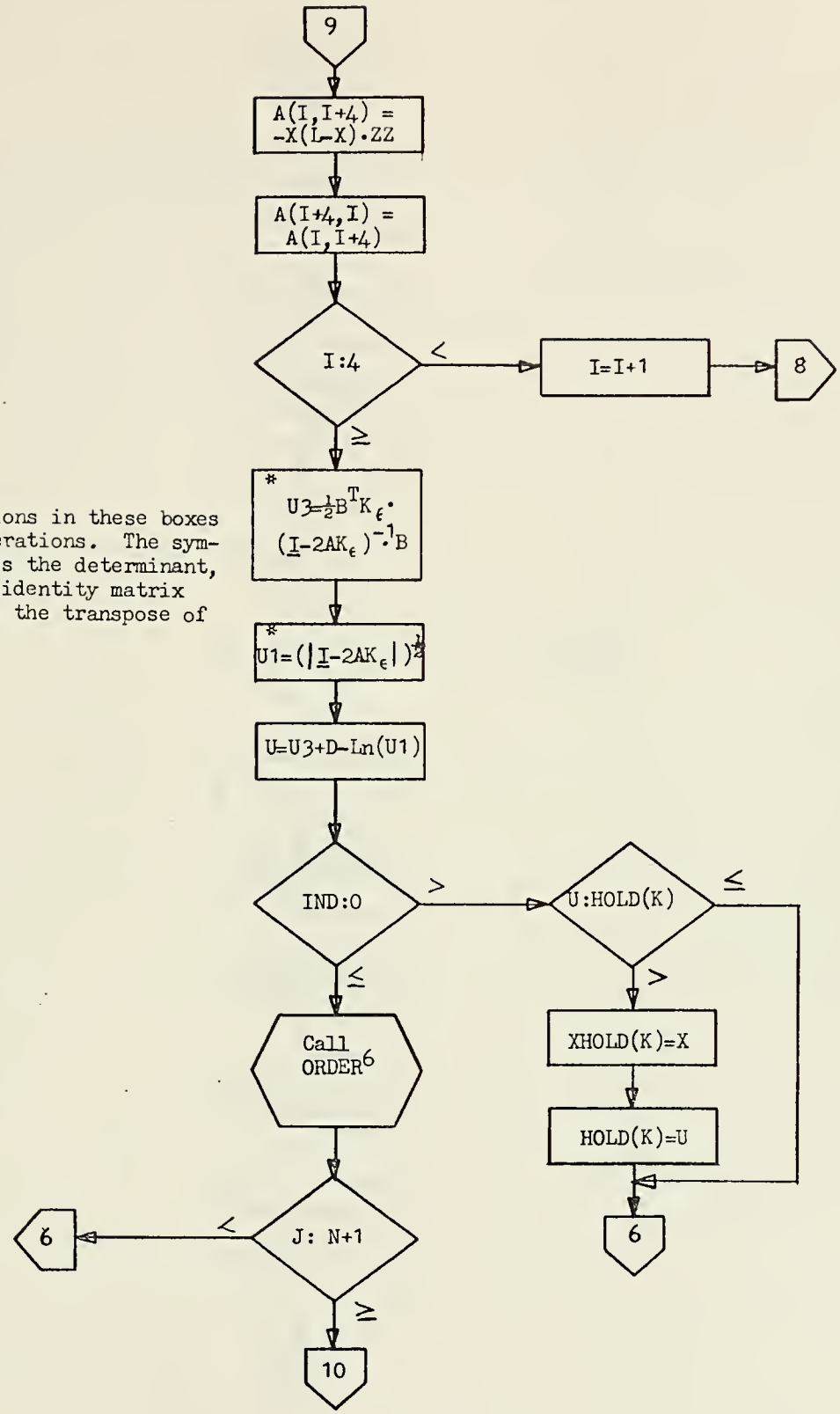

* The operations in these boxes are matrix operations. The symbol $|\cdot|$ denotes the determinant, $\underline{I}$ denotes the identity matrix and B^T denotes the transpose of the vector B.

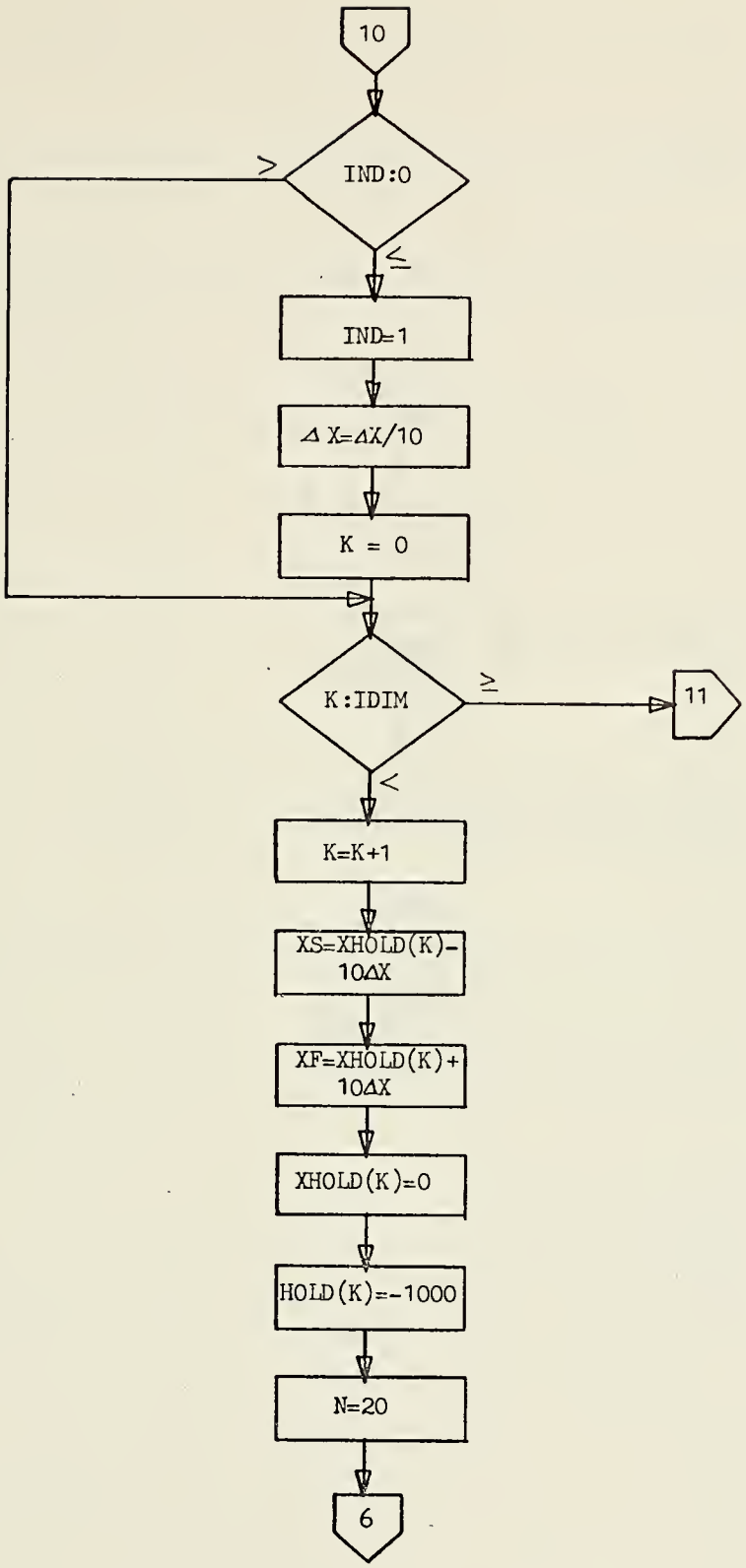
10
IND:0
>
≤
IND=1
ΔX=ΔX/10
K = 0
K:IDIM
≥
11
<
K=K+1
XS=XHOLD(K)-10ΔX
XF=XHOLD(K)+10ΔX
XHOLD(K)=0
HOLD(K)=-1000
N=20
6

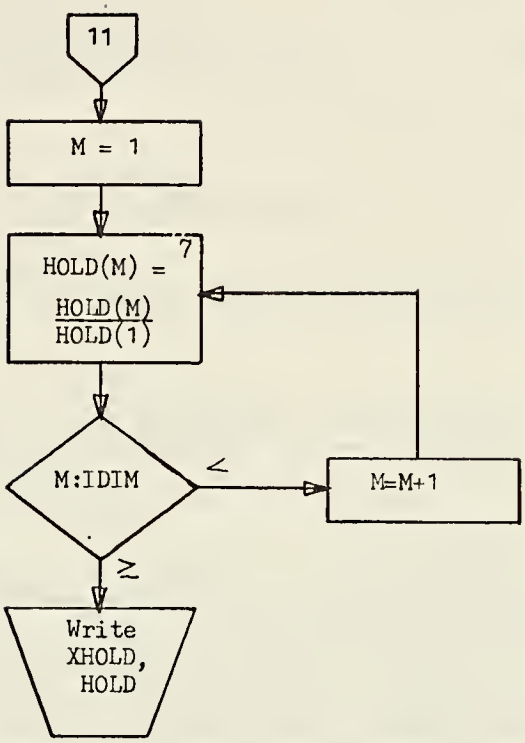
11
M = 1
HOLD(M) = HOLD(M) / HOLD(1)
7
M:IDIM
<
M=M+1
≥
Write XHOLD, HOLD

1 The parameters to be read in are the scalars XS, XF, ΔX, L, FR1, FR2, and IDIM and the matrix K_ε.

2 The invariants to be set up are the scalars π, RNG and c (vel of light in vacuum) and the vectors T, ω, CL, CD and RNG.

3 The (I,J)th data element consists of ec(I,J) and es(I,J) where

$$ec(I,J) = \int_{10(J-1)}^{10(J-1)+T(I)} y(I)\ COS[\omega(I)t]dt \qquad \text{and}$$

$$ec(I,J) = \int_{10(J-1)}^{10(J-1)+T(I)} y(I)\ SIN[\omega(I)t]dt$$

where y(I) is the Ith component of the received signal vector.

4 Subroutine NEST must be provided the vectors R, β and T and returns in R the estimates of the signal amplitude to noise density ratios.

5 The vector SWC must be provided as propagation correction factors for each frequency in the form of station two minus station one corrections. When propagation correction factors are used, all entries in the mean value vectors ν must be set equal to the charting phase velocity which is used in their prediction (1.00261•c). When no propagation correction factors are used, the vector SWC must have all zero entries.

6 Subroutine ORDER must be given the values of the scalars U, X and IDIM and it returns the requested number (IDIM) of most likely estimates of X in the vector XHOLD. The corresponding likelihood function values in the vector HOLD are returned also. The components of these vectors are in descending order of likelihood.

7 The vector HOLD at this point contains the probability ratios.

DEFINITIONS

XS- starting value for X in the iteration

XF- final value for x in the iteration

ΔX- size of incremental steps in X to be used

L- fixed value for L

K_ε- 8-by-8 covariance matrix of ε

CL- 4 element vector for mean values of phase velocity in lighted path

CD- 4 element vector for mean values of phase velocity in dark path

T- 8 element vector for Omega pulse durations

FR1- fraction of path 1 in light

FR2- fraction of path 2 in light

ω- 4 element vector of radian frequencies

γ- 8 element vector of mean values of phase velocity to be computed by the program

SWC- 4 element vector of propagation correction factors in form of station two minus station one corrections for each of four frequencies (to be set equal to zero if no corrections are to be used)

RNG- a predetermined constant in radians equal to the maximum deviation of the phase of any signal from the phase resulting from mean values of phase velocity. These deviations are due to phase velocity uncertainties. (1.5 rad was used in the experiment data processing.)

IDIM- The number of most likely estimates of X to be retained

HOLD- vector of length IDIM of values of the likelihood function to be retained

XHOLD- vector of length IDIM of values of X corresponding to the values of HOLD

μ- 8 element vector of phase angles computed by the program

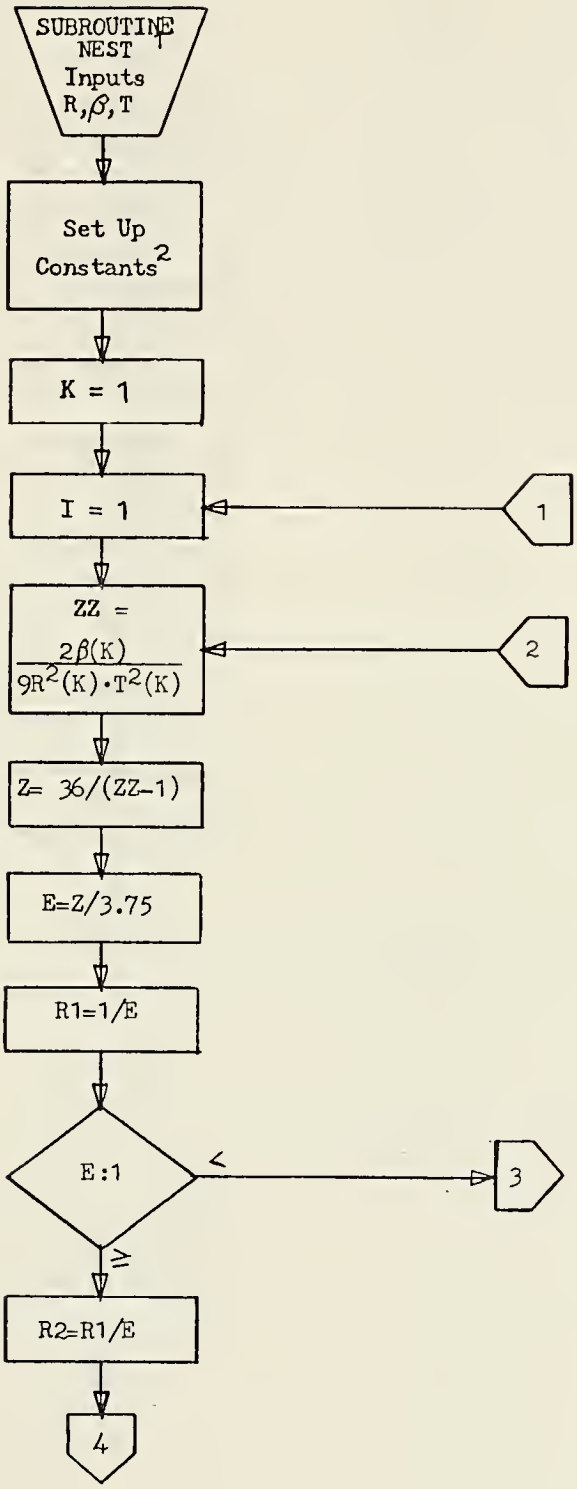
SUBROUTINE NEST
Inputs
R, β, T
Set Up Constants
K = 1
I = 1
1
ZZ = 2β(K) / 9R²(K)·T²(K)
2
Z= 36/(ZZ-1)
E=Z/3.75
R1=1/E
E:1
<
3
≥
R2=R1/E
4

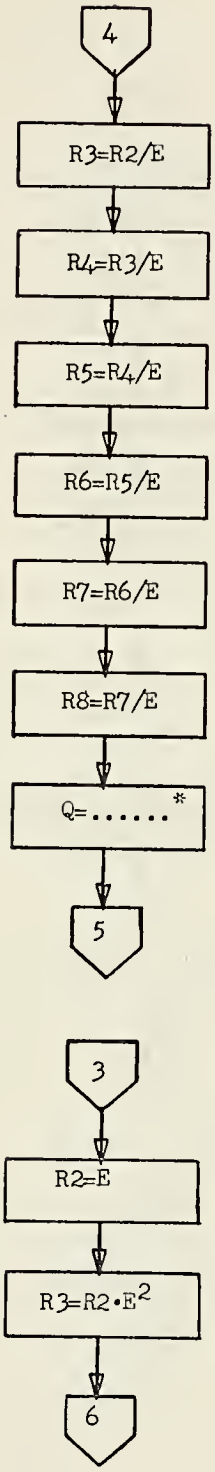

* Q=C1(C2+C3•R1+C4•R2+C5•R3+C6•R4+
C7•R5+C8•R6+C9•R7+C10•R8)

** $Q=D1(D2\cdot R1+D3\cdot R2+D4\cdot R3+D5\cdot R4+D6\cdot R5+D7\cdot R6+D8\cdot R7)$

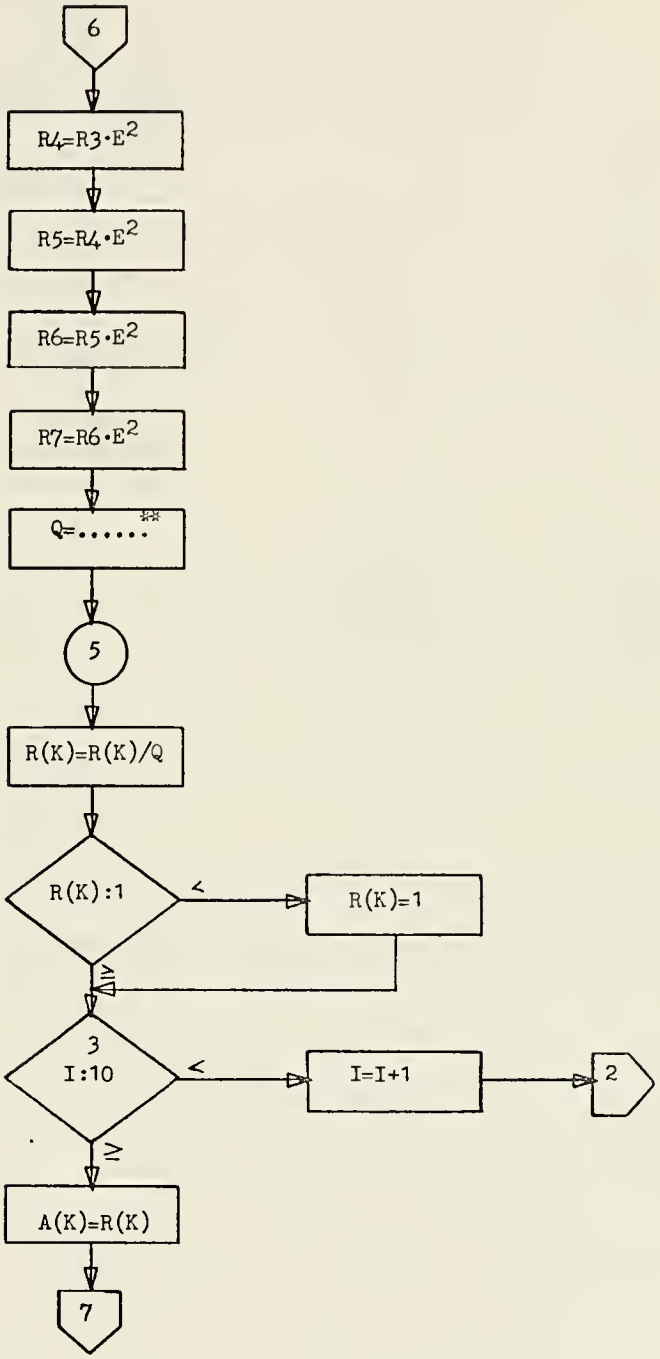

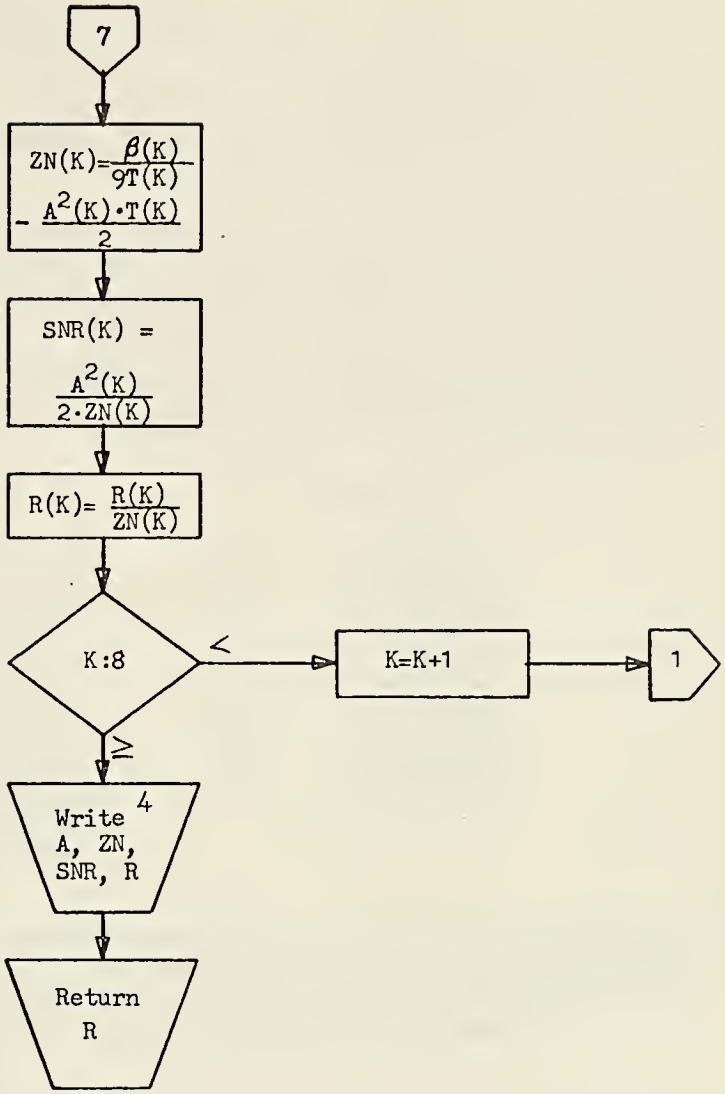
7
ZN(K)=β(K)/9T(K) - A²(K)·T(K)/2
SNR(K) = A²(K)/2·ZN(K)
R(K)= R(K)/ZN(K)
K:8
<
K=K+1
1
≥
Write 4
A, ZN,
SNR, R
Return
R

1 Subroutine NEST computes the joint maximum likelihood estimates of the signal amplitudes and the one-sided noise spectral density heights from the equations

$$N(I) = \frac{\beta(I)}{9T(I)} - \frac{A^2(I)\ T(I)}{2} \quad \text{and}$$

$$A(I) = \frac{SQ(I)}{9 \cdot T(I)} \cdot \frac{I_1[2A(I) \cdot SQ(I)/N(I)]}{I_o[2A(I) \cdot SQ(I)/N(I)]} \ .$$

In these equations the vectors are as defined in the subroutine NEST or the MAIN estimation program. I_1 and I_o are modified Bessel functions of the first kind of order one and zero respectively. The ratio of these Bessel functions is computed by using their polynomial approximations found in Handbook of Mathematical Functions by M. Abramowitz and I. A. Stegun, Dover Publications.

2 The constants required for this subroutine are:

C1	= 2.50662828	D1	= .53333333
C2	= .39894228	D2	= 1.00000000
C3	= .05316616	D3	= 1.75781160
C4	= .01118812	D4	= -1.02993610
C5	= -.00161279	D5	= .90497756
C6	= .01920037	D6	= -.84749981
C7	= -.04017321	D7	= .80494379
C8	= .04837180	D8	= -.76696533
C9	= -.02678420		
C10	= .00532070		

3 It has been found experimentally that 10 iterations are adequate for reasonable convergence of the iterative process for data from the OPLE ground station in SNR environments which can be expected from Omega.

4 The vectors A, ZN, SNR and R written out here are the estimates of signal amplitude, two-sided noise density height, signal to noise density ratio and signal amplitude to noise density ratio respectively.

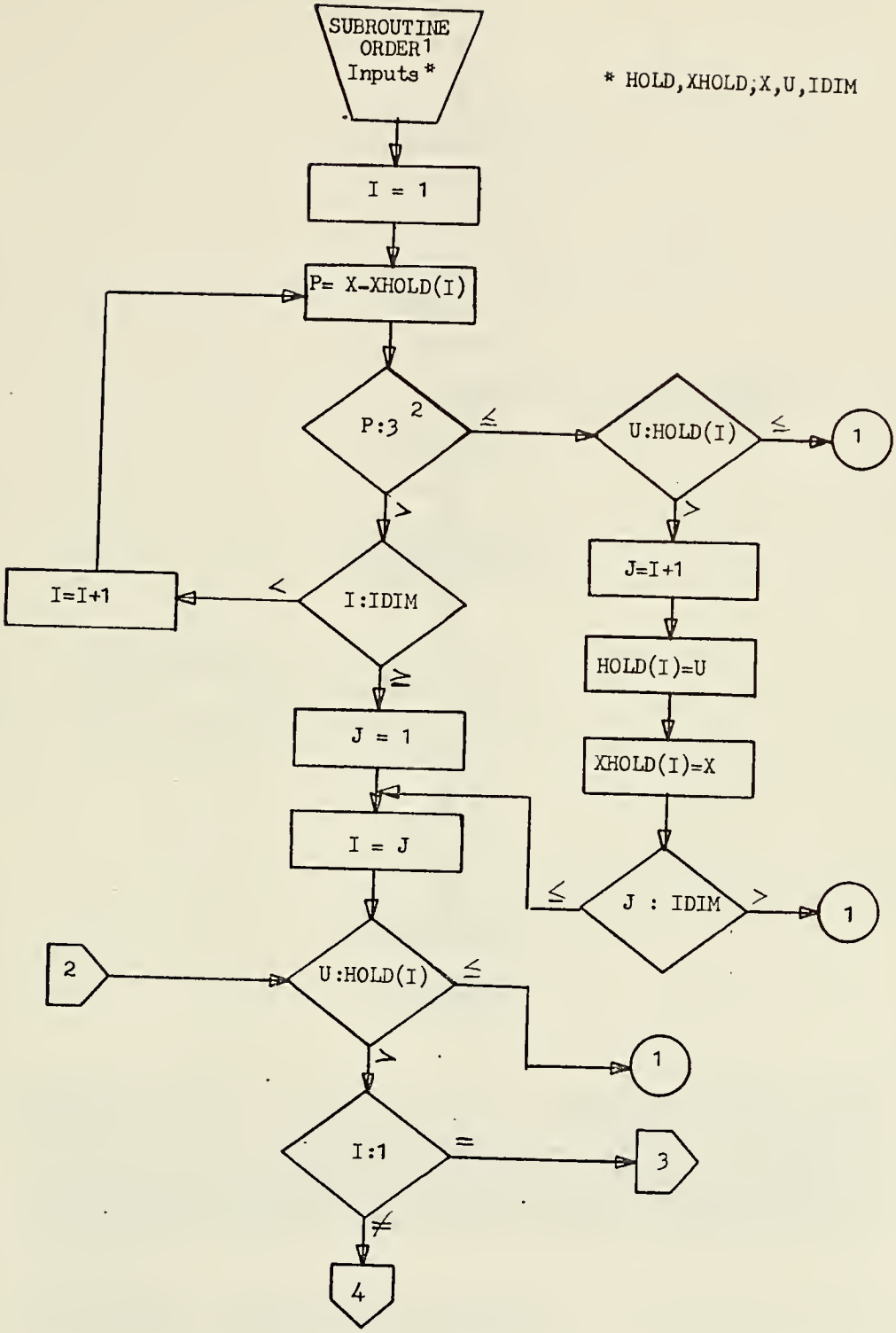
SUBROUTINE ORDER1 Inputs *
* HOLD,XHOLD;X,U,IDIM
I = 1
P= X-XHOLD(I)
P:3 2
≤
U:HOLD(I)
≤
1
>
>
J=I+1
HOLD(I)=U
XHOLD(I)=X
I=I+1
<
I:IDIM
≥
J = 1
I = J
≤
J : IDIM
>
1
2
U:HOLD(I)
≤
1
>
I:1
=
3
≠
4

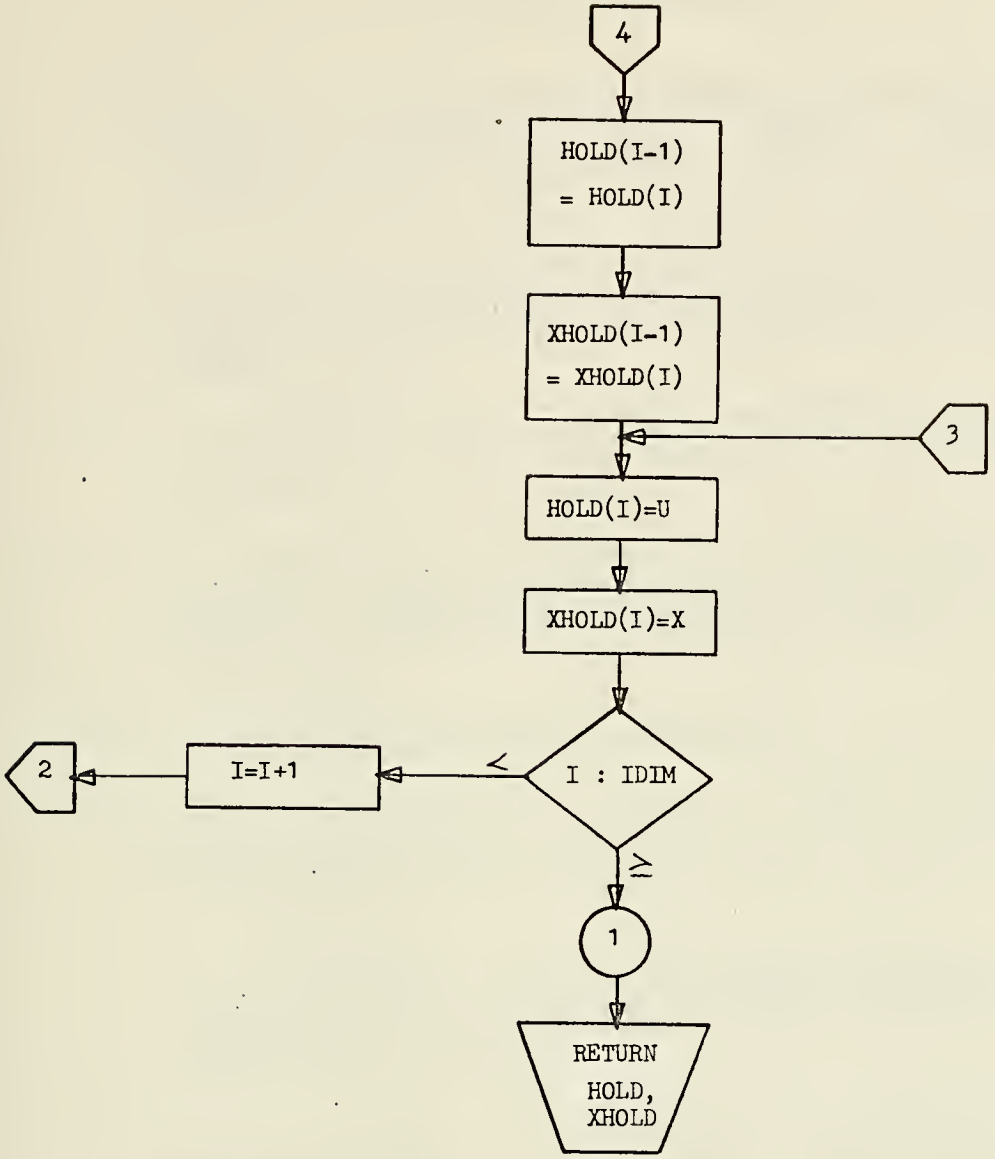

1 Subroutine ORDER receives the scalars X, U (likelihood function value for X) and IDIM. ORDER places U and X into the vectors HOLD and XHOLD of dimension IDIM in their appropriate place. That is, the largest value of U received thus far in the "run" occupies the first component of HOLD, the second largest U occupies the second component, etc. The components of XHOLD are the values of X which correspond to these values of U.

2 This operation insures that only one value of U and X will be retained for each peak of the likelihood function.

LIST OF REFERENCES

1. Naval Electronics Systems Command Letter Ser. 459 PME-119, To: Distribution List, Subject: Current Information on Status of the Omega Navigation System, 1 August 1973.

2. W. R. Crawford and W. E. Rupp, "Locating downed aircraft by GRAN (Global Rescue Alarm Net)," NAVIGATION: Journal of the Institute of Navigation, Vol. 19, No. 4, Winter 1972-73.

3. F. H. Raab et al., "Advanced survival avionics program subsystem design analysis report," Cincinnati Electronics Corp. report 80045 ARS 6/773, 30 June 1973.

4. C. Samek and H. S. Pike, "A precision electronic navigation system using Omega and a synchronous satellite network," NAVIGATION: Journal of the Institute of Navigation, Vol. 13, No. 2, Summer 1966.

5. C. Laughlin et al., "Ople experiment," Goddard Space Flight Center report X-733-67-266, June 1967.

6. W. G. Patton and L. F. Field, "Ninth interim report search and rescue communications Global Rescue Alarm Net (GRAN)," Naval Air Test Center report ST-67R-70, 27 April 1970.

7. J. C. Morakis, "The Global Rescue Alarm Net (GRAN) experiment," Proceedings of the 4th Annual NASA and DOD Precise Time and Time Interval planning conference, 14-16 November 1972.

8. M. E. Langley, "The Global Rescue Alarm Net (GRAN), a systems analysis," Elec. Eng. degree thesis, Naval Postgraduate School, Monterey, California, September 1973.

9. J. A. Pierce and R. H. Woodward, "The development of long-range hyperbolic navigation in the United States," NAVIGATION: Journal of the Institute of Navigation, Vol. 18, No. 1, Spring 1971.

10. J. A. Pierce et al., "Omega: A worldwide navigation system: system specification and implementation," National Technical Information document AD 630 900, May 1966.

11. A. D. Watt, VLF Radio Engineering. New York: Pergamon, 1967.

12. J. R. Wait, Electromagnetic Waves in Stratified Media. New York: Pergamon, 1962.

13. K. G. Budden, The Wave-Guide Mode Theory of Wave Propagation. New Jersey: Prentice-Hall, 1961

14. J. Galejs, Terrestrial Propagation of Long Electromagnetic Waves. New York: Pergamon Press, 1972.

15. E. R. Swanson and R. P. Brown, "Omega propagation prediction primer," Naval Electronics Laboratory Center report TN 2101, 3 August 1972.

16. J. A. Pierce, "Lane identification in Omega," Technical report No. 627, Div. of Eng. and Appl. Physics, Harvard Univ., July 1972.

17. W. D. Westfall and J. A. Ferguson, "A comparison of measured and calculated VLF phase velocities for day and night," Naval Electronics Laboratory Center, Technical document 182, 20 October 1972.

18. E. R. Swanson, "Omega lane resolution," Naval Electronics Laboratory Center report 1305, 5 August 1965.

19. E. R. Swanson and C. P. Kugel, "Omega VLF timing," Naval Electronics Laboratory Center report TR 1740 - revision 1, 29 June 1972.

20. J. A. Pierce, "Measurement and prediction of group velocity at very low frequencies," Technical report No. 535, Div. of Eng. and Appl. Physics, Harvard Univ., July 1967.

21. E. R. Swanson and D. J. Adrian, "Omega envelope capability for lane resolution and timing," Navy Electronics Laboratory Center report TR 1901, 20 November 1973.

22. Texas Instruments Corp., "Report on Omega signal measurement program," Texas Instr. Corp., Dallas, Texas, 14 June 1973.

23. G. Frenkel and D. G. Gan, "Ambiguity resolution in systems using Omega for position location," IEEE Trans. Commun. Technol., COM-22, pp. 305-312, March 1974.

24. Computer Science Corp., "Ambiguity resolution in the advanced OPLE system, final report for phase I," Prepared for NASA Goddard Space Flight Center, Greenbelt, Md., August 1972.

25. Computer Science Corp., "Ambiguity resolution in the advanced OPLE system, final report for phase II," Prepared for NASA Goddard Space Flight Center, Greenbelt, Md., December 1972.

26. H. A. Van Trees, Detection, Estimation and Modulation Theory, Part I. New York: Wiley, 1968, pp. 273-275.

27. M. Abramowitz and I. A. Stegun, Handbook of Mathematical Functions. New York: Dover, 1965, pp. 377.

28. Texas Instruments Corp., "Design study report for Omega position location equipment control center," Texas Instr. Corp., Dallas, Texas, 30 September 1966.

29. Texas Instruments Corp., "Four frequency Omega experiment, final report," Texas Instr. Corp., Dallas, Texas, 27 February 1974.

30. B. O. Shubert, "A sequential method seeking the global maximum of a function," SIAM J. Numer. Anal., Vol. 9 No. 3, September 1972.

INITIAL DISTRIBUTION LIST

		No. Copies
1.	Defense Documentation Center Cameron Station Alexandria, Virginia 22314	2
2.	Library, Code 0212 Naval Postgraduate School Monterey, California 93940	2
3.	Assoc. Professor J. E. Ohlson, Code 5201 Department of Electrical Engineering Naval Postgraduate School Monterey, California 93940	4
4.	Assoc. Professor D. E. Kirk, Code 52Ki Department of Electrical Engineering Naval Postgraduate School Monterey, California 93940	1
5.	Assistant Professor R. W. Adler, Code 52Ab Department of Electrical Engineering Naval Postgraduate School Monterey, California 93940	1
6.	Assoc. Professor T. Jayachandran, Code 53Jy Department of Mathematics Naval Postgraduate School Monterey, California 93940	1
7.	Assistant Professor B. Shubert, Code 55Sy Department of Operations Research and Administrative Sciences Naval Postgraduate School Monterey, California 93940	1
8.	Professor S. R. Parker, Code 52 Department of Electrical Engineering Naval Postgraduate School Monterey, California 93940	1
9.	Commander W. R. Crawford, USN Life Support Systems Branch Service Test Division Naval Air Test Center NAS, Patuxent River, Maryland 20670	2

10. Mr. W. E. Rupp — 2
Life Support Systems Branch
Service Test Division
Naval Air Test Center
NAS, Patuxent River, Maryland 20670

11. Professor J. A. Pierce — 1
311 Cruft Hall
Harvard University
Cambridge, Massachusetts 02140

12. Lieutenant Commander C. J. Waylan — 5
7 Tweed Place
Monterey, California 93940